Università degli studi di Padova

Corso di Laurea Magistrale in Ingegneria
Chimica e dei Processi Industriali

Dipartimento di Ingegneria Industriale

Density-induced segregation in particles flows

Laureando:
Lorenzo Poloni
mtr 1160070

Relatore:
Prof. Andrea Claudio Santomaso

Correlatore:
Prof. Chuan-Yu (Charley) Wu

Anno Accademico 2018/2019

Abstract

Particles mixture segregation may occur during die filling in tablet manufacturing processes, compromising the structural stability of the final product.
An analysis of the behaviour of a binary mixture containing an API, caffeine, and an excipient is presented. Particularly, this research focuses on the density-driven segregation, trying to avoid any other phenomenon, mainly size differences, which may hinder it.
Mixtures of different composition are prepared, at 10%, 25% and 50% of API, and they are stabilized at different relative humidity, 20%, 50% and 80%, to investigate how these conditions affect segregation. Blend segregation results to be favored at ambient relative humidity conditions and with caffeine rich formulations.
The experimental results are compared to DEM simulations, which permit to decouple the drag effect due to air presence from the segregation due only to gravity falling. This comparison is done performing simulations in vacuum condition or with the system filled by air.
DEM simulations are performed at different CAF concentration: 10%, 25% and 50% by mass. Moreover, simulations with equal number of the two blend components particles are generated, permitting the analysis of the effect of the initial blend configuration in the shoe, perfectly or randomly mixed. The results suggest that, increasing the API concentration, segregation is reduced. This result is more evident in the air filled system, suggesting a role of the air presence in mixing the falling powder. The importance of a well mixed blend in the shoe is highlighted.

Riassunto

Il verificarsi di meccanismi di segregazione durante il processo di produzione di compresse medicinali può compromettere l'omogeneità della polvere che le compone. Tale evenienza è intrinseca nella manipolazione delle polveri e può intaccare non solo la quantità di principio attivo presente nella singola compressa, ma anche la sua stabilità strutturale, promuovendo l'insorgenza di fenomeni distruttivi come la laminazione o il distaccamento di una o di entrambe le estremità.
Diversi fattori nella manipolazione delle polveri concorrono nell'instaurare fenomeni segregativi, spaziando dalle modalità operative del processo di manipolazione fino a caratteristiche intrinseche alle polveri stesse. In questa ricerca ci si è focalizzati sull'effetto della differenza di densità di un composto binario, comprendente un principio attivo, la caffeina, e un eccipiente, il dicalciofosfato anidro. Il rapporto tra le loro densità è di 1.96, un valore comunemente riscontrato nelle formulazioni farmaceutiche. Per fare in modo che non intervenissero altri fattori nel fare separare i due materiali (in particolare la differenza di dimensione sarebbe largamente dominante sulla differenza di densità), le polveri sono state accuratamente setacciate, ottendendo due frazioni la cui distribuzione di dimensione fosse la più stretta possibile, di dimensione simile tra loro.

Sono state preparate tre miscele, a 10%, a 25% e a 50% di caffeina, stabilizzate poi a tre livelli di umidità relativa, 20%, 50% e 80%. In questo modo si è cercato di investigare quali fattori favorissero o limitassero l'insorgenza di fenomeni segregativi.
Il processo studiato è il riempimento dello stampo per la produzione di compresse, rappresentato da un modello composto da una scarpetta contenente la polvere che scorre a velocità costante ($150\,mm/s$) sopra un orifizio di sezione quadrata che viene riempito in questo modo. Lo stampo è diviso in cinque cassetti che permettono l'estrazione della polvere nei diversi livelli di altezza. Inoltre, un piccolo recipiente diviso in due parti permette la separazione in ogni cassetto nelle parti sinistra, ovvero quella più distante dal primo lato dello stampo incontrato dallo scarpetta, e destra, quella più vicina. Un Indice di Segregazione ($S.I.$) è stato proposto per confrontare i risultati delle diverse prove.

I risultati mostrano come per ogni concentrazione la condizione di umidità ambientale (50% di umidità relativa) sia quella che più favorisce la segregazione. Nelle condizioni di bassa o alta umidità relativa l'insorgenza di interazioni coesive tra le particelle aiuta il mantenimento dell'omogeneità dopo il riempimento dell'orifizio.
L'andamento con la concentrazione è di più difficile interpretazione. L'entità dei fenomeni segregativi sembra essere mitigata aumentando la concentrazione di principio attivo, a meno che tale variazione non modifichi il comportamento della polvere. Tale evenienza dipende dalle sostanze adottate, il cui utilizzo deve essere quindi contornato da una caratterizzazione completa.
Lo stesso processo è stato analizzato anche tramite simulazioni DEM in condizioni di sistema riempito d'aria o sotto vuoto. Tale studio conferma come l'entità della segregazione diminuisca all'aumentare della concentrazione del principio attivo. La presenza dell'aria all'interno dello stampo sembra inoltre avere un effetto di rimiscelazione delle polveri in seguito alla formazione di vortici, riducendo la segregazione nelle polveri ad alto contenuto di principio attivo.

Contents

List of Figures

List of Tables

Nomenclature

Roman symbols

A	UV-VIS Absorbance	[–]
A_r	Archimedes number	[–]
$A_{i,j}$	Hamaker constant	[J]
d_p	Particle diameter	[μm]
d_{50}	Particle median diameter	[μm]
E	Attraction energy	[J]
F_{VdW}	Van der Waals force	[N]
ffc	Flow-factor	[–]
g	Gravity acceleration	[m/s^2]
H	Height in the die	[mm]
h	Particle distance	[mm]
m	Mass	[g]
m_{CAF}	Mass of caffeine	[g]
m_{DCPA}	Mass of DCPA	[g]
MW	Molecular weight	[g/mol]
q_i	Atomic density of species i	[atoms/cm^3]
R	Radius	[m]
$S.I.$	Segregation Index	[–]
V	Volume	[m^3]

Greek symbols

δ	Filling fraction parameter	[–]
η	Air viscosity	[Pa s]
$\lambda_{i,j}$	London constant	[–]

Φ	Density ratio	[–]
ψ_{eff}	Effective friction angle	[°]
ψ_{in}	Internal friction angle	[°]
ρ_i^*	Skeletal measured density of species i	[g/cm^3]
ρ_a	Solid density	[kg/m^3]
ρ_s	Air density	[kg/m^3]
ρ_t	Skeletal, true density	[g/cm^3]
τ_C	Cohesion value	[Pa]
ξ	Air sensitivity	[–]
ξ_c	Critical air sensitivity	[–]
ζ	Air sensitivity Index	[–]

Subscripts

a	Air
C	Cohesion
c	Critical
CAF	Caffeine
$DCPA$	Dicalcium Phosphate Anhydrous
eff	effective
i	species i
in	internal
j	species j
p	Particle
s	Solid
t	true, skeletal
VdW	Van der Waals

Acronyms

API	Active Pharmaceutical Ingredient
CAF	Caffeine
CFD	Computational Fluid Dynamics
DCPA	Dicalcium Phosphate Anhydrous

DEM	Discrete Element Method
LOD	Limit of detection
LOQ	Limit of quantification
PM	Perfectly mixed
PSD	Particle Size Distribution
RH	Relative Humidity
RM	Random packing
SEM	Scanning electron microscope

Introduction

Background

Tablets are the most common solid dosage form used in pharmaceutical industry for medicine delivery. A tablet is produced by compacting a powder containing a certain amount of an active ingredient mixed with other inactive excipients within a die. The active ingredient is the responsible for healing from diseases. The dosage provided by the pharmaceutical form must be exactly the one specified by the package leaflet, so a person itself or a doctor can easily take or prescribe the correct cure.
Powder handling in tablet manufacturing, mainly during the filling of the die, may lead to segregation of the initial mixed blend. This segregation phenomenon may provoke the active ingredient concentration of the tablet to differ from the required specification, but can more probably lead to a non uniformity of the different components distribution along the tablet. Since the total amount of active ingredient in the produced tablet still remains the formulated one, this event does not compromise the effectiveness of the pill, but the differential distribution of its components can leave unbalanced residual forces within the tablet after the molding, prejudicing its structural stability.
The entity of segregation during die filling depends on several factors, both on powder characteristics and on die geometry and filling operation conditions. In particular, segregation driven by density difference is still a not clarified problem, since it is usually concealed by other factors, such as size differences.

Objectives and challenges

This research aims to:

Quantify the segregation extent caused by density differences
Despite density difference has been often neglected as segregation causing factor, focusing rather on size differences, it may have an important role which needs to be analyzed. All other factors must be removed, producing a mono-dispersed powder mixture, extracting from the commercial powder the desired fraction. The size ratio between the two components must be small. The density ratio must be kept similar to the used pharmaceutical values and it must be possible to analyze the powder mixture concentration.

Find the conditions that favor the rising of segregation phenomena
Different concentrations and different relative humidity conditions will be analyzed, in order to obtain a view of the phenomena that influence the segregation occurring in powder handling. The observations must be quantified and explained, relating the behaviour of the powders to their characteristics, specifically or regardless the die filling process used in the experiments.

Compare the results with DEM simulations
A similar analysis can be performed with computer simulations. Die filling process can be simulated, maintaining at least the die aspect ratio. These tests may be useful to understand the experimental powder behaviour.

Layout of this thesis

Chapter 1 - Literature review
A dissertation on the theory required to understand the analyzed problem and the obtained results is summarized in this chapter, integrated with the results found in literature about die filling or aspects referable to parts of the experiment, which can, together, help to understand the whole process.

Chapter 2 - Experimental set up
This chapter collects all the information about the used powders, how the mixtures are prepared and the procedure to analyze the concentration and the flowability of the experimental samples. The die filling device set up, including the taken operational choices, such as the shoe filling height and its velocity, are here explained.

Chapter 3 - Experimental results
Diagrams of the experimental results are shown in this chapter. The description of a Segregation Index, a parameter to represent the entity of the segregation that has occurred during die filling, is presented. The choice of the tests for data analysis is explained.

Chapter 4 - DEM Simulations
After a small digression on the theoretical and literature background on DEM simulation, in particular on die filling processes, the adopted system is presented. The results obtained from the simulation are reported and compared with the experimental results, commented in their similarities or differences.

Conclusions
Thank to the evidence clarified during the results discussion, some conclusions are drawn, to summarize the outcome of this project.

Chapter 1

Literature Review

1.1 Granular material

Particle technology is aimed at the analysis of discrete, usually solid elements, attempting to explain how the single particles characteristics and environmental conditions affect the bulk powder behaviour [66]. The knowledge of this kind of correlations will permit the prediction of the collective properties, allowing a more refined design of production processes.
Many industrial processes require the manipulation of granular materials. Unit operations involving particles handling are widely present in pharmaceutical industry, in food and cosmetics production, ceramics, metallurgical sector, mining, coating and plastics [22]. The final product properties are affected by a whole range of process and material variables, while a product standard quality must be always guaranteed [9, 20].
Despite their large use in industry and the increasing attention in research, the understanding of granular materials behavior is poor and predominantly empirical. The difficulty of particles characterization leads to very specific, application-oriented studies, permitting only some partial and not exhaustive conclusions in the general vision.
Working with granular material means to handle a large number of discrete particles. Moreover they cannot be treated neither as a liquid, despite in some circumstances they can flow, nor as a solid, though they can show both resistance to deformation or elasticity, nor as gasses, nevertheless they can eventually be compressed.
Differently from all the other states of matter, granular material is affected by segregation. It compromises the blend homogeneity, which is usually adopt as the main quality parameter in industrial powders production and must comply with rigorous standards. For this reason, this is a severe problem, which derives from the particles tendency to de-mix under shear or external excitation, based on differences in particle size, density, shape or surface properties.
This situation is even worse since it can be undetectable during the laboratory research and also in the pilot scale, where the amount of treated powder is relatively small and all the procedure are carried out in a systematic and controlled way, to appear evident later at production scale. The contrast between the large amount of the required powders blend in the industrial reality and the small length-scale in which particles interactions operate leads to the arising of phenomena, such as segregation, stagnant zones, unwanted granulation and compaction, that may hinder or totally avoid an efficient and high quality production.
An universally accepted continuum description for granular material behavior has not been developed to date. Many experimental difficulties arise during laboratory research, due to

the smallness of the particles, the particle size distribution (PSD) in the assembly and their different characteristics, which prevent to discern phenomena contributions and make the tests inaccurate.
It is common practice the usage of empirical relations obtained by trial-and-error approach [7, 56], which are usually applicable to specific working conditions with some approximations.
More recent works try to simulate the particle processes through computational simulations of the particle dynamics, combining the discrete elements method (DEM) and computational fluid dynamics (CFD). These techniques are obtaining good results in terms of reliability and they are often validated with experimental results with a good approximation [12, 22, 23, 29, 79, 80].
The advantage is to simulate the granular behavior at the particle scale, providing information of trajectory and forces acting on every single particle.

1.2 Cohesion

Particles are commonly distinguished between cohesive and free-flowing, according to their flowing behaviour. The determination of powder flowability in process and units design and choice is important, since different powders may behave in opposite ways and the feasibility of their handling largely depends on this parameter.
Particles flowability is affected by different factors related to their size, material and shape, but also to the particular process aimed to powder handling and the conditions in which it will be performed. A large amount of studies in the past was directed to understand cohesionless materials, both for the relative easiness of handling [44] and their industrial importance. Their high tendency to segregate can compromise product quality, explaining the large attention received. Recently, attention were moved to material at a smaller length-scale, in which cohesiveness arises as a consequence of particles interactions. These phenomena occur since inter-particle (cohesion) and particle-wall (adhesion) interactions dominate on gravity effect. Particles interactions derive from Van der Waals, electrostatic and capillary forces.

1.2.1 Free-flowing and cohesive particles

Inter-particles interactions are negligible in the case of dry, relatively large particles. In this situation, particles flow is controlled only by inertial, gravity effects, due to their size and mass, and mechanical and aerodynamic factors, due to non spherical shape.
With particles size decreasing, particles interactions become more evident and the flowability of the powder differs from the free-flowing behaviour. As practical consequence, finer powders become difficult to disperse, to remove from walls and tend to aggregates in clusters [4, 8]. For these reasons, manipulation of very fine particulates becomes difficult and their classification may be very inaccurate. The responsible of dry particles cohesion and adhesion are Van der Waals and electrostatic forces.

1.2.2 Van der Waals forces

Van der Waals interactions are originated from induced polarization mechanisms in electrically neutral material. Since it is a short range interaction, also denoted as contact force, it is very sensible to the microscopic structure of the particles surface. In this regard, surface roughness play a major role in inter-particles interactions, because it may keep two

particles apart. Even a small distance between the particles leads to a drastic fall of the effectiveness of the Van der Waals forces [46].
The quantification of Van der Waals force have had a long story all along the last century. Since their first determination [74], Van der Waals interactions between atoms and molecules were indicated for their non ideal behaviour. Nevertheless, molecules were still considered as static dipoles, assumption that does not explain the presence of this sort of interaction also in non intrinsically magnetic materials. Treating dipoles as dynamic systems, the interaction between two particles becomes strongly dependent on the proximity of these [46]. If they are very close, they are instantaneously turned in phase, resulting in an attraction force between them. Increasing the distance between the two particles, this movement is retarded, due to the establishment of a smaller interaction. The consequence is an out-of-phase oscillation, which leads to a dispersive effect. Because of this damping effect, the attraction between the two particles is lower and lower, increasing their distance. The attraction energy, in vacuum, is:

$$E = -\frac{\lambda_{i,j}}{h^6}; \tag{1.1}$$

with h the distance and $\lambda_{i,j}$ the London constant in the two atoms case, which is function of their atomic number. Due to the strong effect of distance in Van der Waals interaction, it appears evident how surface characteristics may determine important consequences in powder flowability.
These considerations, which describes the interaction of two atoms, can be enlarged to microscopic particles composed by multiple molecules. The overall attraction energy, assuming as additive the effects of interactions, is:

$$E = \frac{-\int\int q_1 q_2 \lambda_{12} dV_1 dV_2}{h^6}; \tag{1.2}$$

with q_1 and q_2 atomic densities ($atoms/cm^3$). This approach is known as the "microscopic approach". Hamaker solved the non-retarded Van der Waals force:

$$F_{VdW} = \frac{\delta E}{\delta h}; \tag{1.3}$$

in the cases of regular, perfectly smooth shapes.
Considering two rigid, smooth, spherical spheres at a distance d, Hamaker obtained the following equation [25]:

$$E(d) = -\frac{AR}{6d} \tag{1.4}$$

obtaining equations with R = reduced radius and $A_{1,2} = \pi^2 q_1 q_2 \lambda_{1,2}$ the Hamaker constant, which is specific for the single material in its medium.
The adhesion force of this particular case is:

$$F_{VdW}(d) = \frac{dE(s)}{ds} = \frac{AR}{6d^2} \tag{1.5}$$

According to this equation, it is evident how the adhesion force increases reducing the distance between the bodies. Moreover it should arise to infinite values at zero distance, so approaching the contact between the particles. This is clearly not physical, thus Eq. 1.5 is valid only since a certain nearness. Under that value, electrons clouds contrast adhesion forces leading to a strong repulsion. The value of $1.65\ 10^{-10} m$ was estimated as a good threshold, in accordance with experimental measurements [28].

In the case of rough surface, moreover, the approximation of perfect additivity in not completely valid. This is called the "macroscopic approach" [45].
Van der Waals forces decrease with humidity since it acts as a medium, screening the interaction between the two particles. Mathematically, the Hamaker constant is lowered since it must consider the presence of a third medium.

1.2.3 Electrostatic forces

Van der Waals interactions are contact forces inherent to every material. Differently from these, electrostatic forces are long range interactions which may arise in many ways during particles handling. The most frequent occurrence is contact charging, by which two electrically isolated surfaces touch and separate, determining an electric exchange between the two particles. Triboelectric charging occurs if a frictional component is added to the contact charging [49]. Electrostatic interaction may also be intentionally inducted by applying an external electric field [17].
These are common consequences deriving from frequently performed operations, such as milling, pneumatic transport, sieving or mixing. Hence, all industrial application involving powder handling must face its electrostatic charging, both in term of processability of the treated material and eventual risks arising [19].
Several practices may be adopted to counteract the onset of electrostatic charging. The machinery may be ground to avoid the electrical charge of the powder during its manipulation [35]. Placing for some time the treated, electrostatic powder in a grounded bin may help reduce the accumulated charge. Since the charge transport within the insulating powder bulk is poor, grounding the bin can enhance the electric discharging only if the material is well dispersed. It can be done only with little amount of particulates and it is also difficult to do in continuous operations. Otherwise, the only option is to directly ground the powder bulk, inserting more electrodes into it [34].
Although the correlation between material properties and electrostatic forces arising is still not totally clarified, some experimental evidences indicate their general effect [31].
Surface resistivity determines the level of exchanged charge between two particles after a collision. Moreover, an higher resistivity implicates increased strength and longer persistence of electrostatic effect. Material resistivity is affected by environmental humidity.
Controlling the shape that the particle will assume is a difficult task. Also, producing particles with a narrow shape distribution, even better with a constant high sphericity, is often impossible. Nevertheless the effect that irregular shapes or irregular shapes distribution have on industrial processes is huge. The consequence is a difference in electric charge distribution in different shape particulates.
Also morphology has an important role. Irregular particles have an unbalanced distribution of the charge along the particle surface, differently from spherical particles, and are more easily subject to friction charge. Roughness also amplifies the heterogeneous distribution of the electric charges on the particle surface, since they tend to concentrate on the peaks of the uneven surface. Hence, asperities increases rough particles specific surface, giving them higher dispersive surface free energy and higher moisture sorption capability than smooth particles [39].
Both electrostatic and Van der Waals forces are affected by the relative humidity. Moisture sorption is the capability of a particle to adsorb water vapour from air, until a dynamic equilibrium is reached. This phenomenon largely depends on the relative humidity of the environment in which the powder is placed [14, 21] its chemical intrinsic hydrophilicity/hydrophobicity and the specific surface of the particles. Electrostatic forces are affected by

the relative humidity since it decreases the surface resistivity [49, 57] and increases the conductivity of the surrounding air, enhancing the electric discharge [33, 53].

1.2.4 Capillary forces

Cohesion may also be induced by capillary forces, when the amount of liquid is high enough to permit the formation of liquid bridges between the particles. In this case, particles are bonded together by the capillary pressure and tensile force, forming agglomerations and significantly changing the flow behaviour of the powder [70]. The establishment of liquid bridges after liquid addition to powder increases cohesion and can prevent segregation in process operations.
Liquid bridges in wet granular materials are categorized in four degree of saturation, see Figure 1.1, depending on the amount of liquid added to the powder: pendular (a), funicular (b), capillary (c) and droplet (d).

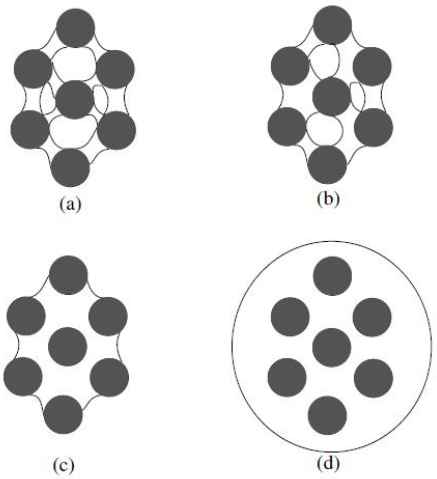

Figure 1.1: Degrees of liquid saturation [44]

Dry particles flow behaviour depends mostly on gravity and contact forces. The assumption in the pendular regime is considering a low liquid amount in the system that permits that each liquid bridge connects two and only two particles, but they are not interconnected each other. Liquid bridges bind the particles together through the surface tension of the liquid-air interface and the hydrostatic suction pressure in the liquid bridge, preventing them from moving independently of one another. Increasing the amount of liquid, bridges can enlarge or coalesce, touching more than two particles in once. Since they are still independent, so air is still present inside the agglomerate, this is called the funicular regime. Increasing more the liquid amount all the liquid bridges coalesce together, expelling all the air from inside the agglomerate, and the powder enters the capillary regime, in which the main factor of cohesion is the liquid-air interface suction. The last one is the droplet or slurry regime, in which particles are also dragged by the liquid.

1.3 Powder Mixing

In industry, the design of the process operations and of the machinery must consider the flowability of the powders blend to be treated. Different powders behave so differently that the equipment and the storage devices completely change their aspect. Since homogeneity

is the goal to maintain, any powder handling must be performed also avoiding or minimizing any segregative phenomena.
Flowability is not an univocally determined parameter in particles technology. Despite the concept is of primary utility in almost all the operations involving powders, all the available procedures can just give an indication of the powder flowability in the particular system in which it is analyzed.
Mixing is the operation to obtain a spatially uniform mixture from two or more ingredients. Usually, these must be as well dispersed as possible to permits to the biggest possible part of the production to satisfy the quality requirements.
Blend mixing is one of the most important process in an industry involving powders. Nevertheless, it is often very inefficient, because the knowledge of the physical phenomena governing solids mixing is not totally clear. Hence, evolution in the procedures and techniques is mainly attributed to trial and error mechanisms [56], act to solve somehow the problems of the previous ones [7]. Only a clear understanding of mixing and segregation phenomena will lead to the development of adequate methods able to guarantee the final homogeneity of the product.
There are three different mechanisms of mixing in granular materials: convective, shear and diffusive (dispersive) mixing [58]. The grade of mixing depends also on the flowability of the powders. Free-flowing powders shows a greater tendency to segregate, which may compromise the operation. On the contrary, cohesive powders generally minimize segregation, but it may be difficult to reach the unswept corners of the mixer in which they lodge as dead spots.
Mixing of solids depends on local conditions, the determination of which is even more difficult the smaller is the particles size. Differently from liquid, in which the concept of well-mixed solution may be applied up to the molecular scale, the nature of solid materials prevents a similar definition, since a single particle is composed by only one ingredient [42]. For this reason, solid mixing needs another definition of well-mixedness. In industrial practice, it is important to guarantee the blend homogeneity in the smallest product scale handled by the costumer (a tablet, a pack,...). For this reason the definition of a *scale of scrutiny* is introduced. It is the minimum solids amount with which the samples can be compared and corresponds to the end use packed amount of product. Variations within the scale of scrutiny are not considered a problem in term of product quality, though it may cause severe mechanical issues [26, 58].

1.4 Tablet manufacturing

The safest and easiest method of taking a drug is through tablets. The dosage of every tablet is clearly specified, so it is difficult to overdose, and the ingestion of the pill is a simple procedure, which hardly leads to complications. Moreover they are compact, easy to carry dispense and storage. Hence, tablets are the most usual way in which people care for themselves.
A tablet is a compacted powder blend, which contains a specific quantity of API (active pharmaceutical ingredient), whose ingestion is addressed for the therapeutic effect, and other substances, excipients, intended to act for example as stabilizers, preservatives, diluents, binders and generally to adjust the release of the active ingredient from the pharmaceutical form.
As shown in Figure 1.2, direct compression in tablets manufacturing comprises three steps: 1) die filling, in which the tablet mold is fulfilled with dry powder by gravity or suction from a feed hopper or shoe, 2) compaction, to obtain a rigid product corresponding to a

calibrated dose of the medicine, and 3) ejection of the tablet from the die [78].

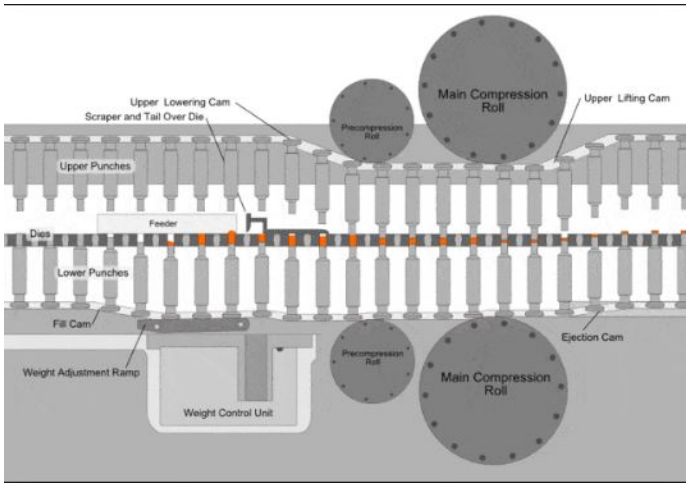

Figure 1.2: Tablet production scheme [1]

During compression, powder is subjected to high stresses by the compacting pressure of two punches, which causes an intensive deformation, both plastic and elastic. Three mechanisms lead to the bonding of the compressed particles [18]. In this situation particles are so close together that Van der Waals forces act consolidating them, according the intermolecular theory. Moreover, particles may be mechanically interlocked. According the liquid surface film theory, the energy of compression causes the fusion or the solubilization of the particles contact surface. After the pressure release, solidification of the material keeps the particles bonded through solid bridges. In this stage the volume of the powder blend is reduce, increasing its density.
The resulting tablet characteristics vary depending on powder compressibility, the ease of a powder to be reduced in volume under pressure, and the compactability, the ability of a material to be formed in tablet of a specific tensile strength.
The displacement of the punches, preceding the ejection of the tablet from the die, causes a decompression, followed by tablet relaxation. This permits the recovery of the elastic compressing strain by the tablet, which partly increases its volume and so reduces its density.
Assuming the starting powder blend uniformly mixed, any difference in the tablet drug concentration detected means that segregation has somehow occurred. Die filling, starting from the moment in which a part of the powder blend is separated from the bulk to be delivered into the tablet mold, during all its filling, is indicated as the critical stage controlling product quality, so the uniformity of concentration in different tablets [80].
Differently, powder compacts properties, such as the mechanical stability, depend on the powder behavior in all of the steps [10].
The role of flowability is of paramount importance either in tablet weight, since it determines different packing fractions within the die, or in tablet strength and drug dosage, because it can favour or avoid segregation during handling.
Die filling and compaction processes may lead to mechanical instability in the produced tablet, that manifest themselves in defects as capping [13] or lamination [50, 51], as visible in Figure 1.3.
Altough they are generally not distinct from each other, they are very different events with different causes. The highlighting of overlapped fractures parallel to the compressing punch face is called lamination, while capping is the following splitting of the top or the bottom

lid of a tablet from its body, which may occur also not during the formation process [18].

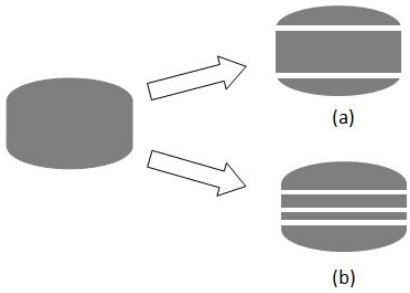

Figure 1.3: Tablet capping (a) and lamination (b)

Several factors concur to determine lamination or capping, such as air entrapment [18, 50], tablet thickness [50], mechanical anisotropy [3, 76], the velocity of recovery of the elastic strain before ejection [76].
The onset of these defects is due to the formation of shear bands during the unloading phase [77]. Shear bands pattern largely depends on tablet shape [76], tablet anisotropy and powder flowability.

1.5 Segregation

All the granular materials are in reality a mixture of particles varying in size, shape, density and surface properties, however small the range of variation is. Under certain condition, these differences may favor segregation, the phenomenon in which particles having the same properties gather together from the rest of a homogeneous mixture. This fact seriously affects the blend uniformity and must be detected and avoided to improve efficiency and quality in all the industries in which the mixing of powder is a crucial quality factor [22].
In particular, in pharmaceutical industry, segregation may lead to variation in compounds concentration from tablet to tablet, which may result in the undesired administration of a wrong dosage of the active ingredient to patients, with all the possible side effects [36], or structural issues in the tablet [13, 50]. Difficulty in maintaining the homogeneity in the product binds pharmaceutical industry to keep the traceability of all different batches, precluding a more efficient continuous mixing route [26].
Segregation is intrinsically caused by the handling of the powders [38], so every industrial process involving it must be carefully designed. During the last decades, several studies focused on some pieces of equipment to understand and solve the occurring segregation mechanisms. Loading and discharging of hoppers received a conspicuous interest, since it is an obligatory step in large production [15, 16, 37, 62, 72], as well as storage [55] and conveyance.
Segregation is found to occur through a total of thirteen different mechanisms [36, 69]:

Rolling: the mechanism by which large and rounded particles roll down the slope during the heap accumulation;

Sieving: the mechanism by which finest particles fall through the interstitial space of rolling or sliding layers of coarser particles;

Push-away: the mechanism by which falling heavy particles push away lighter, equal-size particle from the apex of the heap during its formation;

Angle of repose: this mechanism is caused by different angles of repose when powders of different materials are sequentially stratified. The component with lower angle of repose tends to flow over the component with an higher one, especially during filling operations;

Percolation: the mechanism characterized by a net down-flow of small particles through the gaps in the net of the coarser ones, due to vibrations or localized shears;

Displacement: the mechanism by which vibrations may lead to the rise of the coarser particle to the surface of a small/big particles mixture. Vibrations make the big particles jump, leaving a small gap under them which can be rapidly occupied by the small particles, segregating them in two layers. This phenomena is commonly called the Brazilian Nuts effect [41, 68];

Trajectory: the mechanism by which smaller, lighter or more angular particles are hampered by air frictional effects more effectively than heavier ones, due to their lower inertia;

Elutriation: the mechanism by which lighter particles are dragged by the air currents formed during the powder handling. The extent of this phenomenon is strictly related to the handling process itself;

Fluidization: the mechanism that maintains the lighter or finer particles component on the top of the powder bulk, during powder handling;

Impact: the mechanism by which particles with higher coefficient of restitution bounce further than the other ones from the surface of a heap;

Concentration driven displacement: this mechanism is typical in rotating systems, in which fine particles tends to gather together due to their higher mobility;

Agglomeration: the mechanism by which very fine particles stick together forming larger agglomerates with an higher flowability;

Embedding: the mechanism by which heavier or bigger particles penetrate into the surface of lighter particles and become locked there. It is an inertia driven mechanism.

These phenomena can be better summarized into three key mechanisms considering the others as infrequent or subsets of these: sterical effect, inertial effect and air drag effect.

Chapter 2

Experimental set up

In this chapter the preparation of the experiments is explained in all the solution adopted for the tight constrains to respect in order to perform this particular research. After a view on the materials and the powder characteristics and analysis, some preliminary observation on the die filling process are reported.

2.1 Purpose

Tablets are usually prepared starting from dry powder at wanted API concentration, which is then compressed into a mold to get the final form at exact weight.
The most common pharmaceutical device for tablet manufacturing consists in two parts. An upper rectangular or circular box (called shoe), refilled in turn by an hopper, which aims to provide a constant amount of powder over the lower part. This section must provide an high level of mixing, so one or more impeller can be present to maintain the powder mixed and in motion. The second part of the device is formed by a rotating plate which contains a row of dies. The relative velocity between the two part of the machinery is maintained constant to guarantee the complete filling of any die, which will lead to a constant tablets weight. The adopted shoe velocity in common operations in the pharmaceutical industry is in a range of $50 - 450\, mm\, s^{-1}$, usually around $100\, mm\, s^{-1}$[79]. Once the die is fulfilled, two punches compress the powder within the die and then the final tablet is ejected to be packed.
The final product properties depends on all three the procedure's steps, die filling, compression and ejection. Although this fact, die filling is pointed as the most influencing step to cause quality and mechanical issues in the final tablet [80].
The experiments to perform are studying the effect of density difference in the binary powder mixture during die filling, varying the concentration of API and the relative humidity conditions in which it is stabilized.
What this study may provide is the arising of segregation in the binary blend during the procedure. The establishment of this eventuality may lead to serious problems in the production, forcing to the discard of the final anomalous product. Since the die filling considers the obtaining of a tablet only, so under the scale of scrutiny, eventual detected segregation will not mainly affect the product API concentration. A little variation in the concentration of API in the total tablet may be present do to segregative phenomena during die filling occurring between the die and the shoe or even within the shoe, but this is not a main factor in continuous tablets manufacturing. Anyway, also considering the total API amount inside a tablet to be correct, segregation within the tablet may lead to unwanted effects. Different spots of the tablet may react differently to external stresses,

for example during the compression step, due to an internal anysotropy. Moreover, some residual strain may be maintained after the decompression step and relaxation may happen in a differential way along the tablet. All this facts may induce defects within or over the tablet surface, like cracks or fractures, which can extend leading to the development of defects as lamination or capping.

2.2 Experiment

2.2.1 Experimental apparatus

A model of the shoe filling device, shown in Figure 2.1 is used to perform the experiments. The moving shoe is a rectangular shape box, pulled by a pneumatic system, which is remotely controlled and can move at different velocities, from 0 to 1000 $mm\ s^{-1}$. The shoe is 150 mm long and 30 mm wide.

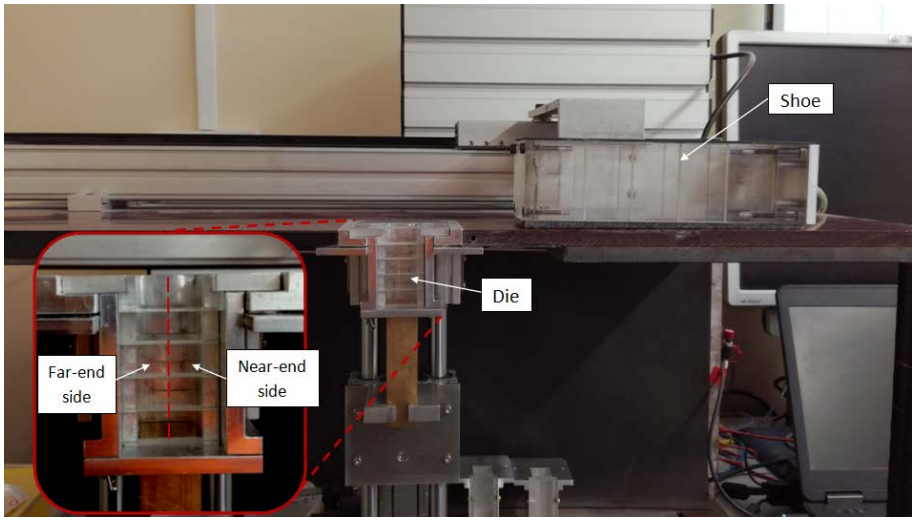

Figure 2.1: The die filling device with detail of the die

The movement of the shoe consists in an initial high acceleration, from right to left. Then a constant velocity is maintained while the shoe pass over the die. After it the shoe rapidly decelerates and stops.

(a) *Die drawers*

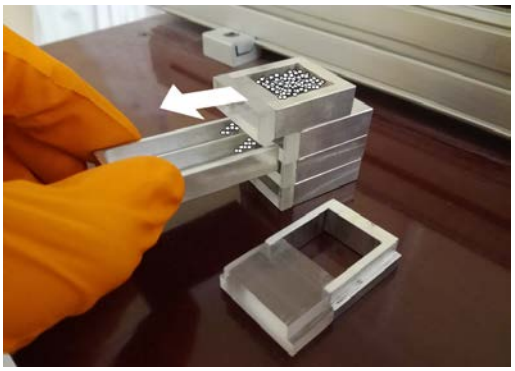

(b) *Sample proving procedure*

Figure 2.2: Die drawers and extraction procedure

The die has a square section with 20 mm of side and is 50 mm high. For the scope of this analysis, the die is divided in five drawers, Figure 2.2.a, each of them can be extracted singularly to probe the different layer powder. Also, every probe is then divided into the left part, the *far-end* side since the shoe moves from right to left, so it starts to surmount the die from its right side, and the right part of the die, the *near-end* one, and the procedure to separate them is represented in Figure 2.2.b.

2.2.2 Materials

The considered powder is a binary blend of caffeine (abbreviated to CAF, provided by Sigma-Aldrich, *ReagentPlus* purity grade) and dicalcium phosphate anhydrous (DCPA, provided by MiSC dispense) at different conditions.
Caffeine, also called 1,3,7-trimethylxanthine or with the IUPAC name 1,3,7-Trimethylpurine-2,6-dione, is a common alkaloid active pharmaceutical ingredient belonging to the methylxanthine class. The molecular formula of caffeine is $C_8H_{10}N_4O_2$, and its molecular structure is shown in Figure 2.3.

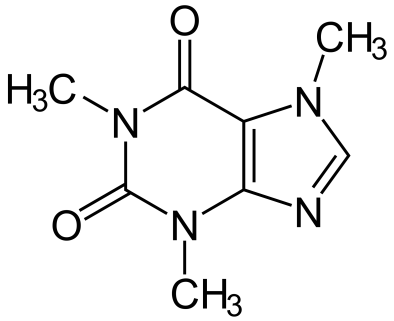

Figure 2.3: The molecule of caffeine

A number of plants are natural sources of caffeine or similar methylxanthines molecules: coffee beans, tea leaves, kola nuts, guaranà, yerba mate leaves.
Caffeine is a stimulant of the central nervous system (CNS), commonly used for its mental alertness effect, concentration, wakefulness and decreasing of reaction time. Caffeine is completely absorbed by the small intestine within 45 min from the ingestion or thought the oral mucosa and distributed throughout the body water to all bodily tissues. Since it is both lipophilic and hydrophilic, it can easily cross cell membranes including the brain. The peak of plasma concentration is reached between half an hour and two hours and its elimination half-life in an healthy adult is about 5 hours. The LD_{50} of caffeine in humans is estimated to be $10 - 15\ g$ ($150 - 200\ mg/kg$ of body mass). Caffeine intoxication due to an over-dosage can cause unpleasant symptoms like irritability, restlessness, insomnia, headaches, and tachycardia. Caffeine clearance required time is affected by environmental and physiological factors, such as smoking, pregnancy, use of oral contraceptives and alcohol assumption. Continuous use may provoke tollerance and addiction.
Its primary stimulatory mechanisms is the blocking of adenosine receptors and inhibition of phosphodiesterases, increasing blood pressure and basal methabolic rate.
Most important characteristics of caffeine as regards the purposes of this research are summarized in Table 2.1. If not differently specified, values are considered at room temperature and atmospheric pressure and are taken from the caffeine supplier data sheet, Sigma-Aldrich, or found in literature [54].
The measured density (ρ measured*) value is the skeletal density of the monosize fraction

Table 2.1: Properties of CAF

Parameter	Value	Units
colour	white	
form	crystalline	
	powder	
odour	odourless	
taste	slightly bitter	
MW	194.19	g/mol
ρ	1.23	g/cm^3
ρ (measured*)	1.46	g/cm^3
water solubility	16 at 20°C	mg/ml
	200 at 80°C	mg/ml
	666 at 100°C	mg/ml

of the powder, obtained using a Helium pycnometer,the *Accupyc* II 1340, Figure 2.4, by Micromeritics. The one reported is the mean value of ten measurements.

Figure 2.4: The Accupyc pycnometer

The skeletal, true, density value is given by:

$$\rho_t = \frac{m}{V_t} \tag{2.1}$$

The volume of the solid is obtain as the difference between the reference volume chamber before and after the introduction of the sample.
Dicalcium Phosphate is commonly used as an excipient in the pharmaceutical industry, due to its good compaction properties. It is also adopted as a calcium source in nutritional supplement and it is a common toothpaste ingredient for its abrasive properties. Its molecular formula is $CaHPO_4$ and its structure is shown in Figure 2.5.

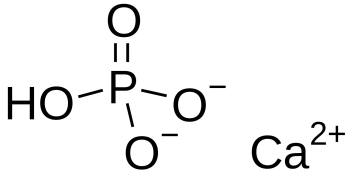

Figure 2.5: The molecule of dicalcium phosphate

Brittle fracture has been observed to be the main deformation mechanism of dicalcium phosphate. For this reason, DCPA tablet deformation is not sensitive to the applied strain-rate, but only to the strain itself.

DCPA can exhibit lamination and capping when compacted at higher pressures, mostly if the percentage of this material in the tablet formulation is high. These phenomena are independent from the rate of compaction. It can be partly mitigated through avoiding a deep concave shape for the produced tablets [61].

DCPA is stable and non-hygroscopic at ambient temperature. It does not hydrate to form the dihydrate.

Main characteristics of DCPA are summarized in Table 2.2. Also in this case, if not differently specified, values are considered at room temperature and atmospheric pressure and are taken from the calcium phosphate dibasic anhydrous supplier data sheet, MISC dispense, or found in literature.

Table 2.2: Properties of DCPA

Parameter	Value	Units
color	white	
odor	odorless	
taste	tasteless	
MW	136.06	g/mol
ρ	2.89	g/cm^3
ρ (measured*)	2.86	g/cm^3
water solubility	0.2 at $20°C$	mg/ml

The resulting density ratio between DCPA and CAF, using the measured values of the skeletal density, is:

$$\frac{\rho^*_{DCPA}}{\rho^*_{CAF}} = \frac{2.86\ g/cm^3}{1.46\ g/cm^3} = 1.96 \tag{2.2}$$

This is the density ratio for which the occurrence and the behaviour of an eventual segregation during die filling is analyzed. This value of density ratio is commonly present in most part of the pharmaceutical formulation.

Images at different magnification are reported in Figure 2.6. They are taken by a scanning electron microscope, the JSM-7100F *Field Emission Scanning Electron Microscope* by JEOL in Figure 2.7.a.

The signal analyzed by the instrument derives from the interaction between the electrons shot by an electron source and the surface of the sample. Non-conductive samples can be analyzed using a metallic coating. A sputter coating of $4nm$ of gold is applied over the powder particle, so the new conductive surface permits to the instrument to examine the morphology of the specimens. The image is rebuilt from the signal detected after the low beam penetration into the sample provided by the low voltage selected, in this case $5\,kV$.

As visible, both powders have very irregular surface, fact that confirms their observed high tendency to be electrostatically charged [31]. Their surfaces probably restrain finer particles which are quite impossible to remove with normal sieving, Figures 2.6.e and 2.6.f. Anyway, they are supposed to remain as an agglomerate along all the experiments, so they can be considered as a solid body.

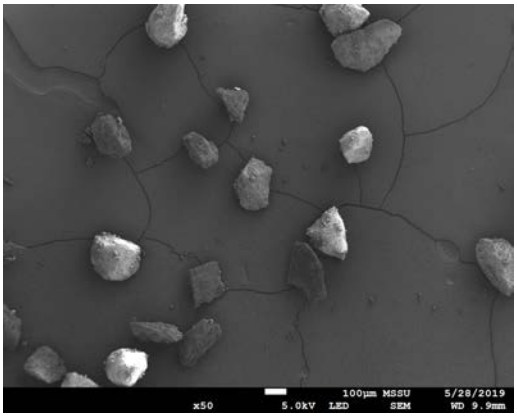

(a) CAF - 50x

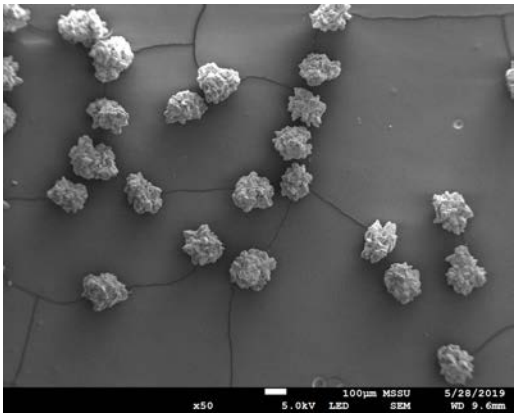

(b) DCPA - 50x

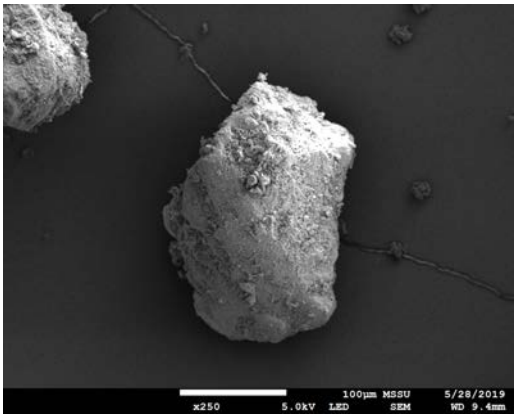

(c) CAF - 250x

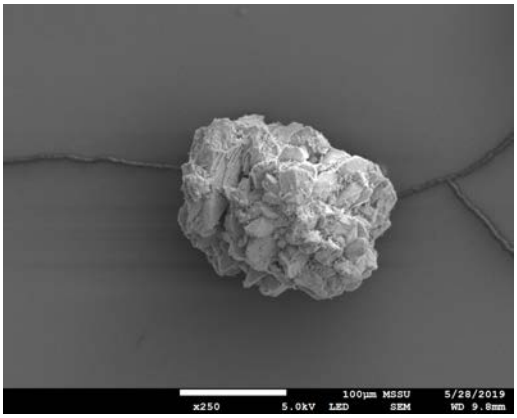

(d) DCPA - 250x

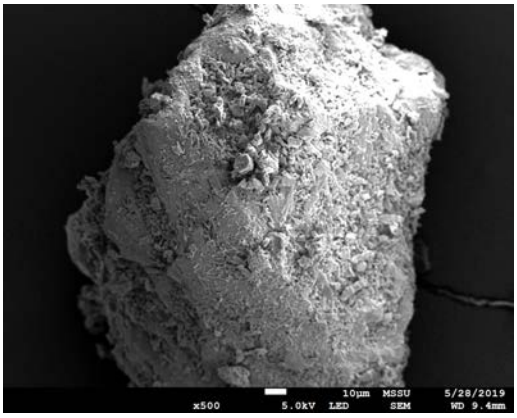

(e) CAF - 500x

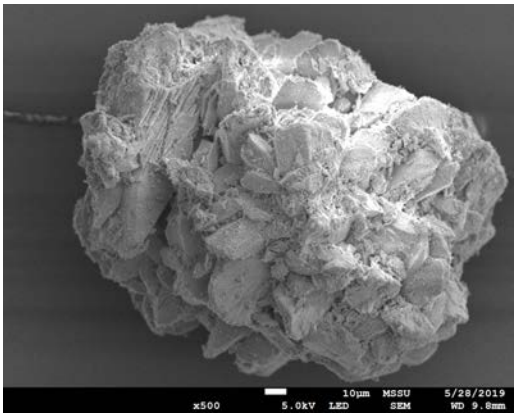

(f) DCPA - 500x

Figure 2.6: Images at different magnification of CAF and DCPA with SEM

(a) The JSM-7100F SEM

(b) The Retsch AS 200

(c) The Qicpic

Figure 2.7: Laboratory instruments

2.2.3 Preparation of the powders

Powder preparation is a critic part of the experiment. Since segregation is due to many factors, the aim of this step is to remove any other one of them that can hinder the segregation driven by density difference. In particular, size ratio, which is one of the main source of segregation during powder motion, must be kept lower than $D/d = 1.2$ for die filling [43]. Other values are found in literature, as $D/d = 1.9$ for hopper discharge [36] or $D/d = 2$ for sieving segregation [72], but the most conservative value was chosen as reference.
Both powders were sieved with a mechanical sieve, *Retsch AS 200*, in Figure 2.7.b, to obtain the fraction between the $150\mu m$ and $180\mu m$, according to the "$R\,40/3$ ISO 3310-1:2006" technical requirements table [2], and the resulting fraction were analyzed with the *Qicpic* by Sympatec, assembled with *Gradis* powder dispenser and *Vibri* components. The instrument set up is visible in Figure 2.7.c.
Some helpful properties are so obtained, as reported in Table 2.3.

Table 2.3: Characteristic parameters of CAF and DCPA

Material	d_{50} $[\mu m]$	Aspect Ratio (at 193.04 μm)	Circularity (at 193.04 μm)
CAF	207.16 ± 1.56	0.704 ± 0.011	0.847 ± 0.008
DCPA	195.73 ± 1.70	0.788 ± 0.002	0.787 ± 0.005

Approximating particles dimension with their respective d_{50} values, the resulting D/d is found:

$$\frac{D}{d} = \frac{d_{50,CAF}}{d_{50,DCPA}} = 1.058 \tag{2.3}$$

which is lower than the lowest required value found in literature.
Moreover, after an accurate sieving, the particle size distribution is narrow, as visible in Figure 2.8 (distribution is based on particles' volume).
Once prepared, the two powders are mixed together in a *Turbula* mixer, the 3-dimensional shaker mixer by Eskens shown in Figure 2.9.a, that works following the Schaltz geometry

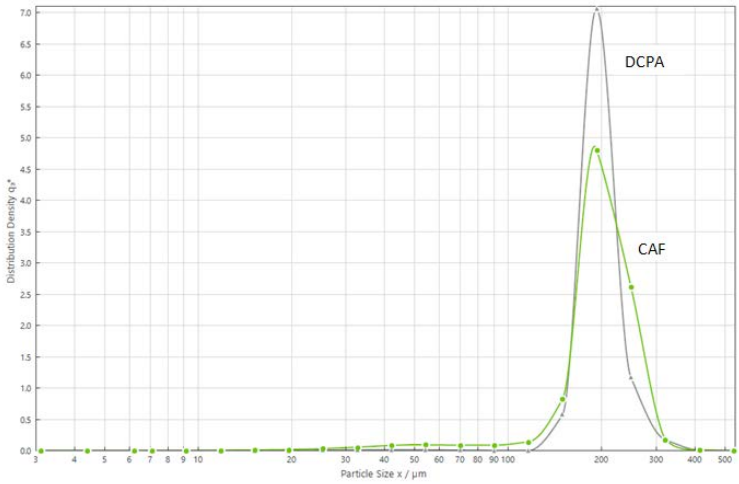

Figure 2.8: CAF - DCPA PSD comparison

theory. Three compositions are prepared, at 10%, 25% and 50% of CAF by weight. Mixing is performed at 22.4 min^{-1} for 10 min [59].

(a) The Turbula 3D mixer (b) The Humidity Chamber (c) The Moisture Analyzer

Figure 2.9: Other laboratory instruments

The result is a well-mixed, almost mono-dispersed binary blend at known composition. The final particle size distribution is a narrow peak at approximately 200μm, shown in Figure 2.10:
The cumulative distribution in Figure 2.10 reports also a little volume of fine particles, very difficult to be totally removed, and a little amount of bigger grains, which can depends both on non-perfect screening during the sieving due to the non-perfect sphericity of the particles and on an incorrect measurement by the *Qicpic*, due to a partial overlapping of projections of the particles on the instrument lens, which considers so a slightly bigger projected area. Anyway, since the distributions are based on particles' volume, the number of bigger particles is smaller than the perceived one from the graph.
At this point, the mixed blend are placed in an humidity chamber, *Climacell* by MMM Group, visible in Figure 2.9.b since their relative humidity is stabilized. Three humidity are imposed, at 20%, 50% ambient humidity and 80%, to analyze the effect of relative humidity on inter-particle interaction and so on die filling operation. The humidity chamber is set

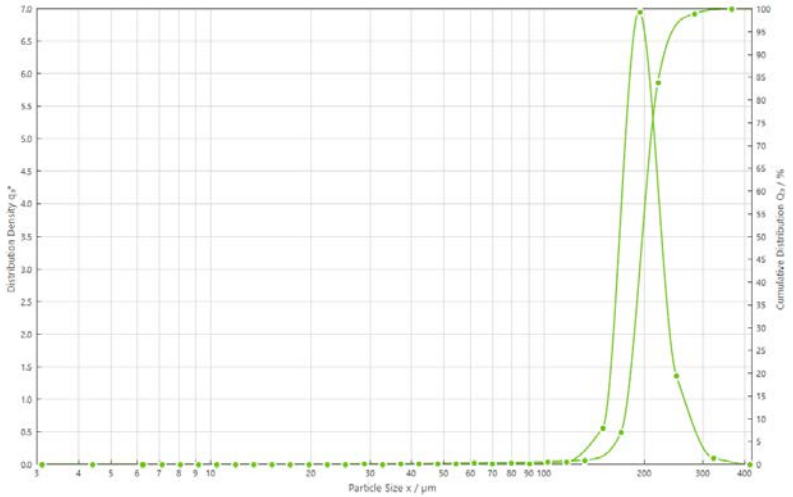

Figure 2.10: Final blend PSD

at the chosen relative humidity and at $23°C$, since the powder is stabilized (more or less one week for 50% and 80% of relative humidity, two weeks to dry the powder up to 20% of relative humidity). Powder humidity is measured with a moisture analyzer, the *Ohaus MB35* by Ohaus, in Figure 2.9.c, always placing approximately the same amount, $0.6g$, well dispersed over the sample plate. The analysis temperature is set at $105°C$.

2.2.4 Die filling set up

In this sections the procedure to conduct the experiments is presented, with all the considerations made and the choices taken to perform them in the most rigorous and reliable way possible. Some of these are strictly related to the specific instrumentation and powders used and to the particular research to be conducted. Anyway, they can certainly be adapted for similar studies at other working conditions.

2.2.4.1 Shoe filling height

Initially the shoe is filled at a constant height of powder (approximately $130\ g$). In this way, in every experiment the air pushed away from the die meets the same resistance passing through the powder [24]. An higher shoe powder height helps preventing nose flow [52], which will be better explained in the next paragraph. Air can exit the system by-passing the shoe too, through the little free layer under it, or, in the initial and final stage, through the free area between the die and the moving shoe side [22].

2.2.4.2 Shoe velocity

The velocity of the shoe is set in order to have a bulk flow in the powder discharging and complete die filling. At a low shoe speed, powder will show the so called *nose flow* [79], in which the first section of the shoe is completely discharged in the die as a landslip, causing an irregular emptying of the shoe and placing the upper part of the shoe bulk in the bottom section of the die. Increasing the shoe velocity, the powder mainly detached from the bottom of the shoe. This is the *bulk flow*, in which the formation of the nose flow is avoided by rapidly translating it over the cavity before any powder falls. If the velocity is too high, the filling of the die remains incomplete, causing an erroneous tablet weight and drug dosage.

The critical shoe velocity before incomplete die filling is calculated with the procedure reported by Wu [79]. A filling fraction parameter is define, as:

$$\delta = \frac{m_{sample}}{m_{max}} \tag{2.4}$$

At this point, several tests are performed increasing the shoe velocity and recording the mass of the powder which falls inside the die, m_{sample}. Since the die is completely filled up, the measured mass corresponds to m_{max}. The evolution of the filling ration is plotted and an exponential regression is made, visible in Figure 2.11.

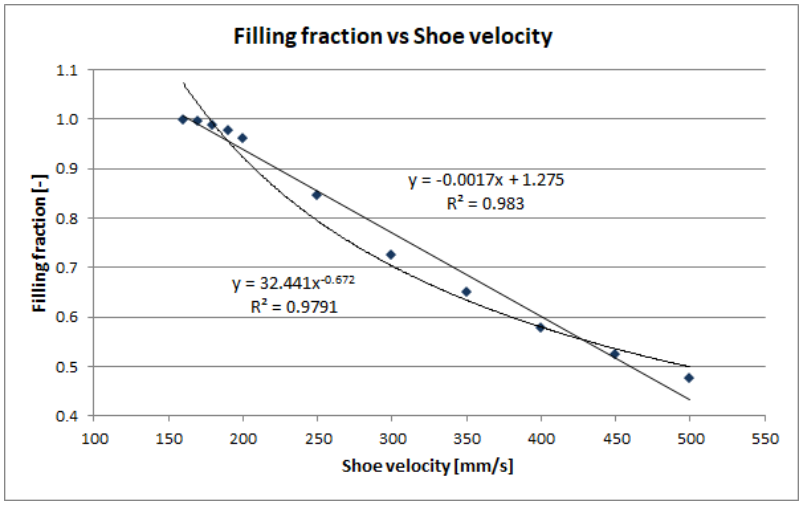

Figure 2.11: Critical velocity analysis

The exponential form provides the equation:

$$y = 32.44x^{-0.67} \tag{2.5}$$

Solving it in x and assigning to the filling ratio the value of 1, which corresponds to complete filling, the critical shoe velocity of 180 mm/s is found. Anyway, it is quite evident in the diagram that this method overestimate the result in this particular case. For this reason a linear regression is added, obtaining the equation:

$$y = -0.0017x + 1.275 \tag{2.6}$$

This equation permits to find a critical velocity of 161 mm/s, which is seems to be more correct.

Anyway, the shoe velocity of 150 $mm\,s^{-1}$ is selected, which seems to be a good compromise between avoiding nose flow and being sure of the complete die filling in any of this analysis condition.

Then the experiment is run and ten samples, far-end and near-end for each of the five layers, are probed. They are weighted in an analytical balance, the *Entris Analytical Balance Sartorious*, Figure 2.12.a, by Kern & Sons. The measured weight registered for the estimation of the CAF weight in case no segregation has occurred (so by considering maintained the initial blend composition), which will be later compared with the composition analysis result. Each experiment is performed three times.

(a) The Entris balance (b) The T.S. Evolution 201

Figure 2.12: The balance and the UV-VIS spectrophotometer

2.2.5 Concentration analysis

Powder concentration is measured using a *Thermo Scientific Evolution 201* UV-VIS spectrophotometer, in Figure 2.12.b, by Thermo Fisher Scientific, measuring the zero-order absorbance of CAF after diluting the sample in a solvent, following the procedure described by Sethuraman [65]. The sample is placed in a quartz cuvette with $10\,mm$ path length during the spectral measurements. The used instrument has a Xenon flash lamp as internal light source, which combined with an internal correction algorithm permits to the instrument to be reliable until $3.5\,A$. Several solvents and the relative absorbance peaks are found in literature for the caffeine. The DCPA presence, dissolved or not in the solvent, is not a problem since it is inert to the analysis. Since it is not dangerous, is largely available and permits the caffeine to be well detectable by UV photometry, Figure 2.13, distillate water is selected as solvent. The solubility of caffeine in water is high enough, Table 2.1, considering approximately $0.8\,g$ as the maximum amount of CAF in one single die slot with the maximum concentration analyzed. Different values of the absorbance peaks wavelenght are found in literature for CAF in distillate water: $270\,nm$ [65], $274\,nm$ [6, 54]. Otherwise, a preliminary analysis has highlighted the different value of $273\,nm$ at $10\,\mu g$ of CAF, as visible in Figure 2.13.

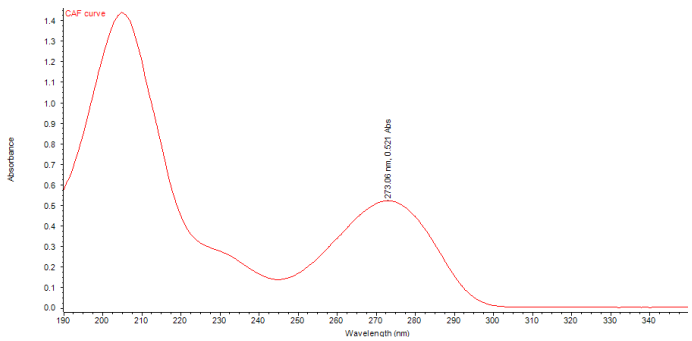

Figure 2.13: Caffeine absorbance peak with Thermo Scientific Evolution 201

2.2.5.1 Preparation of the calibration curve

Following tests permitted to conclude the linearity behaviour of the UV analysis over CAF concentration. For this reason, the method is considered reliable and a calibration curve, in Figure 2.14, is prepared, to relate the sample measured absorbance to its CAF mass content. This calibration curve relates data from solutions prepared from two different standard stock solution. The first of these is made by dissolving $0.0012\ g$ of caffeine in $100\ ml$ of distillate water in a $100\ ml$ calibrated volume flask, a *Fisherbrand* flask. The concentration of this stock solution is $1.2\ \mu g/ml$. Five solution are prepared taking $1, 2, 4, 6, 8$ and $10\ ml$ from this stock solution and fulfilling $10\ ml$ calibrated volume flasks, again by *Fisherbrand*. A second stock solution is prepared dissolving $100\ mg$ of caffeine in $100ml$ of distillate water, similarly as before. Then, $10ml$ of the stock solution are withdraw from there and diluted in another $100\ ml$ flask, obtaining a solution with concentration of $100\ \mu g/ml$. Four solution are prepared by dissolving $2, 3, 4$ and $5\ ml$ of this second stock solution in a $10\ ml$ flask. In this way, all the feasible range of caffeine concentrations detection can be exploited during the experiments. The table 2.4 shows the absorbance data at different caffeine concentration.

Table 2.4: Absorbance values varying caffeine concentration

$CAF[\mu g/ml]$	1.2	2.4	4.8	7.2	9.6	12.0	20.0	30.0	40.0	50.0
$A[-]$	0.063	0.131	0.252	0.363	0.483	0.609	1.039	1.557	2.055	2.551
$StDev(\cdot 10^4)$	4.29	13.63	8.10	8.86	3.72	43.20	7.80	3.04	73.48	25.25

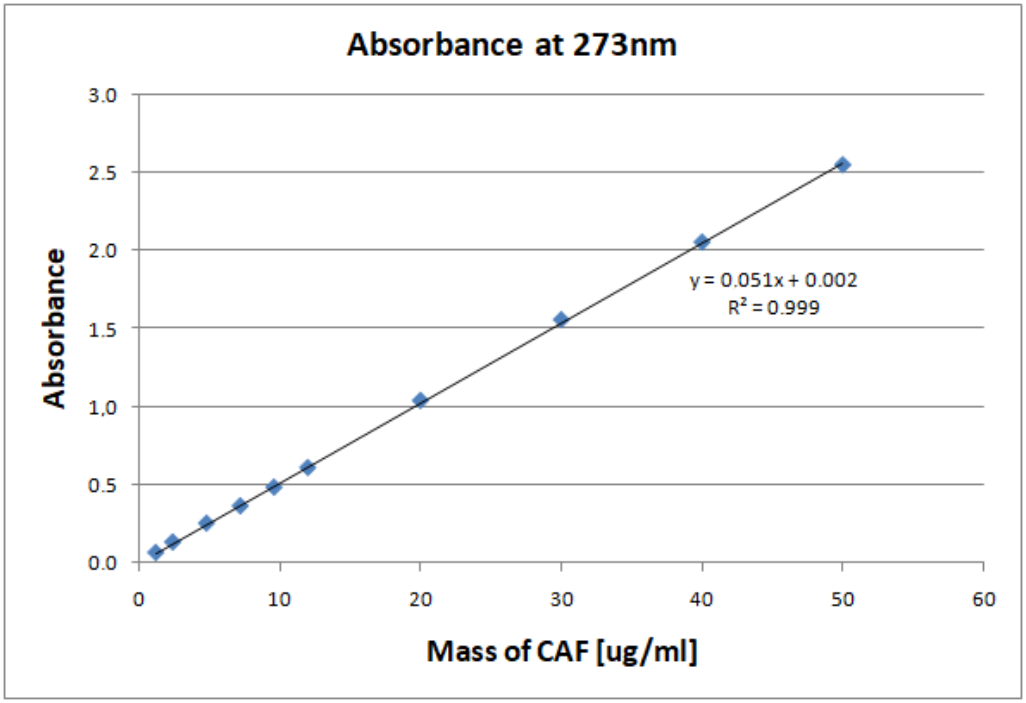

Figure 2.14: Caffeine absorbance calibration curve

A linear regression of the data permits to obtain an equation which is useful to calculate the amount of caffeine present in the sample solution from the signal detected by the

spectrophotometer:

$$A = 0.051\, m_{CAF} + 0.002 \tag{2.7}$$

It follows that the mass estimated in the single sample is:

$$m_{CAF} = \frac{A - 0.002}{0.051} \tag{2.8}$$

The approximation of the absorption data varying the caffeine concentration provide a very good linear dependence in the range between 1.2 μg and 50 μg, as testified by the nearly unitary value of the R^2 reported in Figure Fig.2.14.
Using calibration standards, the Limit of Detection, LOD, and the Limit of Quantification, LOQ, are calculated. LOD is estimated as $3.3s/S$ and LOQ as $10s/S$, with s the standard deviation of the response and S the slope of the calibration curve. The resulting values are:

$$LOD = 0.1238\, \mu g/ml \tag{2.9}$$

and

$$LOQ = 0.3715\, \mu g/ml \tag{2.10}$$

2.2.5.2 Samples analysis

The ten samples from the different die drawers are dissolved in distillate water in ten 100 ml calibrated volume flasks and handly agitated to favor caffeine dissolution. DCPA is insoluble in water, so an amount of powder remains in the bottom of the flask, avoiding to see any difference after the dissolution of caffeine. Anyway, at room temperature caffeine dissolves quite easily in these proportions. For this reason after a short agitation it is considered to be completely dissolved. After permitting to the not dissolved DCPA to settle down in the bottom of the flasks, a certain volume of the solution is withdraw using high precision volumetric pipettes. Since the measurement range for caffeine concentration with the UV-VIS spectrophotometer is limited up to 50μg, different dilution levels must be adopted for the different concentration samples. For 10% and 25% of caffeine concentration samples, 100 μl of solution are withdraw from the first flasks with a *Pipetman p1000* by Gilson, and diluted again in distillate water in 10 ml flasks. For the 50% caffeine concentration samples, 50 μl of solution from the first bigger flasks are withdraw with a *Pipetman p200* by Gilson, and diluted in distillate water in the 10 ml flasks.
At this point the final solutions are analized three times with the spectrophotometer. The results, which contain the detected amount of caffeine in the final diluted solution, are elaborated to obtained the real concentration in each die drawer and compared with the one estimated from the powder mass measured for that drawer considering ideal concentration of the powder blend.

2.2.6 Flowability analysis

The flowability of powder at any composition and humidity condition is analysized using a Schulze ring shear cell, the *RST-XS.s*, Dietmar Schulze shown in Figure 2.15.a. The low shear cell is used, *Type XS-Lr0 "low stress"* visible in Figure 2.15.b, in which the specimen volume is about 70 cm^3.

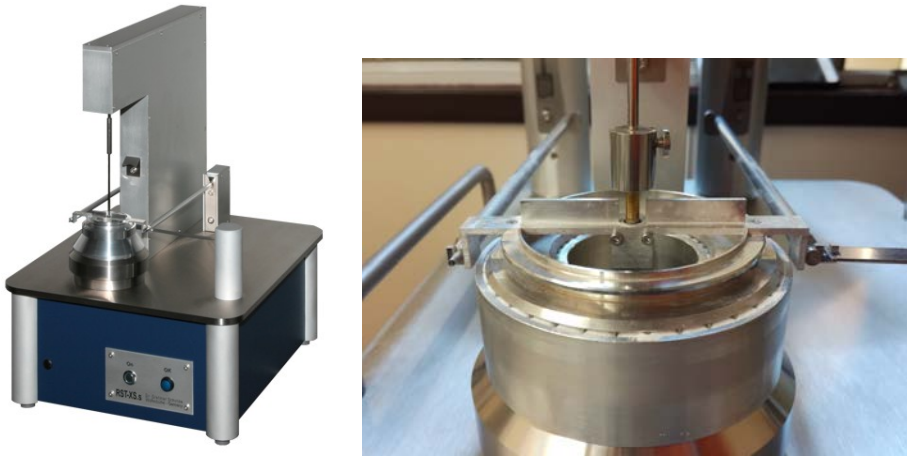

(a) RST-XS.s (b) XS-Lr0 "low stress" cell

Figure 2.15: The Schulze Ring Shear Cell tester

An initial normal preshear stress of 1000 Pa is applied. Then, any test is composed by five normal stresses ($100, 275, 450, 625, 800\ Pa$) to draw the yield loci, alternated by preshear stresses until steady state to erase the history of the material. The cohesion of each sample is extrapolated from the yield loci to zero normal stress. Every test is repeated three times and the mean value is considered. With this analysis, the flow-factor (ffc), the cohesion estimation (τ_c), the effective friction angle (ψ_{eff}) and the internal friction angle (ψ_{in}) are calculated.

2.3 Die filling observations

Die filling is a fast process which steps cannot be distinguished at naked eyes, but the possibility to see what happens is very important to have at least a qualitative understanding of the phenomenon and to relate the results to a precise behaviour.

2.3.1 Die filling mechanism

A series of photos, in Figure 2.16, captured with an High Speed Camera, the *Phantom UHS-12* Ultra-high Speed Camera by Vision research, AMETEK, provides a step by step vision of the die filling process, useful to detect more precisely what is happening in this fast operation. These pictures are taken using the 25% of caffeine powder stabilized at 50% of relative humidity and the set up is shown in Figure 2.17.

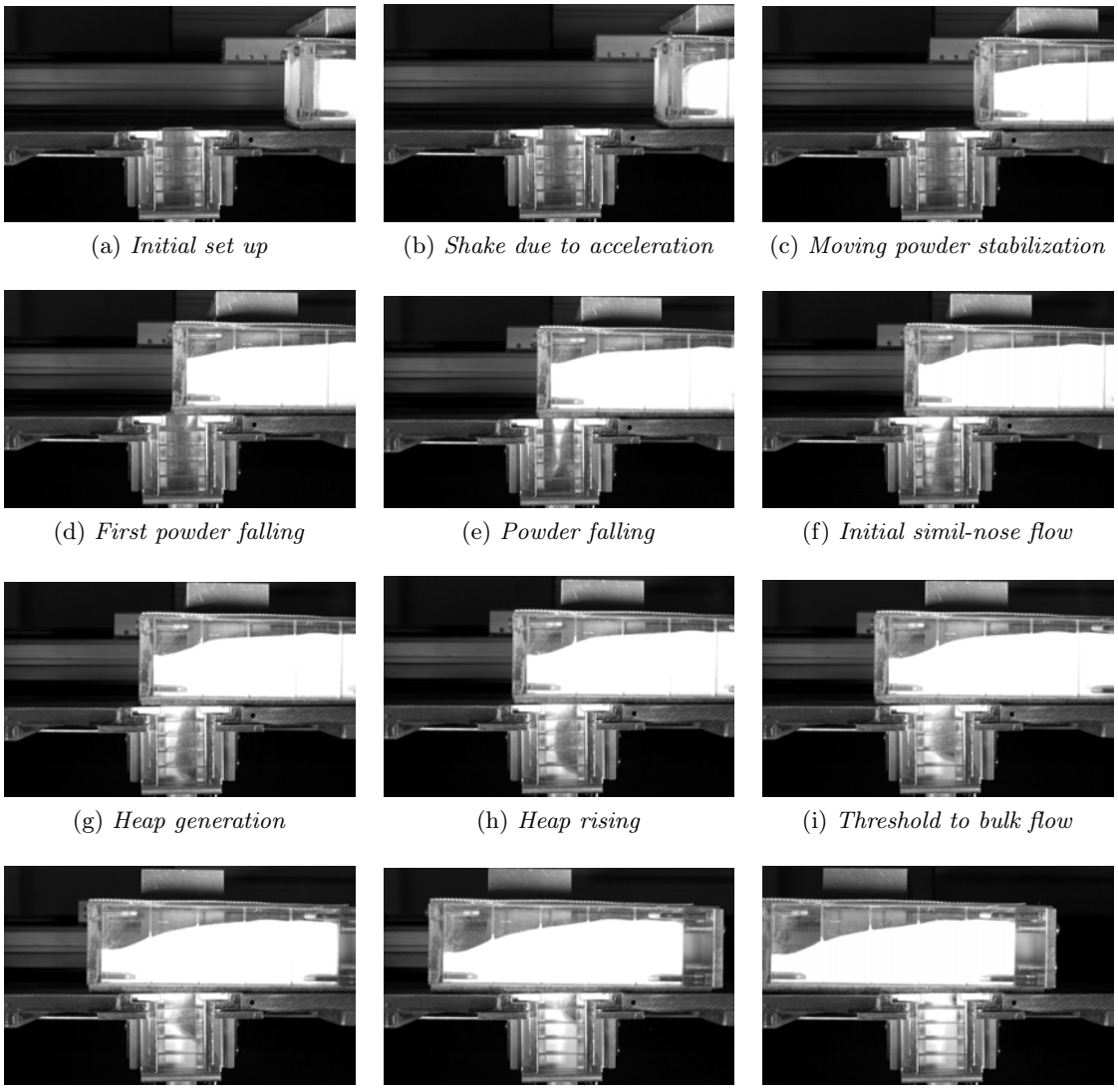

(a) *Initial set up* (b) *Shake due to acceleration* (c) *Moving powder stabilization*

(d) *First powder falling* (e) *Powder falling* (f) *Initial simil-nose flow*

(g) *Heap generation* (h) *Heap rising* (i) *Threshold to bulk flow*

(j) *Heap's rising* (k) *Heap touches the shoe bulk* (l) *Last moment before complete filling*

Figure 2.16: Die filling mechanism

Figure 2.17: The High Speed Camera

The shoe is initially filled with powder, Figure 2.16.a. The starting acceleration makes the powder consistently shake, Figure 2.16.b, until the velocity of the shoe reaches the regime speed, Figure 2.16.c. Then the powder shape inside the shoe stabilizes since it travels at constant velocity. When the shoe starts overhanging the die, the powder has a moment of inactivity and than starts falling, Figure 2.16.d. The flow at the very beginning is small and a little conveyed by the air flows in formation, Figure 2.16.e. Then a simil-nose flow establishes, pointed to the far-end side of the die bottom, Figure 2.16.f, due to its inertia. A complete nose flow, how described by Wu et al. [79], is avoided because of the geometry of the system, the aspect ratio of the die and the height of the powder filling ratio in the shoe. The simil-nose flow is not very sensitive to the presence of air inside the die, so its flux is only marginally penetrated by the forming air flows. In the bottom of the die powders particles bounce and deposit, until a heap is formed, Figure 2.16.g. Heap formation in this case can be divided in three steps. During the simil-nose flow it is formed mainly from the avalancing of the falling flux, Figure 2.16.h. Then, when bulk flow starts, Figure 2.16.i, powder falls from the bottom of the shoe. This kind of flow is much more sensitive to air presence, since they can easily penetrate inside the falling powder section and shape the powder flux. Inertia and drag effects are strongly present. The die is full by an air bag, which need to escape from it through the void spaces between the shoe and the surface or through the shoe powder bulk. The heap rising continues, Figure 2.16.j, until it touches the bottom of the shoe, Figure 2.16.k. After this point the section of the bulk flow diminishes, and so does the section free for air to escape. The air bag is shrunk until complete filling is reached, Figure 2.16.l.

2.3.2 Involved segregation mechanisms

During die filling, differences in size, density, superficial characteristics as well as die geometry, filling mechanism and conditions may induce segregation in the powder blend, causing non homogeneity within the tablet. Assured the API amount provided, such phenomena may lead to undesired effects, mostly represented by structural weakness and defects.
All experiments are performed at the same shoe velocity, $150mm/s$, which has been verified

to permit complete die filling in every condition of API concentration and relative humidity. The selected velocity of the shoe is not the critical one. This fact, added to the high filling ratio of the shoe, which is nearly fulfilled, has an important consequence in the die filling mechanism: the filling sequence can be divided in two different moments. The first one recalls the nose flow described by Wu et al. [79]. The height of the powder bulk in the shoe does not permit the formation of a proper landslide of powder, anyway, a consistent part of the front side of the shoe collapses into the die. After that, the die is filled by bulk flow, so powder from the bottom of the shoe gradually fills the die.
This die filling mechanism, considering only density as driving force for segregation, is subject to different segregation mechanisms:

Electrostatics: small size powders are easily charged electrostatically by handling, such as the mixing before the shoe loading. This means that every process must be performed carefully to avoid the particles to jump away and possibly vary the bulk concentration. Shoe filling is made after a short period of electrostatic relaxation, to reduce this eventuality.

Vibrations: during shoe acceleration, powder is strongly shaken back. Moreover, shoe movement is not perfect because of some friction in the mechanical guide. These events may induce a little segregation in the shoe, due to fluidization of the powder bulk.

Geometry of the system: powder falling is far to be uniform. The first step, in which the simil-nose flow happens, powder falls diagonally to the far end of the die. In this step inertial effect is very important, but is probable that also impact mechanism has a role. Then the bulk flow starts, powder is still mainly directed to the far-end side in the die bottom, but the formation of an heap forces the powder to slide down, filling also the near-end part. In this second part the rolling of falling particles over the heap in formation may have some segregation effects due to the different angle of repose of the two substances. The transition between the two flows as well as the magnitude of these segregation mechanisms strongly depends on the geometry of the die and partly on the characteristics of the powder.

Air effect: gravity die filling is largely affected by the presence of air. Powder falling produces flows of air that tries to escape the die. These currents drag the lighter particles up, separating them from the heavier ones. Moreover, the different inertia of the two substances causes trajectory segregation, since the heavier particles tend to be less affected by the presence of air.

2.3.3 Air sensitivity

During gravity die filling, the presence of air may affect differently particles of different size and/or different density. The general segregation effect of air depends on the formation of local air flows, factor which cannot be easily controlled. Mostly in big size, regular shape dies, these air escaping flows may be unpredictable and vary between the filling experiment repetitions. Air flows entity depends on powder feeding rate and on air extraction rate.
Segregation induced by air presence is reduced increasing the powder feeding rate and with the turbulence within the die and increases if the powder is fed in diluted form [81]. This corresponds, in the case of die filling, to the results found by Wu et al. [79], according to which nose flow is not affected by the presence of air within the die and bulk flow is very sensitive to air induced segregation.

The geometry of the die and the filling procedure should be designed to minimize the rate of air escaping from the die itself. A successful improvement is the suction filling, in which the lower punch moves down at a calibrated velocity to permit complete die filling avoiding the gravity falling of the powder.
Anyway, particles with various size or density are differently affected by the dragging effect of air flows. The sensitivity of a particle to the air presence was analyzed by Guo et al. [22, 23], who formulated a dimensionless parameter to quantify and compare it:

$$\xi = A_r \Phi_\rho \tag{2.11}$$

with $\Phi_\rho = \rho_s/\rho_a$, ratio between the density of the solid particle material ρ_s and the air density $\rho_a = 1.205\, kg/m^3$ and A_r is the Archimedes number for particles in a fluid, given by:

$$A_r = \frac{\rho_a(\rho_s - \rho_a)g d_p^3}{\eta^2} \tag{2.12}$$

where $g = 9.81\ m/s^2$ is the gravitational acceleration, d_p is the particle diameter and $\eta = 1.78 \cdot 10^5\ Pa\ s$ is the air viscosity. This parameter permits to define two regimes in which classify different powders, considering as critical value $\xi_c = 9.56 \cdot 10^6$. Hence, air-sensitive powders are characterized by $\xi < \xi_c$, otherwise they are air-inert.
The air sensitivity index is introduced [67]:

$$\zeta = 1 - \frac{ln\xi}{ln\xi_c} \tag{2.13}$$

Particle are air-inert if $\zeta < 0$ and air-sensible if $0 < \zeta < 1$. In the air-sensitive regime $(0 < \zeta < 1)$, the sensitivity of the particles to the presence of air increases as the index ζ is higher.
Parameters for the particles used in this research are shown in 2.5:

Table 2.5: Air sensibility indexes of CAF and DCPA

Material	d_{50} $[\mu m]$	ρ_s $[kg/m^3]$	Φ_ρ	A_r	ξ	ζ
CAF	207.16	1460	1211.618	483.869	$5.86 \cdot 10^5$	0.174
DCPA	195.73	2860	2373.444	799.781	$1.90 \cdot 10^6$	0.101

The result is that caffeine is a little more affected by the presence of air in the die than DCPA. It follows that some segregation effect may be caused by air escaping currents during gravity die filling.

Chapter 3

Experimental results

The results of the die filling experiments are presented in this chapter. Samples are prepared at three different caffeine concentrations (10%, 25% and 50%) and stabilized at three different relative humidity levels (20%, 50% and 80%).
Results are presented considering the behaviour of each concentration powder in the three relative humidity conditions.
Diagrams are built starting from experimental data, to better visualize what happened within the die during its filling. The reported results are the mean value of three repetitions of experiments at the same conditions. In particular:

- the table summarizes the characteristics of the powder;
- the first diagram shows the concentration of each layer. This is the mean value between the far-end side and the near-end side of any single layer;
- the second diagram shows the mean concentration between the far-end side and the near-end side;
- the third and last diagram shows each single drawer concentration.

Every mean value is accompanied by its standard deviation.

3.1 Segregation index

A non dimensional parameter is introduced to compare the results of the different experiments. This parameter should consider the entity of the segregation in the different die spots, so the difference between their concentrations respect to the mean concentration value of the die. The actual mean value of the API concentration within the die does not affect the Segregation Index value, since it focuses only on the structural stability of the final tablet and not on the total API amount contained in the final tablet. Anyway, different concentrations are analyzed since the segregation phenomena may depend on the powder composition.
The parameter proposed for such a Segregation Index is:

$$S.I. = \sum_{i=1}^{n} \frac{|c_i - \overline{c_i}|}{\overline{c_i}} \tag{3.1}$$

with n number of concentration measurements per die filling run, c_i measured concentration and $\overline{c_i}$ mean concentration of the single die filling run. Then, the segregation indexes from the three single test repetition are averaged.

This parameter is useful to compare results of die filling processes with powders with different characteristics, such as composition, humidity, but also different blend materials, particle size distribution, or operational conditions, so different shoe filling height.
The limitation of this parameter is the possibility to compare results only for the same dimensions and aspect ratio of the die, divided into ten drawers. Also environmental conditions of die filling procedure may affect the results, since air properties changes. Any experiment is performed at ambient room and temperature. The reason is that the main source of segregation is the air currents formation, which largely depends on the geometry of the die.

3.2 Data analysis approach

Segregation has occurred during die filling if the concentration in different spots within the die is different. To clarify if segregation has occurred in a significant way, a statistical test is required to compare group means, the mean values of the concentration in different spots, and state if they are or not different from each other. For this purpose, an analysis of variance, Anova, is adopted. Since nearly all of the reported analysis breaks the assumption of homoscedasticity, so failing the Levene test on the equality of variances, the usual Anova test cannot be applied, but the alternative Welch-Anova test must be adopted. This test permits to obtain information on the means comparison either when their variances are not similar.
The statistical tests are performed using the *Minitab* tool, setting 95% as level of confidence (which means that a p-value under 0.05 is considered statistically significant to denote differences in concentration means values) and two-sides confidential interval.

3.3 Die filling experiments results

3.3.1 10% CAF samples

Powder blend is prepared with the 10% by mass of caffeine and the remaining part of DCPA.
After performing the experiments, the samples concentrations if no segregation has occurred is estimated to be 10% of the weighted samples.
The dilution for the concentration measurement with the spectrophotometer is 1 : 10000.

Table 3.1: Results of die filling for 10% CAF mixture at 20% of relative humidity

10% CAF - RH = 20%						
	Far-end side		Near end side		Layers' mean	
Height $[mm]$	Conc. $[wt\%]$	St. Dev.	Conc. $[wt\%]$	St. Dev.	Conc. $[wt\%]$	St. Dev.
-5	10.9	0.9	10.4	0.3	10.7	0.6
-15	10.6	0.5	10.2	0.3	10.4	0.4
-25	10.5	0.5	10.0	0.3	10.3	0.4
-35	10.3	0.4	10.3	0.4	10.3	0.4
-45	10.2	0.5	10.4	0.5	10.3	0.4
Side's mean	10.5	0.6	10.4	0.4		

Mean concentration $[CAFwt\%]$	10.40%
Mean powder humidity	$0.653 \pm 0.042\%$
Layers Segregation p-value	0.211
Each drawer Segregation p-value	0.032
Segregation Index	0.562 ± 0.241

Table 3.2: Results of die filling for 10% CAF mixture at 50% of relative humidity

10% CAF - RH = 50%						
	Far-end side		Near end side		Layers' mean	
Height $[mm]$	Conc. $[wt\%]$	St. Dev.	Conc. $[wt\%]$	St. Dev.	Conc. $[wt\%]$	St. Dev.
-5	10.4	0.6	10.4	0.1	10.4	0.3
-15	10.2	0.2	10.0	0.2	10.1	0.1
-25	10.0	0.3	9.8	0.0	9.9	0.1
-35	10.1	0.3	10.1	0.5	10.1	0.3
-45	10.4	0.8	10.2	0.1	10.3	0.4
Side's mean	10.2	0.0	10.1	0.1		

Mean concentration $[CAFwt\%]$	$10,17\%$
Mean powder humidity	$1.047 \pm 0.023\%$
Layers Segregation p-value	0.000
Each drawer Segregation p-value	0.000
Segregation Index	0.765 ± 0.150

Table 3.3: Results of die filling for 10% CAF mixture at 80% of relative humidity

10% CAF - RH =80%						
	Far-end side		Near end side		Layers' mean	
Height $[mm]$	Conc. $[wt\%]$	St. Dev.	Conc. $[wt\%]$	St. Dev.	Conc. $[wt\%]$	St. Dev.
-5	10.2	0.1	10.0	0.2	10.1	0.1
-15	10.3	0.1	9.9	0.2	10.1	0.1
-25	10.2	0.1	9.9	0.2	10.1	0.1
-35	10.2	0.2	10.0	0.2	10.1	0.2
-45	9.9	0.3	10.0	0.2	10.0	0.3
Side's mean	10.1	0.1	10.0	0.1		

Mean concentration $[CAFwt\%]$	10.06%
Mean powder humidity	$1.32 \pm 0.04\%$
Layers Segregation p-value	0.407
Each drawer Segregation p-value	0.000
Segregation Index	0.453 ± 0.106

3.3.1.1 10% CAF at 20% of relative humidity

The mean of the results are collected in Table 3.1 The concentration of the different die layers is shown in Figure Fig.3.1.a.

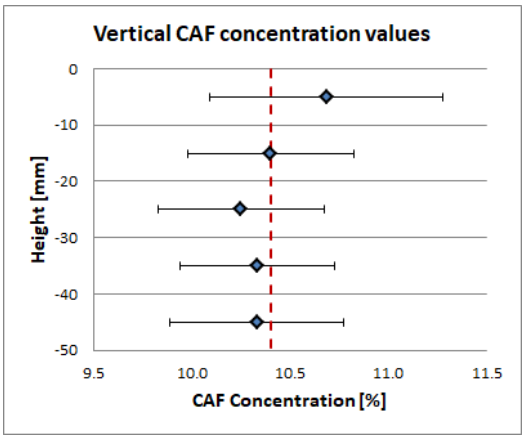

(a) *Different layers CAF Concentration*

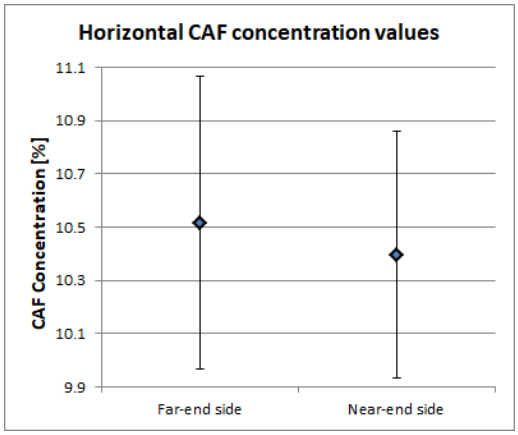

(b) *Different sides CAF Concentration*

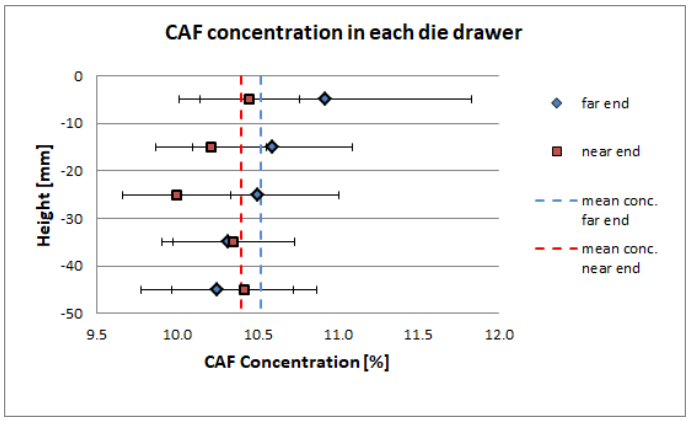

(c) *Different sides CAF Concentration*

Figure 3.1: Vertical, horizontal and each die drawer CAF concentration variations for 10% CAF at 20% of relative humidity

A general tendency to segregate along the different layers is visible. Caffeine tends to concentrate in the upper part of the die. Anyway, since variances are quite high, Welch-Anova test returns a p-value over the acceptable threshold, so the differences across the layers are not statistically significant. It must be concluded that there is no difference in the different layers concentration, so segregation is negligible.
The concentration in the far-end side and the near-end side of the die is shown in Figure Fig.3.1.b. A little difference between far-end and near-end side mean is visible, but the big variances don't permit to conclude that a significant segregation has occurred between the two sides, considering them all along the die height.
The concentration in each one of the die drawer is shown in Figure Fig.3.1.c and the properties are summarized in Table 3.1.
The tendencies of the two different die sides seems to be subject to two segregation phenomena. In the far end side, caffeine concentrates in the upper part of the die. During powder falling, air tends to drag up the light component, caffeine, since it is the most air-sensitive in the binary mixture, increasing the DCPA concentration in the bottom of

the die. In the near-end side, at the bottom an higher concentration of caffeine is present, probably due to a partial nose flow and push-away effect by the heavier particles. Then, looking at the upper part of the die, caffeine concentration tends to be lower than the respective far-end side of the same layer. This occurrence may be provoked by a difference in the angle of repose. Since DCPA has an higher density, its momentum is higher than that of the caffeine, so its particles tends to roll more in the slope of the forming heap, concentrating in the near-end side of the die.

3.3.1.2 10% CAF at 50% of relative humidity

Results of the die filling experiment are collected in Table 3.2.

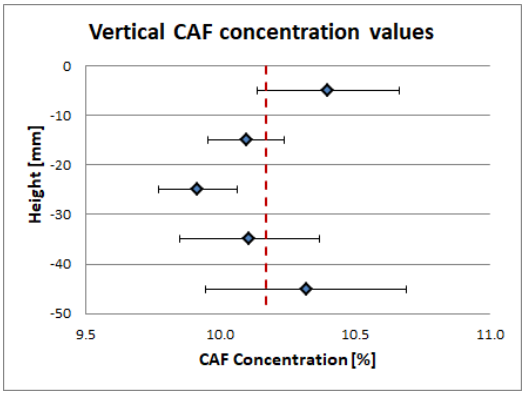

(a) *Different layers CAF Concentration*

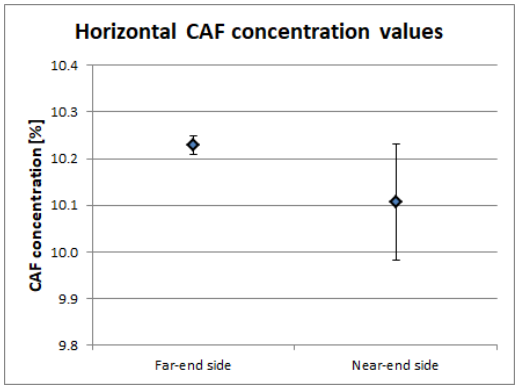

(b) *Different sides CAF Concentration*

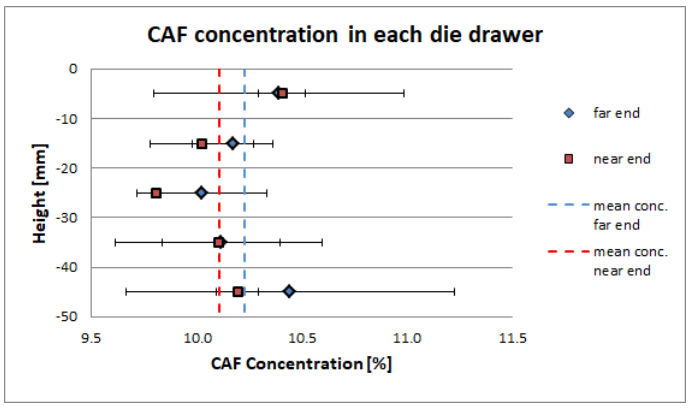

(c) *Different sides CAF Concentration*

Figure 3.2: Vertical, horizontal and each die drawer CAF concentration variations for 10% CAF at 50% of relative humidity

Layers concentration are shown in Figure 3.2.a. At this humidity level, powder blend clearly segregates along the die height, as confirmed by the null p-value, in Table 3.2. The concentration graph assumes a 'C' shape. Since air should drag caffeine particles up, the presence of an high caffeine concentration in the bottom of the die means that this effect has not been effective. An initial important simil-nose flow, which is not sensitive to air presence, may explain this fact. The different rebound of the two substances may be considered a cause of the horizontal segregation at the bottom of the die, Figure 3.1.c. The high concentration of caffeine in the upper part of the die agrees with the air drag effect that holds caffeine back high. Horizontal segregation is not statistically proved.

3.3.1.3 10% CAF at 80% of relative humidity

Table 3.3 contains the mean values of the results and conditions of the experiment.

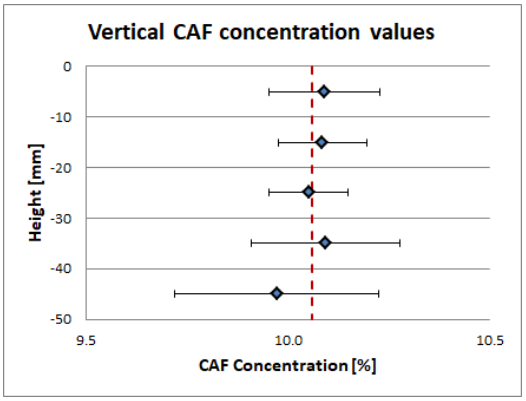

(a) *Different layers CAF Concentration*

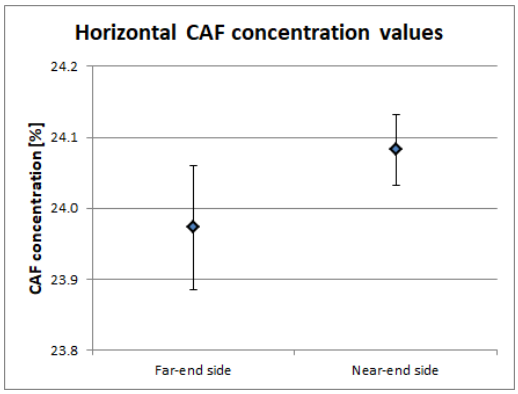

(b) *Different sides CAF Concentration*

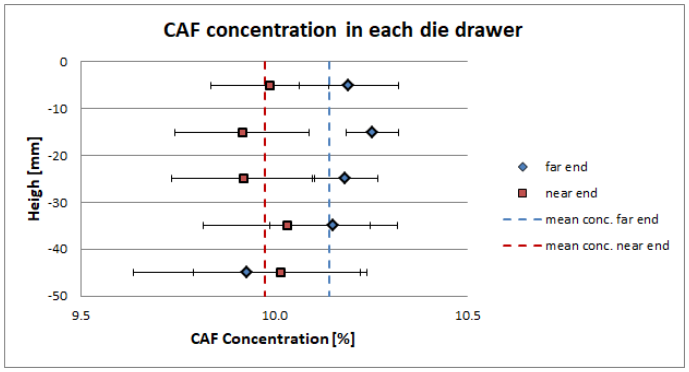

(c) *Different sides CAF Concentration*

Figure 3.3: Vertical, horizontal and each die drawer CAF concentration variations for 10% CAF at 80% of relative humidity

No statistically significant segregation has occurred in the different layers, as indicated by the high p-value, Table 3.3. Mean values are very similar and the relatively little variance is high enough to consider them not different, as shown in Figure 3.3.a. Some segregation occurs in the single drawers, mostly between each layer far-end and near-end sides, Figure 3.3.c. The reason of this behaviour can be the greater rolling of DCPA particles due to their higher inertia. Since liquid bridges formed, air cannot easily extract caffeine from the falling powder column, concentrating it in the far-end side of the die.

3.3.2 25% CAF samples

Powder blend is prepared with the 25% by mass of caffeine and the remaining part of DCPA.
After performing the experiments, the samples concentrations if no segregation has occurred is estimated to be 25% of the weighted samples. The dilution for the concentration measurement with the spectrophotometer is 1 : 10000.

Table 3.4: Results of die filling for 25% CAF mixture at 20% of relative humidity

25% CAF - RH = 20%						
	Far-end side		Near end side		Layers' mean	
Height $[mm]$	Conc. $[wt\%]$	St. Dev.	Conc. $[wt\%]$	St. Dev.	Conc. $[wt\%]$	St. Dev.
-5	25.1	0.4	25.2	0.6	25.1	0.3
-15	25.6	0.6	24.8	0.6	25.2	0.4
-25	24.9	0.3	24.8	0.4	24.8	0.4
-35	25.3	0.2	25.3	0.7	25.3	0.2
-45	24.5	0.3	25.0	0.7	24.7	0.2
Side's mean	25.1	0.2	25.1	0.1		

Mean concentration $[CAFwt\%]$	25.03%
Mean powder humidity	$0.59 \pm 0.03\%$
Layers Segregation p-value	0.004
Each drawer Segregation p-value	0.000
Segregation Index	0.456 ± 0.277

Table 3.5: Results of die filling for 25% CAF mixture at 50% of relative humidity

25% CAF - RH = 50%						
	Far-end side		Near end side		Layers' mean	
Height $[mm]$	Conc. $[wt\%]$	St. Dev.	Conc. $[wt\%]$	St. Dev.	Conc. $[wt\%]$	St. Dev.
-5	26.4	0.4	26.4	0.4	26.4	0.1
-15	26.9	0.7	26.3	0.5	26.6	0.6
-25	26.1	0.3	26.0	1.2	26.1	0.7
-35	25.9	0.4	25.9	0.7	25.9	0.4
-45	25.8	0.6	25.2	1.3	25.5	0.4
Side's mean	26.2	0.1	25.9	0.5		

Mean concentration $[CAFwt\%]$	26.08%
Mean powder humidity	$0.99 \pm 0.05\%$
Layers Segregation p-value	0.000
Each drawer Segregation p-value	0.001
Segregation Index	0.542 ± 0.087

Table 3.6: Results of die filling for 25% CAF mixture at 80% of relative humidity

25% CAF - RH =80%						
	Far-end side		Near end side		Layers' mean	
Height $[mm]$	Conc. $[wt\%]$	St. Dev.	Conc. $[wt\%]$	St. Dev.	Conc. $[wt\%]$	St. Dev.
-5	24.2	1.0	24.4	0.4	24.3	0.6
-15	24.0	0.2	23.6	0.4	23.8	0.3
-25	24.1	0.5	24.1	0.5	24.1	0.5
-35	24.2	0.2	24.1	0.7	24.1	0.4
-45	23.3	0.6	24.2	0.8	23.7	0.5
Side's mean	24.0	0.1	24.1	0.5		

Mean concentration $[CAFwt\%]$	24.03%
Mean powder humidity	$1.19 \pm 0.04\%$
Layers Segregation p-value	0.016
Each drawer Segregation p-value	0.001
Segregation Index	0.456 ± 0.186

3.3.2.1 25% CAF at 20% of relative humidity

As reported in Table 3.4, segregation is statistically proven in the different layers of the die. The concentration has an irregular zigzag shape, Figure 3.4.a. Caffeine particles are dragged up by air, so the concentration at the bottom of the die is quite low, but then it concentrate differently in the layers. Looking at Figure 3.4.c, two 'S' shape caffeine concentration trend are visible, braided together. This effect can be caused by a conflict between the caffeine drag by air and the heaping formation due to falling powder that pushes down the retained particles. In the second layer the inertial rolling of DCPA causes a lower concentration of caffeine in the near-end side of the die. Horizontally there is no segregation evidence, Figure 3.4.b.

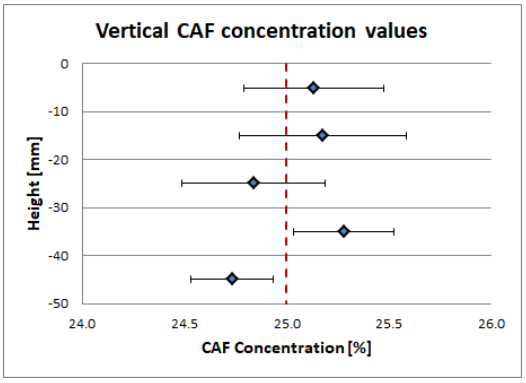

(a) *Different layers CAF Concentration*

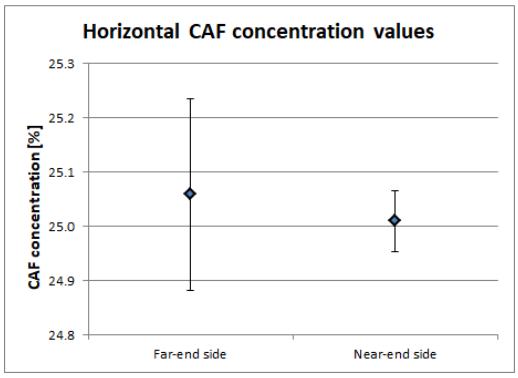

(b) *Different sides CAF Concentration*

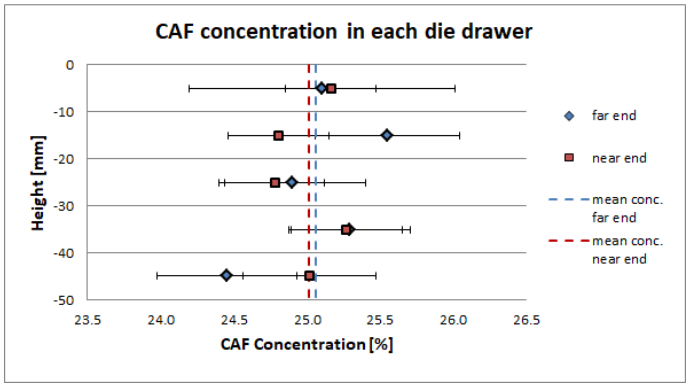

(c) *Different sides CAF Concentration*

Figure 3.4: Vertical, horizontal and each die drawer CAF concentration variations for 25% CAF at 20% of relative humidity

3.3.2.2 25% CAF at 50% of relative humidity

Table 3.5 shows the mean results of the experiment. At this humidity conditions segregation clearly occurs both considering only the layers levels and the single drawers concentrations. The trend is quite similar to the one expected, with the caffeine concentration increasing with the height of the die, because of the air drag effect. A little inversion is present at the top of the die, probably due to the fact that air has not enough space to drag caffeine up, which so deposits in the lower layers. The top layer collect only a bit of the caffeine dragged up, so its concentration stabilizes at a value which is between the mean and the maximum concentration. The near-end side of the bottom layer of the die caffeine concentration is quite lower than the far-end side one, because that side is usually more affected by the air drag effect. However, its variance is very high, because is depends on the specific established powder flow, which may vary in every experiment repetition. Horizontal mean concentration is not statistically different, though a little variation is present. In the single layers, instead, it is more evident, and caffeine tends to concentrate in the far-end side of the layers, as expected.

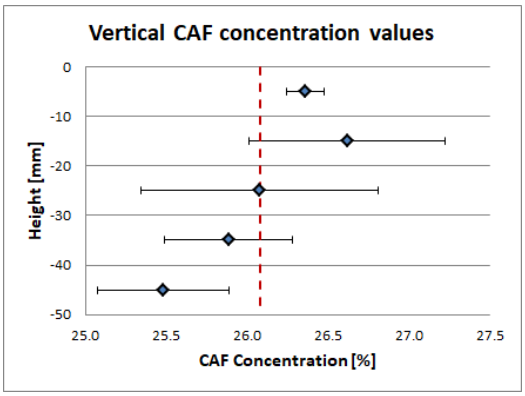

(a) *Different layers CAF Concentration*

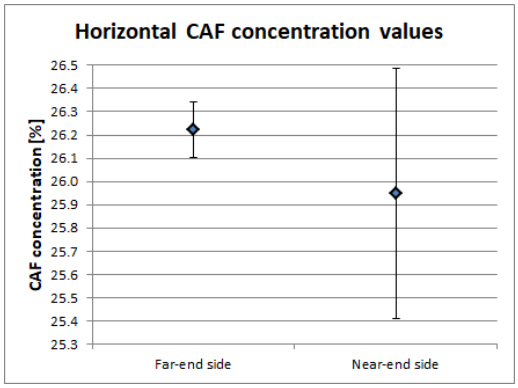

(b) *Different sides CAF Concentration*

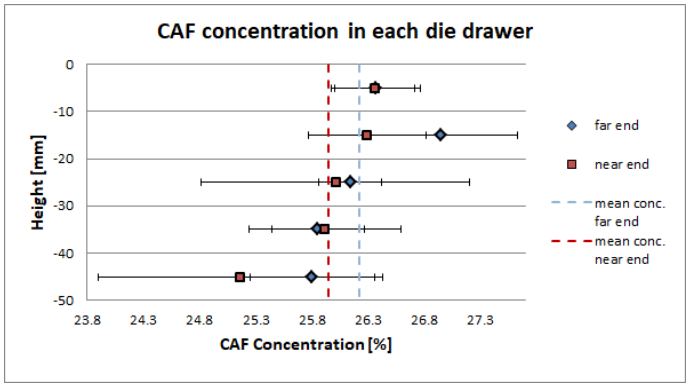

(c) *Different sides CAF Concentration*

Figure 3.5: Vertical, horizontal and each die drawer CAF concentration variations for 25% CAF at 50% of relative humidity

3.3.2.3 25% CAF at 80% of relative humidity

Results collected in Table 3.6 and represented in Figure 3.5 show a quite particular trend. Caffeine concentration increases going up from the die bottom, as expected. Then, at the second layer it decreases consistently, to increase again at the top. In Figure 3.5.c is visible that along the die the two sides concentration is similar, still, concentration in the far-end side is a little higher than that in the near-end side. At the bottom of the die the near-end side concentration is higher, probably due to the deposition of the caffeine extracted by air from the falling powder column. At the top, again, caffeine concentrates in the near-end side. Horizontal differences in the mean concentration value are not significant.

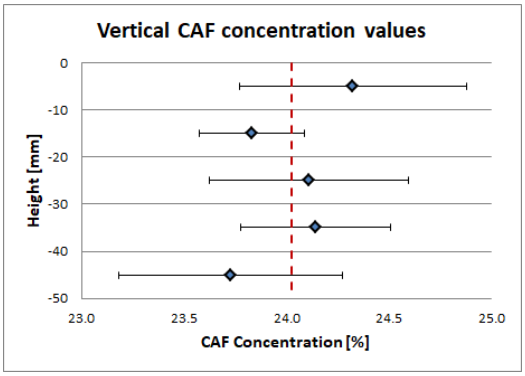

(a) *Different layers CAF Concentration*

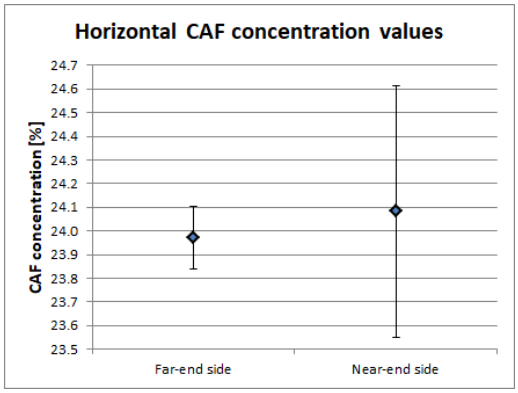

(b) *Different sides CAF Concentration*

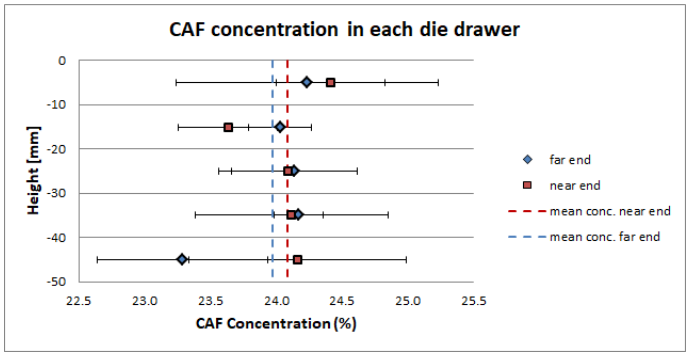

(c) *Different sides CAF Concentration*

Figure 3.6: Vertical, horizontal and each die drawer CAF concentration variations for 25% CAF at 80% of relative humidity

3.3.3 50% CAF samples

Powder blend is prepared with the 50% by mass of caffeine and 50% by mass of DCPA. After performing the experiments, the samples concentrations if no segregation has occurred is estimated to be 50% of the weighted samples.
The dilution for the concentration measurement with the spectrophotometer is 1 : 20000.

Table 3.7: Results of die filling for 50% CAF mixture at 20% of relative humidity

50% CAF - RH = 20%						
	Far-end side		Near end side		Layers' mean	
Height $[mm]$	Conc. $[wt\%]$	St. Dev.	Conc. $[wt\%]$	St. Dev.	Conc. $[wt\%]$	St. Dev.
-5	60.6	0.8	60.3	0.8	60.4	0.2
-15	60.4	0.8	60.3	1.0	60.3	0.7
-25	59.7	1.5	59.6	0.8	59.7	0.6
-35	60.2	0.4	60.2	0.4	60.2	0.4
-45	58.8	1.1	58.6	3.3	58.7	1.6
Side's mean	60.0	0.6	60.0	0.5		

Mean concentration $[CAFwt\%]$	59.87%
Mean powder humidity	$0.56 \pm 0.01\%$
Layers Segregation p-value	0.000
Each drawer Segregation p-value	0.006
Segregation Index	0.413 ± 0.184

Table 3.8: Results of die filling for 50% CAF mixture at 50% of relative humidity

50% CAF - RH = 50%						
	Far-end side		Near end side		Layers' mean	
Height $[mm]$	Conc. $[wt\%]$	St. Dev.	Conc. $[wt\%]$	St. Dev.	Conc. $[wt\%]$	St. Dev.
-5	57.5	3.2	55.0	2.2	56.3	2.3
-15	51.2	5.5	45.2	4.2	48.2	4.1
-25	47.2	3.7	51.0	3.8	49.1	3.3
-35	48.3	6.0	47.3	3.5	47.8	4.4
-45	47.5	4.9	45.6	2.6	46.5	3.5
Side's mean	50.3	3.0	49.2	2.7		

Mean concentration $[CAFwt\%]$	49.57%
Mean powder humidity	$0.95 \pm 0.04\%$
Layers Segregation p-value	0.000
Each drawer Segregation p-value	0.000
Segregation Index	2.290 ± 0.731

Table 3.9: Results of die filling for 50% CAF mixture at 80% of relative humidity

50% CAF - RH =80%						
	Far-end side		Near end side		Layers' mean	
Height $[mm]$	Conc. $[wt\%]$	St. Dev.	Conc. $[wt\%]$	St. Dev.	Conc. $[wt\%]$	St. Dev.
-5	54.4	4.1	56.2	2.9	55.3	3.5
-15	53.9	1.7	53.1	4.0	53.5	2.7
-25	49.4	4.0	52.3	4.1	50.8	3.5
-35	48.6	2.9	50.3	3.0	49.5	2.0
-45	46.2	3.5	48.5	3.6	47.3	3.6
Side's mean	50.5	3.1	50.5	2.1		

Mean concentration $[CAFwt\%]$	51.30%
Mean powder humidity	$1.16 \pm 0.01\%$
Layers Segregation p-value	0.000
Each drawer Segregation p-value	0.000
Segregation Index	1.760 ± 0.357

3.3.3.1 50% CAF at 20% of relative humidity

Results are reported in Table 3.7. Segregation is statistically evident both in layer levels and considering each drawer, Figure 3.7.a/c. It is not considering the horizontal length, both in the total far-end/near-end side mean values and in the single levels, 3.7.b. The concentration of caffeine is on average higher than the target one. A similar deviation may be due to the increased electrostatic force of the powder. DCPA presents an high tendency to be electrically charged, making its particles jump away and stick on the plastic bailer during powder handling. Since the same mean concentration is present in all three the test repetitions, so they are consistent, and because the aim of the research is analyzing the differences within the die, the results are kept and compared with the others.

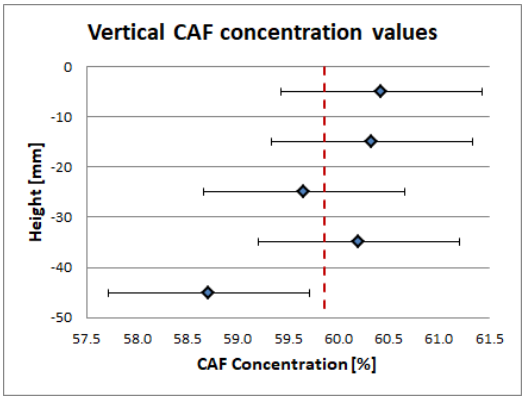

(a) *Different layers CAF Concentration*

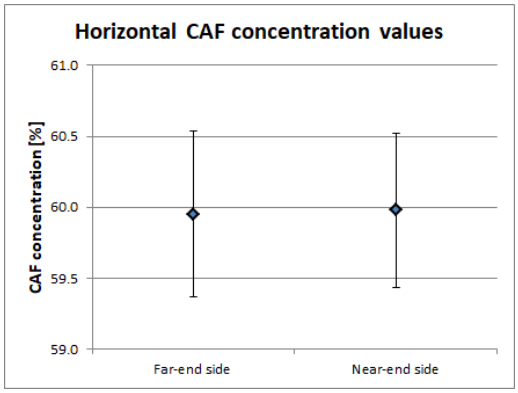

(b) *Different sides CAF Concentration*

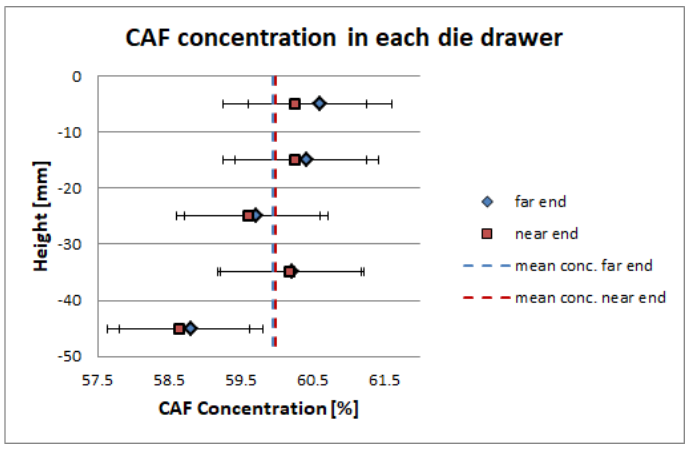

(c) *Different sides CAF Concentration*

Figure 3.7: Vertical, horizontal and each die drawer CAF concentration variations for 50% CAF at 20% of relative humidity

3.3.3.2 50% CAF at 50% of relative humidity

The results in Table 3.8 shows that segregation occur in layer levels, confirmed by the p-value in Table 3.8, and also single drawers concentration is different. The general trend, shown in Figure 3.8a, is a quite constant concentration for all the layers and then a high value at the top. Looking at Figure 3.8.c, the behaviour seems to be more complex. At the bottom layers of the die, the shortage of caffeine is due to the air drag effect, as expected. Then, during the heap growing, it happens that caffeine deposits in a concentrated way. Differences along a layer between the far-end and the near-end sides are present. No important segregation seems to occur in the horizontal mean values. Very high differences in concentration are present probably due to the high caffeine concentration, which avoid to DCPA particles to prevent caffeine particles to be dragged up by air.

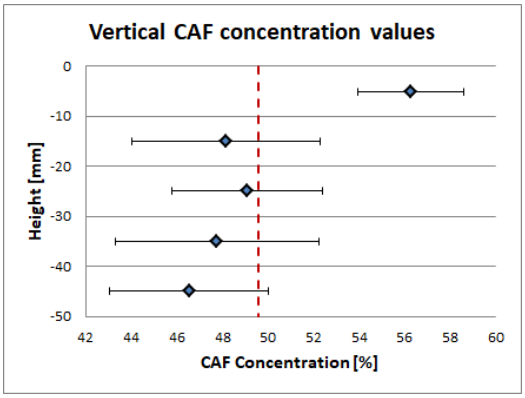

(a) *Different layers CAF Concentration*

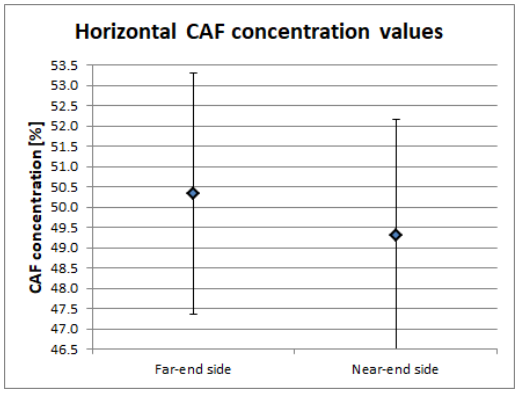

(b) *Different sides CAF Concentration*

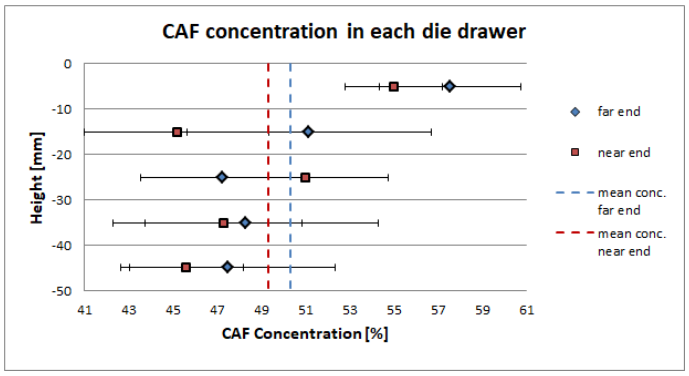

(c) *Different sides CAF Concentration*

Figure 3.8: Vertical, horizontal and each die drawer CAF concentration variations for 50% CAF at 50% of relative humidity

3.3.3.3 50% CAF at 80% of relative humidity

Results collected in Table 3.9 are represented in Figure 3.9. Concentration increases with the height of the die, as normally expected because of air drag effect. Along nearly all the die, caffeine concentration in the near-end side is higher than in the far-end side. This probably happen because extracting effect of air over caffeine is exacerbate by the high caffeine concentration, so it is easy to retain important quantity of CAF particles. Since the DCPA has a lower sensitivity to air presence, it falls, concentrating in the far-end side. Caffeine particles number is high enough not to permit to DCPA particles to drag them down, so an high segregation occurs. No horizontal mean segregation occurs.

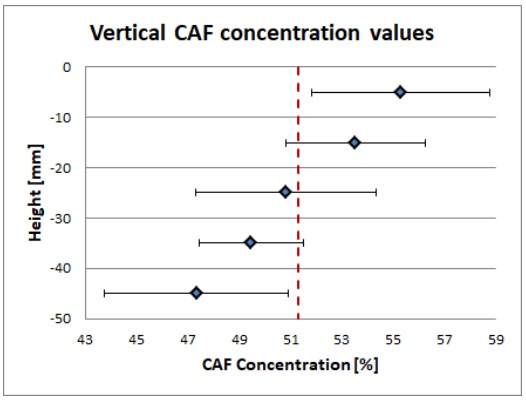

(a) *Different layers CAF Concentration*

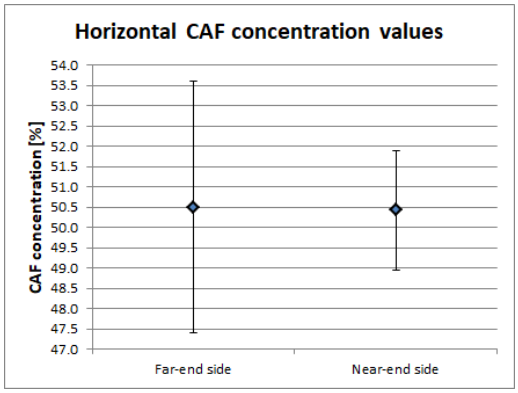

(b) *Different sides CAF Concentration*

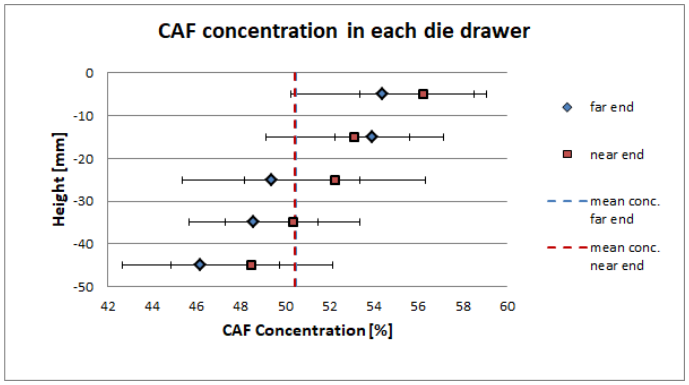

(c) *Different sides CAF Concentration*

Figure 3.9: Vertical, horizontal and each die drawer CAF concentration variations for 50% CAF at 80% of relative humidity

3.3.4 Segregation Index trend

The proposed Segregation Index quantifies the sum of the percentage deviation in each die drawer respect to the mean concentration within the die.
The Segregation Index mean value of anyone of the nine experiments is collected in Table 3.10. Since the variance is quite high, these results cannot be used to denote precisely the behaviour of the powders, but can be an useful outline at least to draw some qualitative conclusions. Results are shown in Figure 3.10.

Table 3.10: Segregation Index results

	Relative Humidity		
	20% RH	**50% RH**	**80% RH**
10% CAF	0.5624 ± 0.2412	0.7653 ± 0.1500	0.4532 ± 0.1063
25% CAF	0.4562 ± 0.2768	0.5419 ± 0.0870	0.4559 ± 0.1855
50% CAF	0.4129 ± 0.1843	2.2899 ± 0.7307	1.7595 ± 0.3569

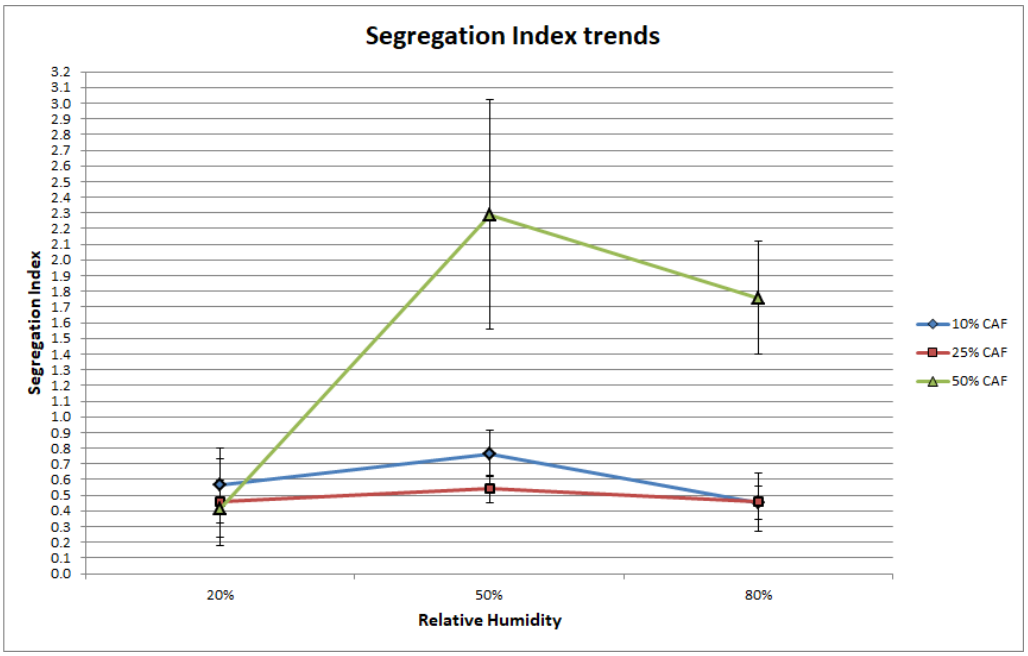

Figure 3.10: Segregation Index trends

3.4 Ring Shear tests results

The mean values of flow-factor (ffc), the cohesion estimation (τ_c), the effective friction angle (ψ_{eff}) and the internal friction angle (ψ_{in}) from the Schulze Ring Shear tests are collected in Table 3.11. The mean value of all the concentration powders results at each relative humidity condition is also included.

Table 3.11: Shear test results

Relative Humidity	CAF concentration	τ_c $[Pa]$	ffc	ψ_{eff} [°]	ψ_{in} [°]
20%	10%	21.67 ± 2.08	21.86 ± 1.99	38.30 ± 0.50	37.23 ± 0.51
	25%	24.58 ± 0.52	18.83 ± 0.18	38.57 ± 0.31	37.43 ± 0.38
	50%	21.00 ± 0.58	24.79 ± 1.06	37.83 ± 0.38	36.90 ± 0.36
	mean	22.30 ± 2.08	21.92 ± 2.89	38.23 ± 0.47	37.19 ± 0.43
50%	10%	20.33 ± 3.51	23.53 ± 4.14	38.23 ± 0.23	37.20 ± 0.10
	25%	15.67 ± 1.53	29.35 ± 3.13	37.83 ± 0.65	37.03 ± 0.61
	50%	20.00 ± 3.00	25.43 ± 4.02	36.63 ± 0.12	35.73 ± 0.21
	mean	18.67 ± 3.32	26.10 ± 4.17	37.57 ± 0.80	36.66 ± 0.77
80%	10%	17.33 ± 4.51	27.41 ± 6.75	38.90 ± 0.26	38.03 ± 0.21
	25%	16.00 ± 4.00	29.98 ± 6.72	38.10 ± 0.44	37.27 ± 0.55
	50%	16.00 ± 3.61	31.38 ± 7.81	36.87 ± 0.15	36.10 ± 0.30
	mean	16.44 ± 3.57	29.59 ± 6.40	37.96 ± 0.93	37.13 ± 0.91

3.4.1 Flowability results discussion

Flowability of a powder is characterized by the flow-factor ffc, which is the ratio between the consolidation stress, σ_1 and the unconfined yield stress, σ_c [64]:

$$ffc = \frac{\sigma_1}{\sigma_c} \tag{3.2}$$

The flow-factor permits the quantitative description and comparison of not free-flowing powders, so until its value remain under 10. From 0 to 10 in fact, the flow-factor value well categorizes the entity of cohesiveness of a material [66]. Above 10, instead, it only indicates a free-flowing powder, but it cannot be used quantitatively to compare different results. For this reason, since the obtained results are placed largely under the free-flowing threshold, Figure 3.11, the flow-factor values cannot be considered as reliable for a quantitative powder flowability description.
Moreover, it appears useless the measure of the complete flow-functions, measuring other flow-factors at different preshear stresses, since the result would not provide any additional information on the powder flowability.
The same reasoning is valid for the cohesion estimation. Having said this, the general trend can be detected by looking at the mean values: increasing powder humidity, the flow-factor value increases, meaning that the powder is more free-flowing. Considering the formation of liquid bridges at high relative humidity, powder should become more cohesive, so the trend highlighted by the ring shear cell seems to be ambiguous. Actually, powder becomes more cohesive at high relative humidity conditions, but this eventuality manifests

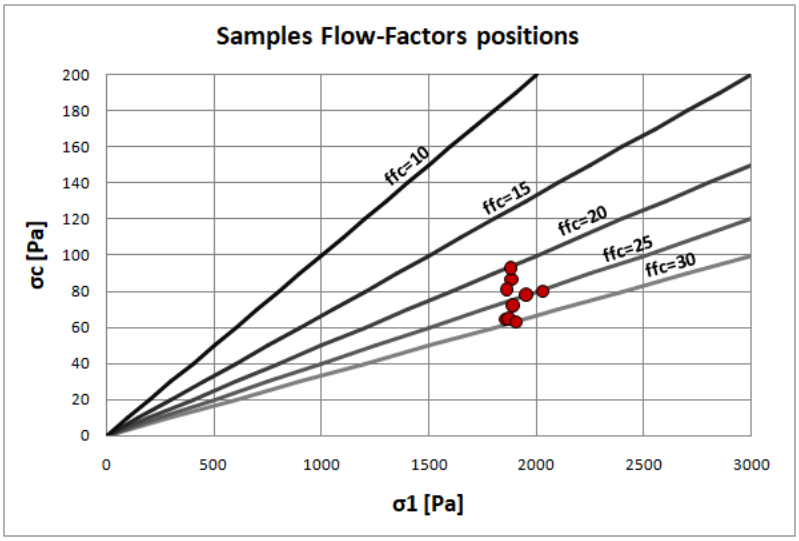

Figure 3.11: Flow-Factors at 1 kPa of preshear

in dynamic operations, which is not the case of a shear test. In fact, in static or nearly-static processes water acts as a lubricant between the particles, easing their scrolling and apparently increasing their flowability [63]. For this reason, only the difference between the low and the ambient relative humidity conditions can be considered to explain the results in a dynamic operation as the die filling.

Also the cohesion strength extrapolated from the flow-function cannot be considered quantitatively, but it just generally indicates a free-flowing powder. During the die filling process, however, the powder has already overcome the failure stress and is moving. The effective friction angle describes

Both the flow-factor and the cohesion are 'static' measures, as they indicates the strength required to initiate the flow of a bulk solid. The effective friction angle is the slope of the loci of the effective failure points, passing through the origin, so with cohesion null value. This is the state of any moving granular material. Since cohesion is negligible, it can be generally described by $\tau = \mu_{eff}\,\sigma$, in which $\mu_{eff} = tg(\Phi_{eff})$.

The trend described by the effective friction angles is quite different and seems to be more adapt to describe the physical behaviour expected from the powder. In particular they suggest that the powders are less free-flowing at low and high relative humidity conditions and more free-flowing at ambient condition. The differences, however, are minimal. The reason of this behaviour is that if the powder is dry, electrostatic charges on particles from triboelectric effect persist longer, as water presence helps their discharging. At ambient conditions electrostatic charges are not more present [60] due to liquid bridges formation, but these are not yet strong enough to induce an important cohesive effect. This state is associated with the more free-flowing conditions for the powders. At high relative humidity, instead, liquid bridges are strong enough to have an important role in changing the flowability of the particles, making the powder more cohesive.

Except for the low relative humidity condition, they tends to decrease if more caffeine is present in the blend, becoming quite lower in the 50% of caffeine cases at ambient and high relative humidity conditions. The explanation of this behaviour may be related to materials characteristics as well as operating conditions. It is possible that caffeine acts as a free-flowing powder, and when it is concentrated it is easier for particles to scroll. Moreover, the reason of this behaviour may be the fine, very cohesive caffeine particles strongly stuck over

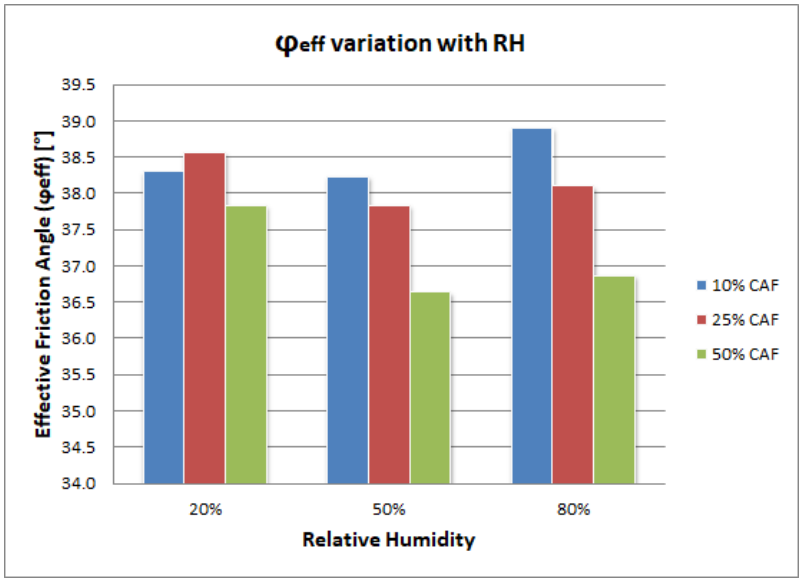

Figure 3.12: Effective Friction Angle variation with Relative Humidity conditions

the coarser particles that shear test may help the scrolling. Another possible explanation could be related to mechanical constrains of the two materials particles. As visible in Figure 2.6, the shape of DCPA particles lends itself to mechanically lock the shifting of other particles. Also it tends to be more electrostatic, due to the richness of tips and edges, but also humidity sorption is favored by surface asperity [39]. This fact can explain both the higher cohesiveness of caffeine poor blends and the lower cohesiveness at ambient and high relative humidity conditions.

3.5 Comments on experimental results

Powders behaviour observed in the experiments is rather complex and can be controlled by many factors.

Humidity effect

Before performing the experiments, powders are placed as thin layers in an humidity-controlled chamber until they stabilize.

Moisture equilibrium between powder and air at a certain relative humidity strongly affects the properties of the material. The appreciable effect of this conditioning is evident in Figure 3.10, as the occurrence of segregation phenomena depends on powder humidity. As visible, segregation seems to be favored at ambient relative humidity, while it decreases consistently both at low and high relative humidity conditions.

The entity of segregation is mainly related to powders cohesiveness, so the highlighted trend must be related to powder characteristics to be clarified.

The used powders has a strong tendency to become electrostatically charged during their handling, due to friction between particles, and to maintain the charge for a longer time in some conditions. This condition causes an high cohesiveness of the powder, and is maximum when it is dry. For this reason the low relative humidity condition is associated with low segregation index values at any powder concentration.

This electrostatic effect is mitigated with powder humidity. The formation of liquid bridges between particles helps the discharging of electric charge, reducing cohesiveness. The minimum of cohesion forces is considered to be between 30% and 50% of the relative humidity [47, 60]. Since capillary forces are not strong yet, ambient condition is associated with the maximum of flowability of the powders. For this reason, the ambient relative humidity condition causes the higher segregation index values for all the three powder API concentrations.

At high relative humidity condition the pendular liquid bridge regime is well established. Over 40% of relative humidity triboelectric charge during powder handling are drastically weakened [60], but liquid bridges induce significant cohesive forces that help reducing the segregation tendency.

API concentration effect

At 20% of relative humidity

Cohesiveness is high at this relative humidity condition due to the electrostatic charges. They are prevented to be discharge by the lack of liquid bridges between particles because of the small amount of moisture in the powder. Because of this cohesive forces, it is difficult for air to extract caffeine particles from the falling powder column even considering the different air sensitivity of the two materials.

Segregation index value seems to decrease with the increasing API concentration in the blend. The greater tendency of low dosage powder blends to show higher segregation is acknowledged in the literature [38, 73]. This can be due to the

lower number of caffeine particles dragged up by air during die filling required by lower dosage blend to show an high segregation index.
Moreover, considering that the powder is not totally dry, a small amount of humidity is present. Since DCPA shows a greater hydroscopic capacity due to its greater surface asperity [39], the effective powder humidity decreases at high caffeine concentrations. Humidity facilitates the electrostatic discharge from the powder, so low caffeine concentrations blends will have higher humidity content and a lower electrostatic charge. For this reason their cohesion will be lower and the respective segregation index value will increase.

At 50% of relative humidity

At ambient humidity conditions powder cohesiveness is minimized. Air escaping from the die can easily drag caffeine since no cohesive forces avoid it. At lower API concentrations it is still quite difficult for air to extract caffeine particles from the falling stream of powder, since DCPA particles are dense and push caffeine down, avoiding an high segregation. Certainly, a quantity of caffeine particles are dragged by air, so the final bulk in the die will be not uniform. Increasing the API concentration in the blend, an higher number of separated caffeine particles is required to obtain the same segregation index value. Since the cloud of falling DCPA particles is still quite dense, the 25% of caffeine powder shows a lower segregation index value. Air can more easily separate the particles on the sides of the falling column of in the cloud that overlooks the heap, instead of the powder inside the column in the far-end side of the die [48]. The result is completely different in the 50% of caffeine case. The number of DCPA particles is not dense enough to avoid caffeine to be dragged up. It is probable the formation of paths in which caffeine can easily escape from the falling powder cloud. This effect is emphasized by a limited presence of liquid bridges that forms agglomerates. During powder falling, agglomerates containing more caffeine particles are more easily dragged up, accentuating the segregation in the die. Moreover, it is more frequent to find caffeine particles in the falling cloud. Considering the flowability of the powder, given by the internal of the effective friction angles, see Paragraph 2.2.6, it is evident the difference between the lower caffeine concentration blends and the 50% one. At this relative humidity condition, electrostatic charges are weak [40, 53]. The humidity content decrease as the amount of caffeine in the blend increases. Hence, the powder becomes more free-flowing and segregation is favored.

At 80% of relative humidity

Capillary forces are stronger at high relative humidity conditions, so cohesiveness plays again a role in avoiding segregation. Since the pendular regime is well established, it is difficult for air to extract caffeine particles from the falling powder when its concentration is lower than the DCPA one. Agglomerates with high caffeine content are more easily subject to extraction by air. In particular, in the 50% CAF powder, the high caffeine content may favor segregation, since less amount of DCPA pushes down the API. Flowability must be taken into account also in this case, since for the 50% case it is quite different. As electrostatic charge is strongly weakened by the great water amount, only liquid

bridges may play a role in changing the cohesiveness of the powder. Again, at high caffeine content the quantity of water is minimum, so powder is more free-flowing and segregation is favored.

Effective friction angle

Graph 3.13 shows the Segregation Index values over the relative effective friction angles.

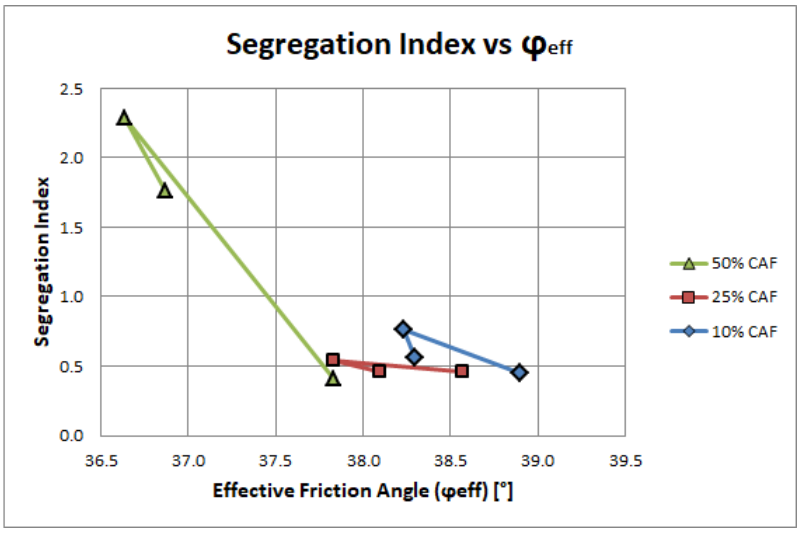

Figure 3.13: Segregation Index behaviour over Effective Friction Angle

Each powder at the same composition shows that at different humidity conditions its friction angles changes. Its seems that considering each of them singularly, the Segregation Index value increases at the decreasing of the friction angles.

Chapter 4

DEM Simulation

Some DEM simulations are performed at different caffeine concentration at ambient relative humidity, to compare their results to the experimental ones. In this chapter, after a short contextualization of this topic literature, the used model and its results are presented.

4.1 Introduction to Discrete Element Method

The Discrete Element Method (DEM) is a numerical method for modeling the dynamics of discrete particles.

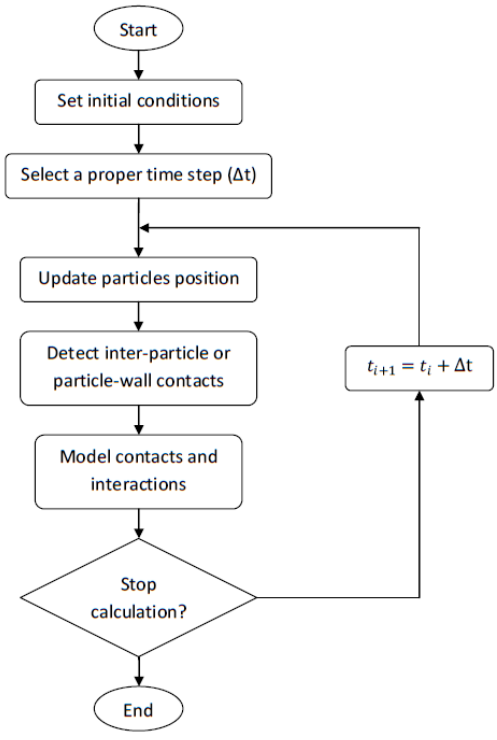

Figure 4.1: Algorithm flowchart

The position, velocity and interactions of each particle is updated with cyclic calculations at short time increments. In this way the trajectory of each single particle is followed in its spacial and time evolution. This method permits to simulate processes involving particles assemblies with a good accuracy.
Different methods are developed to simulate different systems.
The *Hard-sphere* model can be applied in the case of rapid, non dense flows, since particles collisions can be approximate to be instantaneous and binary. Particles are considered to rebound away after the impact, following the conservation of linear and angular momentum. Collisions are usually simulated as inelastic, so the new trajectory is determined only from the incident velocities and the relative friction coefficient, for tangential impact, and restitution coefficient, for normal impact.
In slow, dense flows, in which multi-particles collisions are possible and contacts may endure in time, the *Soft-sphere* model better fits the situation to simulate. With this model it is possible to update the particles trajectory via explicit solution of the Newton second law of motion. Particles can deform microscopically in the contact point due to the external stresses, but, since the variation is considered to be small [12], the deformation does not remarkably ex-

tend to the macroscopic scale. The contact forces caused by the impacts must be modeled to calculate the trajectory evolution. In the simulation, such deformation is represented by a small overlap between the two particles.
The general algorithm, schematized in Figure 4.1, is based on three steps [66]:

1. **Update particle positions**
   Each particle change in position is governed by Newton's second law of motion. Integrating it in the simulation, the movements of the particles are updated.

2. **Detect inter-particle or particle-wall contacts or detachments**
   The shift of the particles in a complex system may lead to the establishment of new contacts between them or to the detachment of particles that were attached. This eventuality must be checked for every particle in every simulation cycle and considering the huge number of particles that a simulation can involved makes this operation very delicate and computational demanding. Because of this reason, an important feature to employ in the algorithm is an efficient contact searching scheme, which helps reducing the computational cost by dividing the operations in two steps. The first one, the *presorting phase*, which has a skimming purpose, deals with reducing the number of particles to consider to the only ones that physically could be in contact with the considered particle, so the ones in its local vicinity. The breadth of zone are determined by the interactions to which the particles may be subject (if long range interaction are negligible, only mechanical contact are considered so the size of the vicinity zone reduces to the size of the attached particles, if not, it enlarges to the length of effect of interaction forces).The contacts detection can be carried out adopting two approaches:

   (a) the *Grid method*: the simulation environment is divided in regular cells and particles are mapped according to their position into one or more of these cells. Contacts are check for the particles that share the same cells.

   (b) the *Verlet list method*: a cut-off radius, which length must be carefully chosen, around the particle is built to consider those that can be in contact with that analyzed one. Subsequently, a *precise contact detection phase* is performed in the reduced neighborhood of particles. This part is easier if the particles are simulated as spheres and needs specific complex algorithms if they have irregular particular shapes [12].

3. **Model of contacts and interactions**
   Particle trajectories are continuously diverted by contacts with other bodies. At each time step, once its occurring has been ascertained, any contact must be modeled in order to quantify the contact forces acting on the particle so that its trajectory can be updated. Contact models are based on theoretical contact mechanics (the Hertz theory, the JKR model) or on phenomenological models (the linear spring model for purely elastic impacts or the spring, dashpot and slider model).

   The **spring, dashpot and slider model**, in Figure 4.2, represents the impacts between particles as a system including a spring, which approximates the elastic deformation, and a dashpot which permits to account the energy dissipation due to viscoelastic deformations. The normal interaction represents the compressive forces, while the shearing forces are represented by the tangential spring-slider-dashpot scheme.

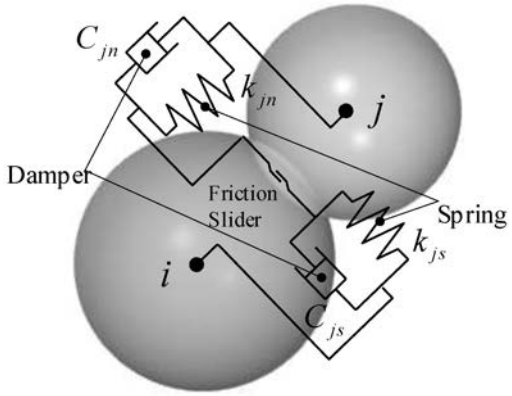

Figure 4.2: The spring and dashpot model [71]

External particles interactions such as Van der Waals or capillary forces [5, 27, 32, 70, 75] or can be easily included in the models, so the system forces calculated by this method usually include only the gravity and the contact ones. [44].

An appropriate selection of the time step (Δt) is required to perform the cyclic calculations in a reliable way. If the time step is reduced too much, computational costs will increase rapidly. On the other side, it must be kept low enough to permit the calculations to be stable. In fact, a low value of the time step will avoid new contacts to occur during the current algorithm cycle. Hence, the effective contacts considered are exactly those which were detected at the beginning of that cycle. If the selected time step is not appropriate, the balance can result to be not closed. Not physical events can show up during the simulation due to an erroneous time step selection, with the consequent unreliability of the results.

4.2 Computational model set up

Numerical simulations are successfully applied in die filling investigations [22, 23, 78, 80]. In this study, the work of Guo [24] is continued and adapted to the conducted experimental research. The code is an evolution of the TRUBAL code, initially developed by Cundall [11]. A 2D model is built, visible in Figure 4.3, representing a die filling device similar to the one used in the laboratory experiments. The results of a 2D system in the case of die filling is found to be in good agreement with the results of a similar 3D system [24]. The reduction of the degrees of freedom of movement of the particles may lead to a small overestimation of the segregation in the simulations. Anyway, the two dimensional construction is supposed to be accurate enough to be compared with the experimental behaviour.
The DEM is coupled to a CFD method, following the scheme developed by Kafui et al. [30] for the modeling of two phase systems (gas-solid or liquid-solid). This model permits the simulation of the solid particles with the DEM method and the inclusion of air dynamics with the CFD one. Hence, it is possible to simulate the die filling process taking into account the particle-air interaction, which is far from being negligible.
Although the aspect ratio and the circularity of the particles is known (and similar, so a common value could have been chosen for both the particles) the particles are simulated as round disks. This is done to emphasize the role of inter-particles interactions, which are based on contact mechanics and rigorously modeled only for spheres (or, in the case of 2D

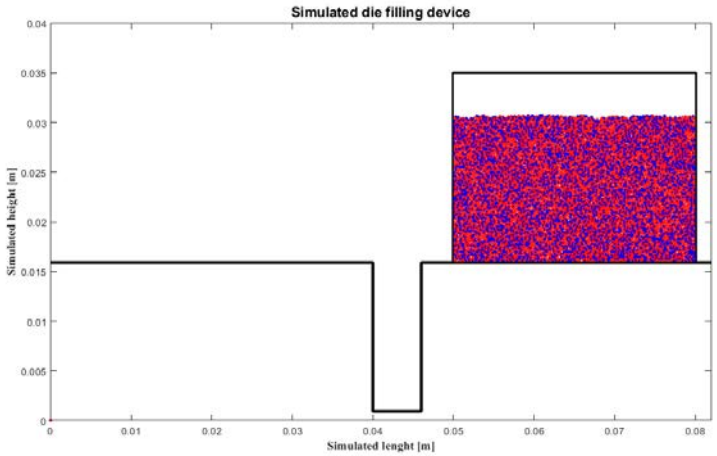

Figure 4.3: Simulation set up (50% of caffeine case)

simulations, disks) [66].
The aspect ratio of the real die used in the experimental part of this research is maintained in the computational simulation. However, its real dimensions are too big to be implemented in the code, since they would lead to the generation of too many particle, increasing the computational cost over the computer limits. The computer is a *Fedora* system (release 12, Constantine), with Linux kernel, Gnome 2.28.2, using an Intel(R) Core(TM) i7, 960 @ 3.20 GHz processor. For this reason a smaller system is built, with the dimensions reported in Table 4.1. Because of the smaller die dimensions, an higher shoe velocity must be used to avoid the fast die filling to happen only in the first part of the shoe movement. After some preliminary tests, a velocity of $240\,mm/s$ is set, which is still under the critical velocity (which seems to be around $250\,mm/s$ for the air-filled die case and $260\,mm/s$ for the vacuum case), but close enough to it to avoid a premature complete die filling with its consequent effect, described in Paragraph 4.3.1.

Table 4.1: Experimental and Simulation characteristics comparison

Set up	Experimental	Simulation
Particles		
CAF diameter $[\mu m]$	207.16 ± 1.56	207
DCPA diameter $[\mu m]$	195.73 ± 1.70	196
Die		
Height $[mm]$	50	15
Lenght $[mm]$	20	6
Aspect Ratio	2.5	2.5

The dimensional difference may lead to a difference in the segregation phenomena during die filling, since the formed air flow will be different. This fact will be considered in the comments of the results comparison.
The simulation requires the number of particles of each species as input. Since experimental powders concentration is based on mass, also in the simulation the mass ratio is maintained. A few calculations are necessary because the only parameter to adjust in order to correct the blend concentration is the number of particles added. Using equation 4.1, the number

of particles of DCPA is calculated, starting from a guess number of caffeine particle. The only issue is to maintain the total number of particles under the computational limiting value. In this case, the number of particles is kept under 12000.

$$n_{DCPA} = \frac{n_{CAF} \cdot V_{CAF} \cdot \rho_{CAF}}{V_{DCPA} \cdot \rho_{DCPA}} \cdot S(\%) \tag{4.1}$$

with n_i in the number of species i particles, V_i their volume, ρ_i their density and $S(\%)$ is a number which depends on the desired caffeine mass concentration in the blend ($S(10\%CAF) = 9$, $S(25\%\, CAF) = 3$ and $S(50\%\, CAF) = 1$). The results of this calculation are reported in Table 4.2.

Table 4.2: Number of particles calculation results

Particle	CAF	DCPA
Density $[kg/m^3]$	1460	2860
Volume $[m^3]$	$4.644e^{-12}$	$3.882e^{-12}$
Case	Particles quantity	
10% by mass	1750	9618
25% by mass	4000	7328
50% by mass	7000	4275
50% by number (perfect mixing)	5907	5901
50% by number (random mixing)	5900	5900

Subsequently they are generated in the area inside the shoe walls with the *FreeDrop* program. Except for the perfectly mixed case, in which each particle of one species is placed alternating from those of the other one, in the other cases each particle is generated randomly. A relaxation step follow the particles generation, in which they settles down under gravity force to form a stable, densely packed bed at the bottom of the shoe, until the kinetic energy of the system reaches a negligible value (until the mean particle velocity is lower than $10^{-6}\ m/s$). At this point the system is ready for the second step, actuated with the *RunVac* program, in the case of vacuum die filling, or *RunAir*, in the case of die filling in air, so the shoe moves from left to right, over the die, pouring the particles into it. The possibility of running the same simulation in the presence of air in the die or in vacuum conditions permit to decouple the segregation factors, highlighting the entity of segregation contributed by the drag effect of air.

4.3 Observations

4.3.1 Die filling segregation effect

The premature die filling, consequent of a shoe velocity too low compared to the critical one, has a very unpleasant effect. Since the die is filled with powder, the bottom part of the shoe powder bulk rubs on the top of the die powder. The vibration causes an intense shear on the powder on the top of the die. This fact triggers the mechanism that moves upwards the lighter particles, so the caffeine one, reducing its concentration in the upper part of the die and inducing also a mixing effects in the top layers, as evident in the Figure 4.4.c/d. In this simulation the velocity is $230\,mm/s$, to much below the critical one which is approximately $250\,mm/s$ for the air-filled die case.

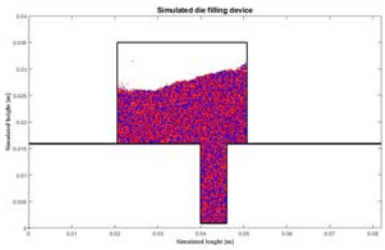

(a) *Premature die filling moment*

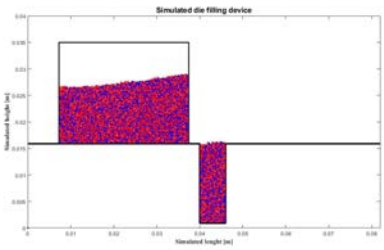

(b) *Situation after rubbing*

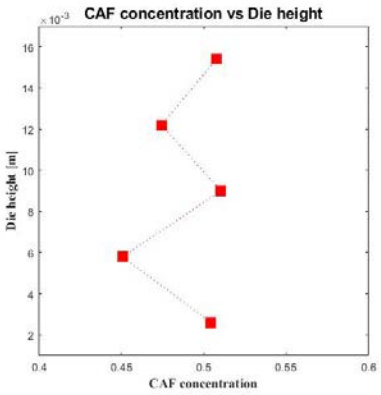

(c) *Layers concentration at premature complete die filling moment*

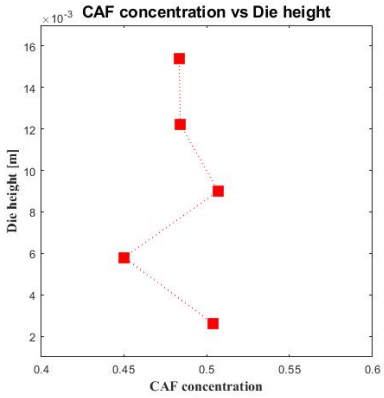

(d) *Layers concentrations after rubbing*

Figure 4.4: Rubbing effects on the concentration of the upper die part

4.4 Simulations and Experimental results comparison

Simulations are performed for the two cases of vacuum condition and air-filled system. This expedient is useful to decouple the effects involved in segregation, permitting a better understanding of what is happening also in the laboratory experiments.
In these simulations no electrostatics and humidity effects are considered. Particles segregation will be related only to inertial differences and, in the air-filled system condition, air drag. Moreover, dimensions of the die filling device and shoe velocity are completely different between the real set up and that simulated. For this reason, simulation results cannot be properly compared to those obtained from the experiments. Nevertheless reducing the involved factors may help the clarifications of the phenomena. Anyway, they will be matched to appreciate if a similar trend can be recognized. Since the low relative humidity experiments have the most similar conditions to those simulated (the major difference is the presence of electrostatic phenomena), their results are chosen to be compared.

4.4.1 Simulated die filling mechanism

The die filling mechanism in the simulated case is quite different from the real one. The initial shake due to acceleration causes an huge inertial accumulation in the tailing side of the shoe, Figures 4.5.b/c. This can be induced both from the higher shoe velocity and the simulation $2D$ structure, which does not permit an horizontal distribution of particles. The huge shake is also responsible of an high caffeine segregation in the shoe, as visible in Figure 4.5.g, in which several caffeine particles accumulate on the top of the front side of the shoe. This behaviour was already shown by Guo et al. [22]. The main difference between the real experiment and the simulated die filling is that in the first one a cloud of falling powder forms in the near-end side of the die and it is very sensitive to air drag. In the simulation die filling proceeds by a column of falling particles, which is intrinsically less likely to be subjected to caffeine extraction by air presence. This fact may be due to the higher shoe velocity, in the simulation with respect to the real experiment.

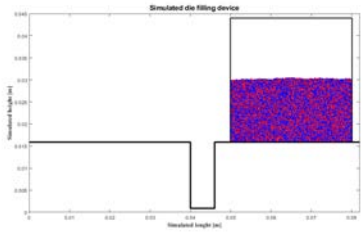

(a) *Initial set up*

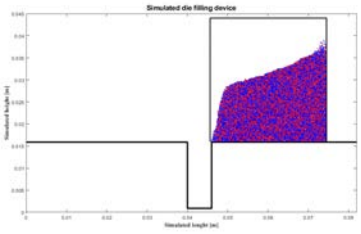

(b) *Shake due to acceleration*

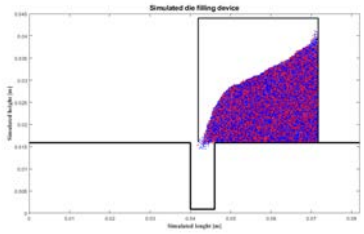

(c) *First powder falling*

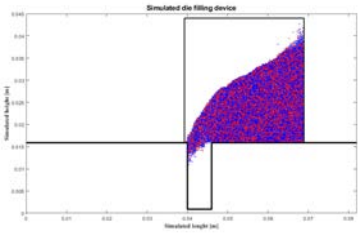

(d) *Powder falling*

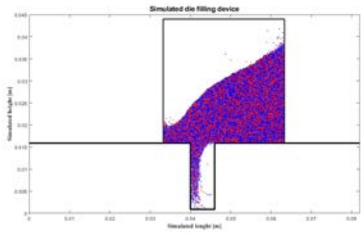

(e) *Threshold to bulk flow*

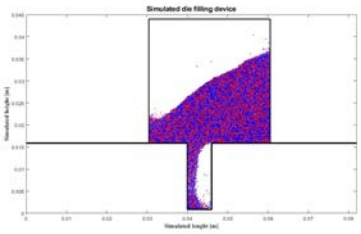

(f) *Heap generation*

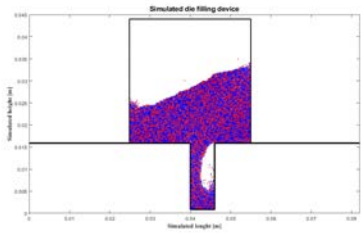

(g) *Heap's rising*

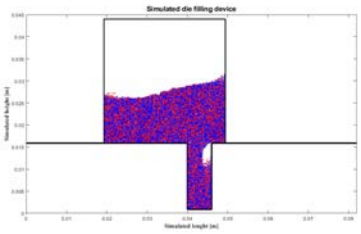

(h) *Air bag shrunk*

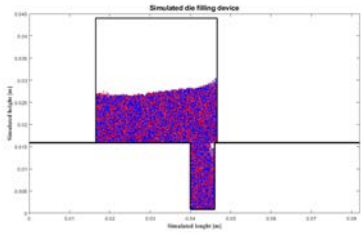

(i) *Last moment before complete filling*

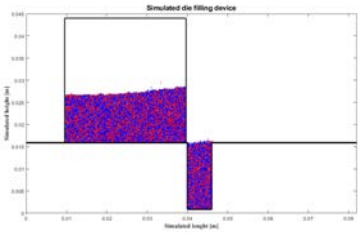

(j) *Complete die filling*

Figure 4.5: Simulated die filling mechanism (25% of caffeine, 240mm/s of shoe velocity)

4.4.2 Simulation results

Similarly to the laboratory experiments, the die is divided in ten drawers and the caffeine concentration is evaluated in each one, using the *Matlab* code reported in Appendix A.4, and the segregation is presented considering horizontal far-end and near-end sides, vertical layers and each drawer differences. In the left side of any group of figures the air filled die results are reported, while in the right side there are the vacuum cases.

4.4.2.1 10% of caffeine

The shoe is fulfilled randomly placing 1750 particles of caffeine and 9618 particle of DCPA. After their gravity settling, the shoe runs over the die at $240\,mm/s$.
The behaviour shown in Figures 4.6 is quite different from the experimental one reported in Figures 3.1. Considering first the air filled die, the horizontal segregation trend is similar, but the vertical one as a few important differences. The main one is the concentration of caffeine particle in the bottom of the die, shown by the simulation but not by the experiments. The initial huge shoe shake causes the segregation of caffeine in the shoe. Then the important nose flow which is evident in the simulations provokes the accumulation of CAF in the lowest die layer, in particular in the near-end side. In the middle part of the die, DCPA tends to concentrate in the near-end side of the die, due to its higher inertia. Caffeine is retained and concentrate again in the upper, near-end side die drawer. The segregation index value is $S.I.(10\%CAF, air) = 0.5390$. In the vacuum case the main difference is the lower concentration of caffeine at the bottom of the die, in correspondence to a lack of caffeine at the near-end right die drawer. A possible explanation is that inertia works vertically, but the absence of air within the die avoid the formation of vortex during the heap formation and arising. The segregation index value in the vacuum case is $S.I.(10\%CAF, vacuum) = 0.4261$.

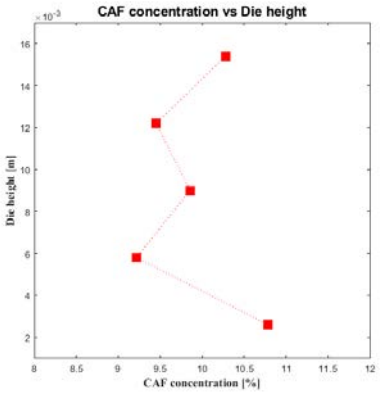

(a) *Different layers CAF Concentration*

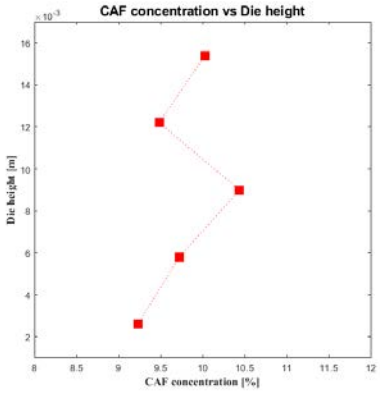

(b) *Different layers CAF Concentration*

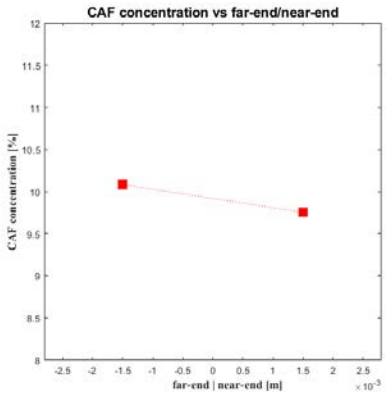

(c) *Different sides CAF Concentration*

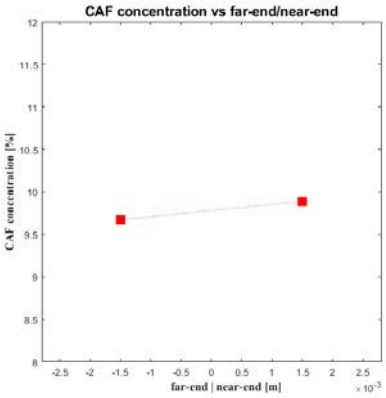

(d) *Different sides CAF Concentration*

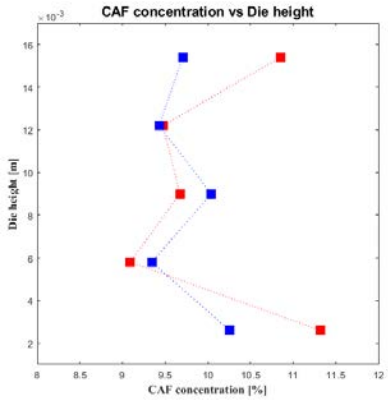

(e) *Every drawer CAF Concentration (blue for far-end side and red for near-end side)*

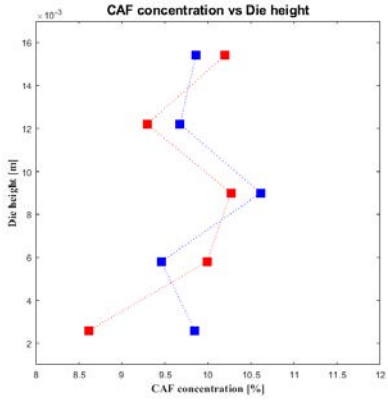

(f) *Every drawer CAF Concentration (blue for far-end side and red for near-end side)*

Figure 4.6: Vertical, horizontal and each die drawer CAF concentration variations in the 10% CAF case in air (left side) or under vacuum (right side)

4.4.2.2 25% of caffeine

This simulation involves 4000 caffeine and 7328 DCPA particles, randomly placed. This case is the one reported in Figure 4.5 to show the die filling mechanism.
The result is quite different from the experimental one. In the air filled die case, caffeine concentrates in the middle of the die height and blend is poor in the bottom and in the top, Figure 4.7. Air presence in the die has succeeded in drag caffeine up from the head of the falling powder column, which concentrates in the medium layer. The segregation index value is $S.I.(25\%CAF, air) = 0.5199$. In the vacuum case segregation is less emphatic, in particular there is not a peak in the middle height of the die, but concentration remains approximately constant. Again, a lack of caffeine is visible at the bottom of the die, due to inertia retaining during the falling. The segregation index value is $S.I.(25\%CAF, vacuum) = 0.3237$

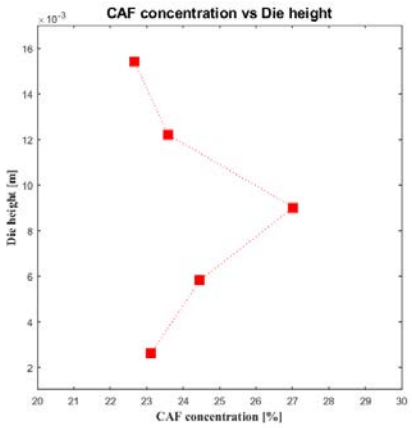

(a) *Different layers CAF Concentration*

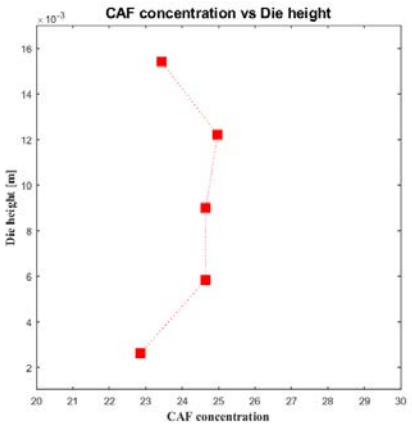

(b) *Different layers CAF Concentration*

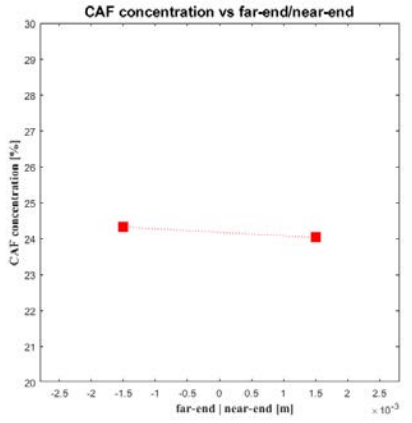

(c) *Different sides CAF Concentration*

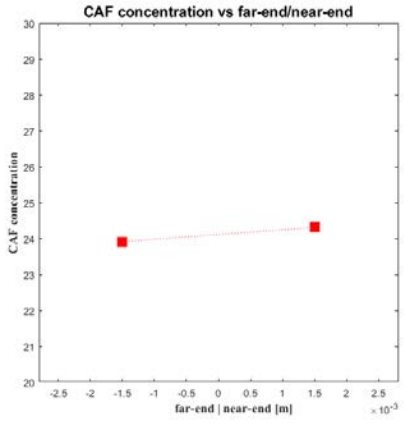

(d) *Different sides CAF Concentration*

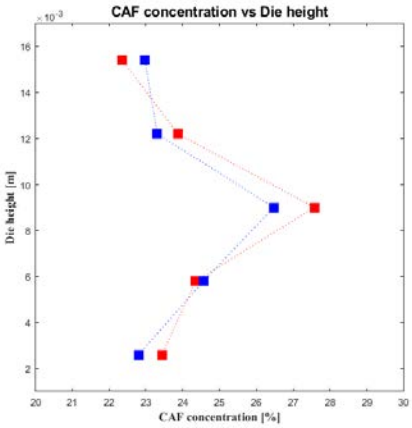

(e) *Every drawer CAF Concentration (blue for far-end side and red for near-end side)*

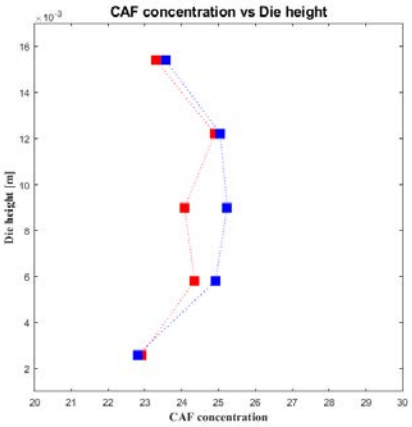

(f) *Every drawer CAF Concentration (blue for far-end side and red for near-end side)*

Figure 4.7: Vertical, horizontal and each die drawer CAF concentration variations in the 25% CAF case in air (left side) or under vacuum (right side)

4.4.2.3 50% of caffeine

The powder blend is generated randomly placing 7000 CAF and 4275 DCPA particles in the shoe.
The zig-zag pattern is quite similar in the lower part of the die between the experiment and the simulation. Horizontal segregation is negligible in both cases. Caffeine tends to accumulate in the middle part of the die and blend is importantly impoverished near the bottom and near the top of the it. Increasing the quantity of caffeine in the edge of the falling powder column it is easier for air to retain it up, so its concentration is more stratified. The segregation index value is $S.I.(50\%CAF, air) = 0.3040$. Also in the vacuum case the general trend is a zig-zag shape along the die height. Caffeine tends to concentrate at the bottom of the die. This fact is anomalous respect to the other two concentration cases. It must be considered that in the vacuum case the critical shoe velocity is higher that the air filled die case, so, since the shoe velocity is maintained at $240\,mm/s$, a larger simil-nose flow is present. This could explain the high caffeine concentration at the bottom. Moving up, a caffeine poor layer is present, partly deposited at the bottom and partly concentrated in the upper part of the die. The high segregation may be due to the high caffeine concentration easing the inertial separation of the two powders. The segregation index value is $S.I.(50\%CAF, vacuum) = 0.4064$. The presence of air in this case may have prevented segregation to be more important. Since both powders are air-sensitive, air may have weakened the inertial separation of the different particles.

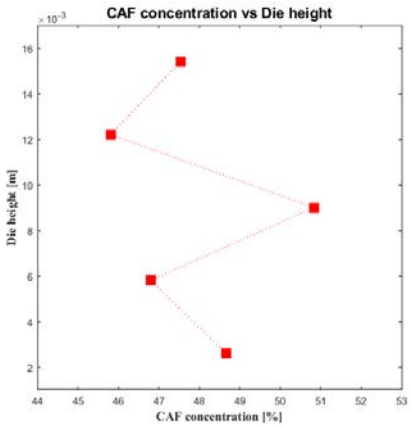

(a) *Different layers CAF Concentration*

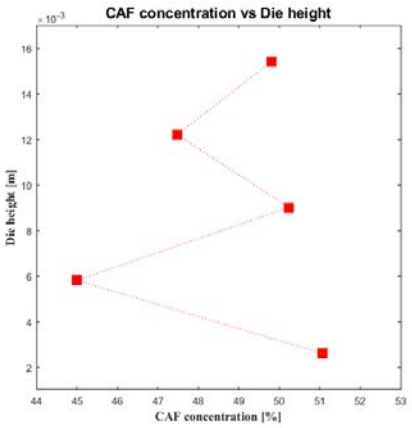

(b) *Different layers CAF Concentration*

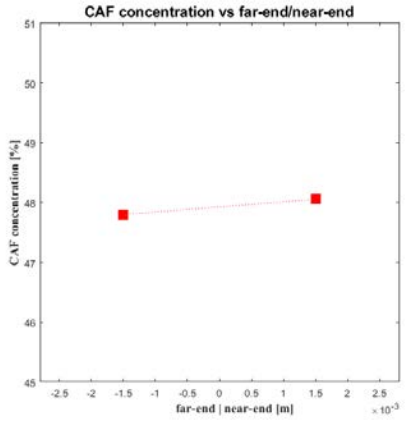

(c) *Different sides CAF Concentration*

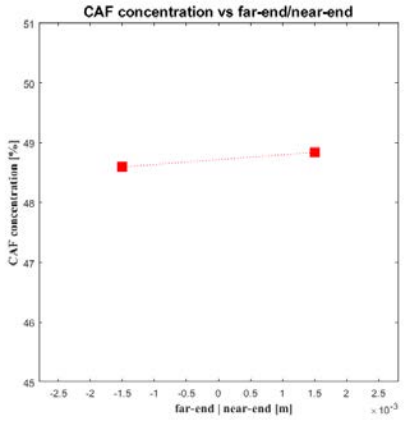

(d) *Different sides CAF Concentration*

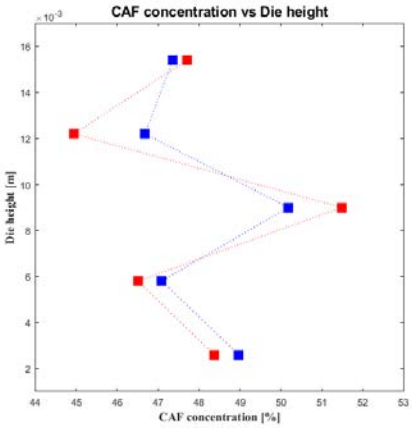

(e) *Every drawer CAF Concentration (blue for far-end side and red for near-end side)*

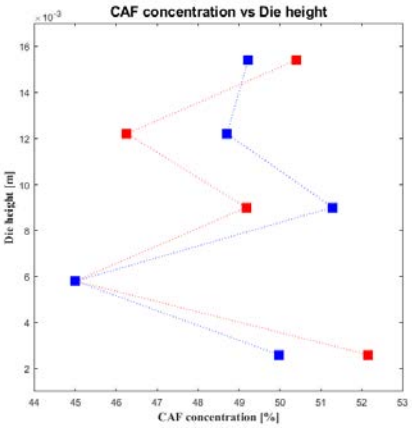

(f) *Every drawer CAF Concentration (blue for far-end side and red for near-end side)*

Figure 4.8: Vertical, horizontal and each die drawer CAF concentration variations in the 50% CAF case in air (left side) or under vacuum (right side)

The following two simulations are made to investigate the importance of the shoe initial filling procedure on the final segregation index value. Two similar concentration blends are generated, one randomly filled, Figure 4.9.a, and the other perfectly mixed, Figure 4.9.b.

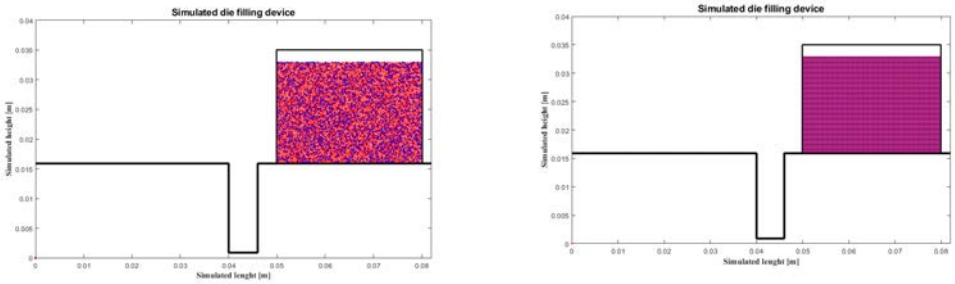

(a) *Randomly mixed initial set up* (b) *Perfectly mixed initial set up*

Figure 4.9: Different shoe filling approaches

Since the concentration of the simulations so far were based on mass and the following two are based on particles number, they are slightly different. Anyway, the concentration are still represented by mass. Obviously, perfectly mixed blend is impossible to be prepared experimentally.

4.4.2.4 Same particle number in the blend, random packing

This simulation involved 5900 CAF and 5900 DCPA particles, approximately the same number of the perfectly mixed case. In this case they are randomly generated within the shoe. For comparison with the other simulations, the concentration by weight of these cases is approximately 37.9%.
The high caffeine concentration in the bottom of the die in the air filled die case may be due to the initial segregation in the shoe due to the shake and then to the initial nose flow. Anyway, the greater concentration in the near-end side can be attributed to the air presence in the die. Then, the high caffeine concentration in the falling powder column may induce the easy extraction of caffeine by air from the edge of the powder falling column, producing the stratified concentration along the die height. The lower concentration in the middle of the die height may be due to the greater inertia of the DCPA particles, that tend to roll more than the caffeine along the heap in formation. The segregation index value is $S.I.(same\,number,\ randomly\,generated, air) = 0.3201$. The vacuum case is quite similar. The main exception is the lack of caffeine at the bottom of the die, that, due to inertial separation, tends to concentrate in the middle-upper part of the die. The segregation index value is $S.I.(same\,number,\ randomly\,generated, vacuum) = 0.3447$.

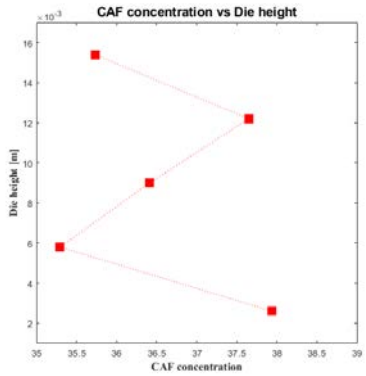

(a) *Different layers CAF Concentration*

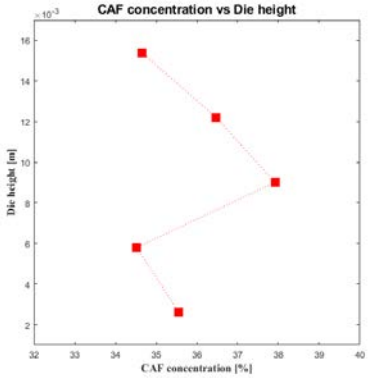

(b) *Different layers CAF Concentration*

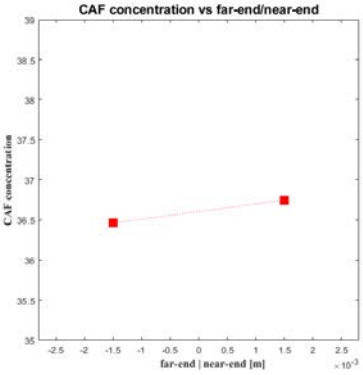

(c) *Different sides CAF Concentration*

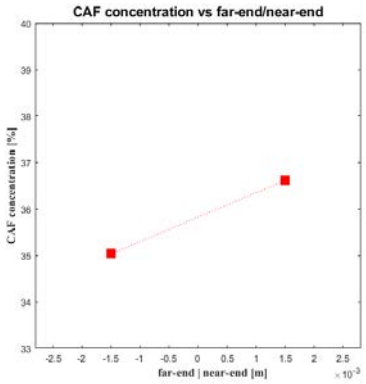

(d) *Different sides CAF Concentration*

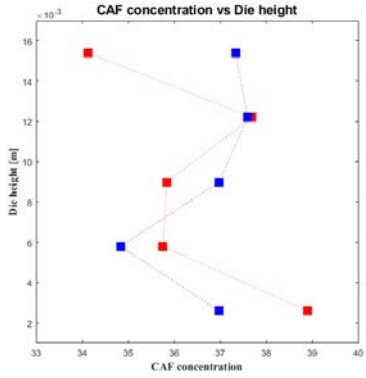

(e) *Every drawer CAF Concentration (blue for far-end side and red for near-end side)*

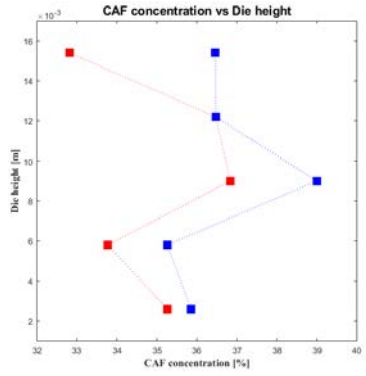

(f) *Every drawer CAF Concentration (blue for far-end side and red for near-end side)*

Figure 4.10: Vertical, horizontal and each die drawer CAF concentration variations in equal number of particles, randomly mixed case in air (left side) or under vacuum (right side)

4.4.2.5 Same particle number in the blend, perfectly mixed packing

Particles are generated specifying their position in such a way that they are perfectly alternated, Figure 4.11.a. This is done by imposing the position of the first particles of CAF and DCPA in one corner and setting the vertical and horizontal distance where placing the others, inside the area formed by the shoe walls.
In the code, this operation is performed with the comand `agenerate` instead of `rgenerate`, adopted in all the other simulations.
After the generation, particles settles under the gravity force, as described in the other cases, until the kinetic energy reaches a negligible value, Figure 4.11.b.

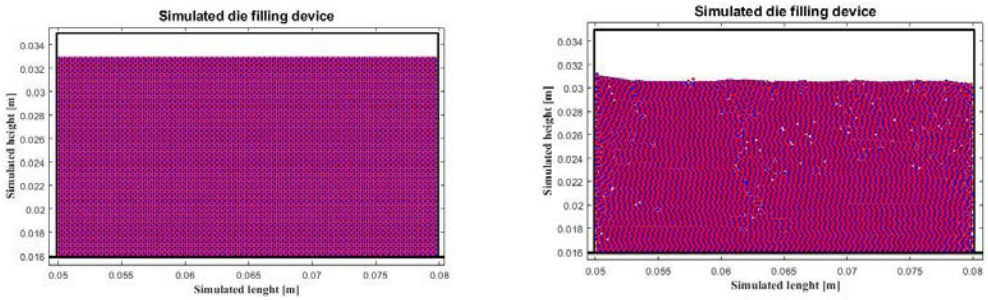

(a) *Perfectly mixed particles generation* (b) *Settled particles*

Figure 4.11: Perfectly mixed shoe filling approach

The initial perfect mixing of the powder has an huge effect on the segregation occurred during die filling. The lower part of the die is poor in caffeine in both the simulations, which concentrates in the middle-top part. Looking at the air filled die case, it is evident that the initial falling powder is depleted of caffeine, which settles in the near-end side of the die bottom. In the middle part of the die height, where air cannot easily penetrate the falling column to extract caffeine, it concentrates, because DCPA tends to roll more than it to the near-end side. In the top die layer there is no enough space for the blend to segregate consistently. The segregation index value is $S.I.(same\ number,\ perfectly\ mixed, air) = 0.1827$. An higher horizontal segregation is present in the vacuum case, in which caffeine tends to concentrate in the upper, far-end side part of the die. This can be due to the bouncing of DCPA particles further down the forming heap. Since the initial powder is well mixed, it is easier to the particle to separate during the falling. The segregation index value is $S.I.(same\ number,\ perfectly\ mixed, vacuum) = 0.2853$. Also in this case air may have helped powder mixing thanks to the similar air-sensitivity of the two powders and to the formation of turbulence inside the die, which may have helped containing the segregation.

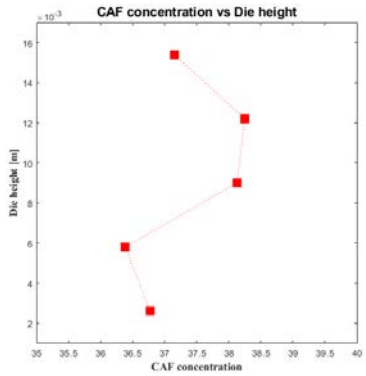

(a) *Different layers CAF Concentration*

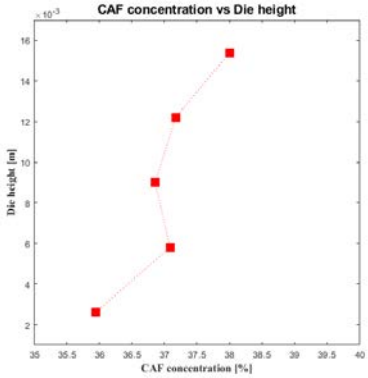

(b) *Different layers CAF Concentration*

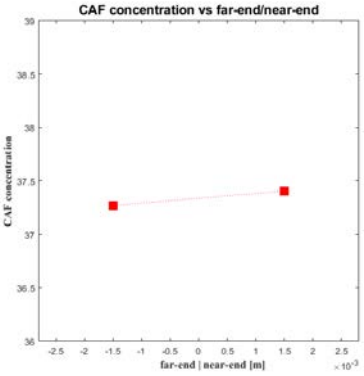

(c) *Different sides CAF Concentration*

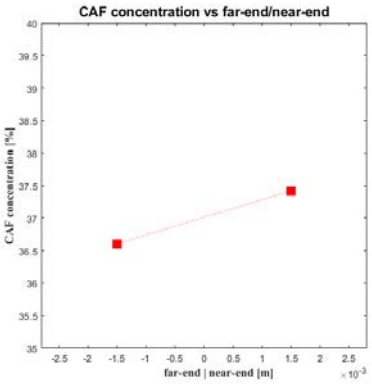

(d) *Different sides CAF Concentration*

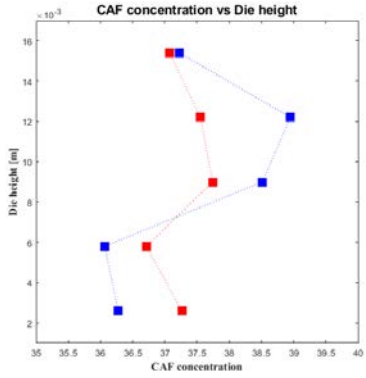

(e) *Every drawer CAF Concentration (blue for far-end side and red for near-end side)*

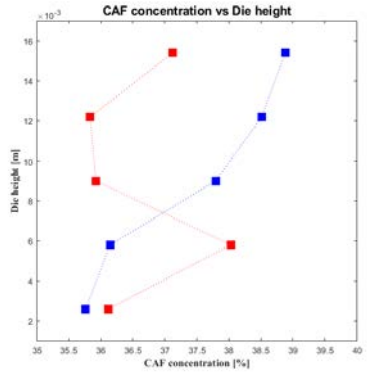

(f) *Every drawer CAF Concentration (blue for far-end side and red for near-end side)*

Figure 4.12: Vertical, horizontal and each die drawer CAF concentration variations in equal number of particles, perfectly mixed case in air (left side) or under vacuum (right side)

4.4.3 Segregation Index of the simulations

In Table 4.3 the values of the segregation index for the performed simulations are collected together. In the cases in which an equal number of particles is involved, **RM** means *random packing* and **PM** means *perfectly mixed*.

Table 4.3: Simulatons Segregation Index values

CAF Concentration	Sim. S.I. air	Sim. S.I. vacuum	Exp. S.I. 50% RH
10% CAF	0.54	0.43	0.77
25% CAF	0.52	0.32	0.54
50% CAF	0.30	0.41	2.29
37.9% CAF, RM	0.32	0.34	-
37.9% CAF, PM	0.18	0.29	-

It can be notice that the segregation index trend in the air filled cases follows the one reported by Kukkar et al. and Tovey et al. [38, 73], in which increasing the API concentration the overall segregation would tend to diminish. The trend is similar to the experimental one stabilized at low relative humidity. This could mean that considering powder with similar flowability, the general behaviour should be the one described here. If the powder flowability changes because of phenomena similar to the ones considered in the ambient and high relative humidity experiments, the resulting segregation may change unexpectedly. Moreover, the huge effect of a perfectly mixed initial set up, especially in the air case, is evident in reducing the final segregation after die filling. This fact suggests to concentrate more effort in guaranteeing the best mixing possible in the shoe before die filling.
The vacuum case Segregation Index values are more homogeneous. Sometimes the Segregation index value in the air filled die case is higher than the one in the vacuum case. It seems like air could, under some circumstances, help mixing within the die or avoid a powder component separation, reducing the general segregation.
It must be specified that, since the shoe velocity is quite high, simulated powders fall nearly totally in a column in the far-end side of the die, not forming a cloud of powder in the near-end side as in the laboratory experiments. For this reason air has only partially the potential to segregate caffeine from the falling powder and the Segregation Index values remain approximately similar in both cases.
The experimental case which is more similar to the simulation set up is the one at 50% of relative humidity. In this case, in fact, inter-particle interactions are weak. Cohesion is on its minimum, so powder behaves more as driven only by gravity, as those simulated. The comparison between the simulations and the experimental results can be only qualitative. Since it is not possible to simulate a full-scale die-filling device, the shoe velocity must be adapted to the simulated size. Moreover, the change in flowability observed in the real powder at high caffeine content makes the comparison more difficult. Anyway, the trend in the 10% and 25% of caffeine cases is similar, so it tends to decrease with the increasing of the API content. The Segregation Index value of the 10% CAF case, excluding the 50% CAF one, is higher than the value of the simulation. Since the simulated shoe velocity is higher than the experimental, bulk flow in the simulations is limited and occurs only through a falling column of powder. In the real experiments a cloud of falling powder is observed, which is more sensitive to segregation by air drag effect.

Chapter 5

Conclusion

5.1 Summary

The main objectives of this research were:

- **Quantify the segregation extent caused by density differences**
- **Find the conditions that favor the rising of segregation phenomena**
- **Compare the results with DEM simulations**

5.2 Conclusions

Density-driven segregation is not negligible also with small density differences as the one reported for the caffeine-DCPA binary blend. This fact has important implications in the pharmaceutical industry since density ratios around 2 are very common in tablet formulations. Underrating this phenomenon may lead to wrong API dosage or structural instability of the tablets. It may result in disruptive effects such as lamination or capping, leading to the withdrawal of entire batches of finished product.
Segregation occurrence was analyzed in different concentration blends and different relative humidity conditions, to obtain a view of the operative conditions which may help reducing it. Segregation is favored at ambient humidity conditions for every powder concentration, since cohesion is at its minimum. At low relative humidity condition electrostatic forces induce particles interaction and at high relative humidity conditions capillary forces arise due to the formation of liquid bridges. In both cases cohesion is increased, avoiding segregation to occur. Since stabilizing big amount of powders at non-ambient relative humidity is a slow process, which must be carried out with attention, this may complicate tabletting operations.
Increasing the API concentration in the blend, segregation should decrease. This has been observed to happen if no other phenomena occur, varying the flowability of the powder. Such an eventuality could be used to detect critical conditions before running tablets production processes, to adapt theirs formulation to the powder characteristics.
DEM simulations permitted to confirm the general decreasing of the segregation, increasing the CAF concentration. Moreover, it highlighted the effect of air in this behavior, which helps maintaining the mixing in high caffeine content blends.

5.3 Future works

Suggestion on the possible future researches with the die filling device are as follows:

- To explore different pharmaceutical materials and different particles sizes to find if the behavior observed in this research, or part of it, can be generalized;
- To verify the possible correlation between a change in the effective friction angle and a variation of the Segregation Index value;
- To develop an adimensional number which considers the effective friction angle with the relative humidity of the powder (or the electrostatic charge and the capillary force) and relates it to the Segregation Index. This may lead to a characterization process that permits to establish the best formulations and conditions to carry out the die filling process without directly testing everyone of them.

Bibliography

[1] Working and principles of tablet compression machine. `https://www.pharmaguideline.com/2016/02/principle-of-tablet-compression-machine.html`. Accessed: 04/06/2019.

[2] BS ISO 3310-1:2016 test sieves — technical requirements and testing. *The British Standard Institution*, 2016.

[3] I. Akseli, B.C. Hancock, and C. Cetinkaya. Non-destructive determination of anisotropic mechanical properties of pharmaceutical solid dosage forms. *International Journal of Pharmaceutics*, 377:35–44, 2009.

[4] Anshu Anand, Jennifer S. Curtis, Carl R. Wassgren, Bruno C. Hancock, , and William R. Ketterhagen. Experimental study of wet cohesive particles discharging from a rectangular hopper. *Industrial Engineering Chemistry Research*, 54:4545–4551, 2015.

[5] Mohammadmehdi Ataei, Huanchen Chen, Tian Tang, and Alidad Amirfazli. Stability of a liquid bridge between nonparallel hydrophilic surfaces. *Journal of Colloid and Interface Science*, 492:207–217, 2017.

[6] Showkat Ahmad Bhawani, Sim Siong Fong, and Mohamad NasirMohamad Ibrahim. Spectrophotometric analysis of caffeine. *International Journal of Analytical Chemistry*, 2015.

[7] John Bridgwater. Mixing of particles and powders: Where next? *Particuology*, 8:563–567, 2010.

[8] M. Capece, Z. Huang, D. To, Marie Aloi, Charles Muchira, R.N. Davé, and A.B. Yu. Prediction of porosity from particle scale interactions: Surface modification of fine cohesive powders. *Powder Technology*, 254:103–113, 2014.

[9] Rohana Chandratilleke, Aibing Yu, John Bridgwater, and Kunio Shinohara. Flow and mixing of cohesive particles in a vertical bladed mixer. *Industrial Engineering Chemistry Research*, 53:4119–4130, 2014.

[10] O. Coube, A. C. F. Cocks, and C.-Y. Wu. Experimental and numerical study of die filling, powder transfer and die compaction. *Powder Metallurgy*, 48(1):68–76, 2005.

[11] P. A. Cundall. Computer simulations of dense sphere assemblies. *Studies in Applied Mechanics*, 20:113–123, 1988.

[12] Peter A. Cundall and Roger D. Hart. Numerical modelling of discontinua. *Engineering Computations*, 9:101–113, 1992.

[13] Siddhi M. Dudhat, Charles N. Kettler, and Rutesh H. Dave. To study capping or lamination tendency of tablets through evaluation of powder rheological properties and tablet mechanical properties of directly compressible blends. *AAPS PharmSciTech*, 18(4):1177–1189, 2017.

[14] J. Eilbeck, G. Rowley, P.A. Carter, and E.J. Fletcher. Effect of contamination of pharmaceutical equipment on powder triboelectrification. *International Journal of Pharmaceutics*, 195:7–11, 2000.

[15] N. Engblom, H. Saxén, R. Zevenhoven, H. Nylander, and G. G. Enstad. Segregation of construction materials in silos. part 1: Experimental findings on different scales. *Particulate Science and Technology*, 30(2):145–160, 2012.

[16] N. Engblom, H. Saxén, R. Zevenhoven, H. Nylander, and G. G. Enstad. Segregation of construction materials in silos. part 2: Identification of relevant segregation mechanisms. *Particulate Science and Technology*, 30(2):161–178, 2012.

[17] James Q. Feng and Dan A. Hays. Relative importance of electrostatic forces on powder particles. *Powder Technology*, 135–136:65–75, 2003.

[18] Shayne Cox Gad. *Pharmaceutical Manufacturin Handbook - Production and Processes*. John Wiley Sons Inc., 2008.

[19] Glor and Martin. *Electrostatic hazards in powder handling*. Research Studies, 1988.

[20] J. M. N. T. Gray and A. R. Thornton. A theory for particle size segregation in shallow granular free-surface flows. *Proceedings of the Royal Society*, 461:1447–1473, 2005.

[21] William D. Greason. Investigation of a test methodology for triboelectrification. *Journal of Electrostatics*, 49:245–256, 2000.

[22] Y. Guo, C.-Y. Wu, K.D. Kafui, and C. Thornton. Numerical analysis of density-induced segregation during die filling. *Powder Technology*, 197:111–119, 2009.

[23] Y. Guo, C.-Y. Wu, and C. Thornton. The effects of air and particle density difference on segregation of powder mixtures during die filling. *Chemical Engineering Science*, 66:661–673, 2010.

[24] Yu Guo. A coupled dem/cfd analysis of die filling process. phd thesis. *Department of Chemical Engineering*, 2010.

[25] H. C. Hamaker. The London-Van der Waals attraction between spherical particles. *Physica*, 4(10):1058–1072, 1937.

[26] Norman Harnby. An engineering view of pharmaceutical powder mixing. *PSTT*, 3(9):303–309, 2000.

[27] Yurong He, Wengen Peng, Tianyu Wang, and Shengnan Yan. DEM study of wet cohesive particles in the presence of liquid bridges in a gas fluidized bed. *Mathematical Problems in Engineering*, 2014, 2014.

[28] J. N. Israelachvili. *Intermolecular and Surface Forces*. Elsevier, 1991.

[29] Kunal Jain, Deliang Shi, and J. J. McCarthy. Discrete characterization of cohesion in gas–solid flows. *Powder Technology*, 146:160–167, 2004.

[30] K. D. Kafui, C. Thornton, and M. J. Adams. Discrete particle-continuum fluid modelling of gas–solid fluidised beds. *Chemical Engineering Science*, 57:2395–2410, 2002.

[31] Waseem Kaialy. A review of factors affecting electrostatic charging of pharmaceuticals and adhesive mixtures for inhalation. *International Journal of Pharmaceutics*, 503:262–276, 2016.

[32] Hiroyuki Kan, Hideya Nakamura, and Satoru Watano. Numerical simulation of particle–particle adhesion by dynamic liquid bridge. *Chemical Engineering Science*, 138:607–615, 2015.

[33] Stefan Karner and Nora Anne Urbanetz. The impact of electrostatic charge in pharmaceutical powders with specific focus on inhalation-powders. *Journal of Aerosol Science*, 42:428–445, 2011.

[34] Stefan Karner and Nora Anne Urbanetz. Arising of electrostatic charge in the mixing process and its influencing factors. *Powder Technology*, 226:261–268, 2012.

[35] John H. Kassebaum and Richard A. Kocken. Controlling static electricity in hazardous (classified) locations. *TRANSACTIONS ON INDUSTRY APPLICATIONS*, 33(1):209–215, 1997.

[36] William R. Ketterhagen, Jennifer S. Curtis, Carl R. Wassgren, and Bruno C. Hancock. Modeling granular segregation in flow from quasi-three-dimensional, wedge-shaped hoppers. *Powder Technology*, 179:126–143, 2008.

[37] William R. Ketterhagen, Jennifer S. Curtis, Carl R. Wassgren, Angela Kong, Padma J. Narayan, and Bruno C. Hancock. Granular segregation in discharging cylindrical hoppers: A discrete element and experimental study. *Chemical Engineering Science*, 62:6423–6439, 2007.

[38] Vipin Kukkar, Vikas Anand, Mahesh Kataria, Manoj Gera, and Pratim Kumar Choudhury. Mixing and formulation of low dose drugs: underlying problems and solutions. *Thai Journal of Pharmaceutical Sciences*, 32:43–58, 2008.

[39] J. W. Kwek, Desmond Heng, S. H. Lee, W. K. Ng, H.-K. Chan, S. Adi, Jerry Heng, and Reginald B. H. Tan. High speed imaging with electrostatic charge monitoring to track powder deagglomeration upon impact. *Journal of Aerosol Science*, 65:77–87, 2013.

[40] Philip Chi Lip Kwok and Hak-Kim Chan. Effect of relative humidity on the electrostatic charge properties of dry powder inhaler aerosols. *Pharmaceutical Research*, 25(2):277–288, 2007.

[41] l. Trujillo, M. Alam, and H. J. Herrmann. Segregation in a fluidized binary granular mixture: Competition between buoyancy and geometric forces. *EUROPHYSICS LETTERS*, 64(2):190–196, 2003.

[42] P. M. C. Lacey et al. The mixing of solid particles. *Trans IChemE*, 21:49–55, 1943.

[43] L. R. Lawrence and J. K. Beddow. Powder segregation during die filling. *Powder Technology*, 2:253–259, 1968.

[44] Hongming Li and J. J. McCarthy. Controlling cohesive particle mixing and segregation. *The American Physical Society*, 90(18), 2003.

[45] E. M. Lifshitz. The theory of molecular attractive forces between solids. *Soviet Physics*, 2(1):73–83, 1956.

[46] F. London. The general theory of molecular forces. *Trans. Faraday Soc.*, 33:8b–26.

[47] G. Lumay, K. Traina, F. Boschini, V. Delaval, A. Rescaglio, R. Cloots, and N. Vandewalle. Effect of relative air humidity on the flowability of lactose powders. *Journal of Drug Delivery Science and Technology*, 35:207–212, 2016.

[48] Jingsen Maa, Wei Gea, Xiaowei Wang, Junwu Wang, and Jinghai Li. High-resolution simulation of gas–solid suspension using macro-scale particle methods. *Chemical Engineering Science*, 61:7096–7106, 2006.

[49] S. Matsusaka, H. Maruyama, T. Matsuyama, and M. Ghadiri. Triboelectic charging of powders: A review. *Chemical Engineering Science*, 65:5781–5807, 2010.

[50] V. Mazel, V. Busignies, H. Diarra, and P. Tchoreloff. Lamination of pharmaceutical tablets due to air entrapment: Direct visualization and influence of the compact thickness. *International Journal of Pharmaceutics*, 478:702—704, 2015.

[51] Vincent Mazel, Harona Diarra, Jérôme Malvestio, and Pierre Tchoreloff. Lamination of biconvex tablets: Numerical and experimental study. *International Journal of Pharmaceutics*, 542:66–71, 2018.

[52] L.A. Mills and I.C. Sinka. Effect of particle size and density on the die fill of powders. *European Journal of Pharmaceutics and Biopharmaceutics*, 84:642–652, 2013.

[53] Toshiyuki Nomura, Takeshi Satoh, and Hiroaki Masuda. The environment humidity effect on the tribo-charge of powder. *Powder Technology*, 135–136:43–49, 2003.

[54] S. Oestreich-Janzen. Caffeine: Characterization and properties. *Encyclopedia of Food and Health*, pages 556–570, 2016.

[55] Chalak S. Omar, Ranjit M. Dhenge, Stefan Palzer, Michael J. Hounslow, and Agba D. Salman. Roller compaction: Effect of relative humidity of lactose powder. *European Journal of Pharmaceutics and Biopharmaceutics*, 106:26–37, 2016.

[56] J. M. Ottino and D. V. Khakhar. Mixing and segregation of granular materials. *Annu. Rev. Fluid Mech.*, 32:55–91, 2000.

[57] J. Paasi, S. Nurmi, R. Vuorinen, S. Strengell, and P. Maijala. Performance of ESD protective materials at low relative humidity. *Journal of Electrostatics*, 51–52:429–434, 2001.

[58] Edward L. Paul, Victor A. Atiemo[U+2010]Obeng, and Suzanne M. Kresta. *Handbook of Industrial Mixing: Science and Practice*. John Wiley Sons Inc., 2004.

[59] Patrice Poriona, Nathalie Sommier, Anne-Marie Faugere, and Pierre Evesque. Dynamics of size segregation and mixing of granular materials in a 3D-blender by NMR imaging investigation. *Powder Technology*, 141:55–68, 2004.

[60] Antonella Rescaglio, Julien Schockmel, Nicolas Vandewalle, and Geoffroy Lumay. Combined effect of moisture and electrostatic charges on powder flow. *Powders Grains*, 140:1–4, 2017.

[61] Raymond C. Rowe, Paul J. Sheskey, and Marian E. Quinn. *Handbook of Pharmaceutical Excipients*. Pharmaceutical Press, American Pharmacists Association, 2009.

[62] Azadeh Samadani, A. Pradhan, and A. Kudrolli. Size segregation of granular matter in silo discharges. *PHYSICAL REVIEW E*, 60(6):7203–7209, 1999.

[63] Dietmar Schulze. Round robin project - shear tests on limestone powder crm-116 with ring shear testers rst-xs and rst-01.pc. 2009.

[64] Dietmar Schulze. Flow properties of powders and bulk solids. 2011.

[65] S. Sethuraman, K. Radhakrishnan, and T. Arul Solomon. Analytical method development and validation of caffeine in tablet dosage form by using UV-spectroscopy. *INTERNATIONAL JOURNAL OF NOVEL TRENDS IN PHARMACEUTICAL SCIENCES*, 3(4):2277–2282, 2013.

[66] Jonathan Seville and Chuan-Yu Wu. *Particle Technology and Engineerin. An Engineer's Guide to Particles and Powders: Fundamentals and Computational Approaches*. Elsevier, 2016.

[67] Yu Shen, Guo Yu, and Wu Chuan-Yu. Dem/cfd modelling of the deposition of dilute granular systems in a vertical container. *Chinese Science Bulletin*, 54(23):4318–4326, 2009.

[68] Troy Shinbrot. The brazil nut effect — in reverse. *Nature*, 429:352–353, 2004.

[69] Sunil R. De Silva, Are Dyroy, and Gisle G. Enstad. Segregation mechanisms and their quantification using segregation testers. 2000.

[70] Xiaosong Sun and Mikio Sakai. A liquid bridge model for spherical particles applicable to asymmetric configurations. *Chemical Engineering Science*, 182:28–43, 2018.

[71] Yoshihiro Takahashi and Mika Sekine. Examination of particle behavior in container on multi-particle collision damper. *Machines*, 3:242–255, 2015.

[72] P. Tang and V. M. Puri. Methods for minimizing segregation: A review. *Particulate Science and Technology*, 22:321–337, 2004.

[73] Geoffrey D. Tovey. *Pharmaceutical Formulation: The Science and Technology of Dosage Forms*. Cambridge, UK: The Royal Society of Chemistry, 2018.

[74] Johannes Diderik van der Waals. Over de continuiteit van den gas-en vloeistoftoestand (on the continuity of the gas and liquid state). *Ph.D. Thesis*, 1873.

[75] Kimiaki Washino, Ei L. Chan, Taku Matsumoto, Seiji Hashino, Takuya Tsuji, and Toshitsugu Tanaka. Normal viscous force of pendular liquid bridge between two relatively moving particles. *Journal of Colloid and Interface Science*, 494:255–265, 2017.

[76] C.-Y. Wu, B.C. Hancock, A. Mills, A.C. Bentham, S.M. Best, and J.A. Elliott. Numerical and experimental investigation of capping mechanisms during pharmaceutical tablet compaction. *Powder Technology*, 181:121–129, 2008.

[77] C.-Y. Wu, O.M. Ruddy T, A.C. Bentham, B.C. Hancock, S.M. Best, and J.A. Elliott. Modelling the mechanical behaviour of pharmaceutical powders during compaction. *Powder Technology*, 152:107–117, 2005.

[78] Chuan-Yu Wu, Brian Armstrong, and Nikolaus Vlachos. Characterization of powder flowability for die filling. *Particulate Science and Technology*, 30(4):378–389, 2012.

[79] Chuan-Yu Wu, Luiza Dihoru, and Alan C.F. Cocks. The flow of powder into simple and stepped dies. *Powder Technology*, 134:24–39, 2003.

[80] Chuan-Yu Wu and Yu Guo. Numerical modelling of suction filling using DEM/CFD. *Chemical EngineeringScience*, 73:231–238, 2012.

[81] Stefan Zigan, Rex B. Thorpe, Ugur Tuzun, and Gisle G. Enstad. Air current segregation of alumina powder. *Part. Part. Syst. Charact.*, 24:124–135, 2007.

Appendix A

Simulations input files

Simulation are divided into two steps. The first one consists in the die filling structure generation and the particles settling until their kinetics energy is negligible. The second one deals with moving the show and follow the die filling.

A.1 Simulation system generation - *FreeDrop* algorithm

With the following code the die filling simulation replica is generated. In the code, caffeine is particle `1`, DCPA is particle `2` and walls are `3` and they are characterized with general properties.

Define the computational domain of the simulation (domain maximum dimension, number of boxes, particles and walls):

```
start 0.0830 0.0470 0.00065 2520 15000 12 log
```

Name of the simulation:

```
Filling in Air
```

Switch on the 2D simulation:

```
2-D
```

Specify particle properties:

Particle diameters:

```
dia 0.000207 1
dia 0.000196 2
```

Elasticity Young modulus:

```
ymd 8.7e9 1
ymd 8.7e9 2
ymd 210e9 3
```

Poisson ratio value:

```
prat 0.30 1
prat 0.30 2
prat 0.29 3
```

Particle densities:

```
dens 1.46e3 1
dens 2.86e3 2
dens 7.9e3 3
```

Friction coefficients:

```
fric 0.30 1
fric 0.30 2
fric 0.30 3
```

Large yield stress value to guarantee that deformations are only elastic:

```
yie 1.9306e30 1
yie 1.9306e30 2
yie 1.9306e30 3
```

Specify 5% ball-ball and 10% ball-wall damping:

```
damp 0.05 0.5 1 0 1
damp 0.10 0.5 1 0 0
```

Specify the gravitational acceleration:

```
grav 0.0 -9.81 0.0
```

Die generation:

```
   dwall fp(0.0400 0.0010 0.000325 0.0400 0.0160 0.000325)
vel(0.0 0.0 0.0) mat(3)
   dwall fp(0.0460 0.0010 0.000325 0.0460 0.0160 0.000325)
vel(0.0 0.0 0.0) mat(3)
   dwall fp(0.0400 0.0010 0.000325 0.0460 0.0010 0.000325)
vel(0.0 0.0 0.0) mat(3)
```

Shoe sliding plane:

```
   dwall fp(0.0010 0.0160 0.000325 0.0400 0.0160 0.000325)
vel(0.0 0.0 0.0) mat(3)
   dwall fp(0.0460 0.0160 0.000325 0.0820 0.0160 0.000325)
vel(0.0 0.0 0.0) mat(3)
```

Device cover generation (to avoid the loss of particles)

```
   dwall fp(0.0010 0.0160 0.000325 0.0010 0.0460 0.000325)
vel(0.0 0.0 0.0) mat(3)
   dwall fp(0.0820 0.0160 0.000325 0.0820 0.0460 0.000325)
vel(0.0 0.0 0.0) mat(3)
   dwall fp(0.0010 0.0460 0.000325 0.0820 0.0460 0.000325)
vel(0.0 0.0 0.0) mat(3)
```

Shoe generation:

```
   dwall fp(0.0500 0.0160 0.000325 0.0500 0.0440 0.000325)
vel(0.0 0.0 0.0) mat(3)
   dwall fp(0.0800 0.0160 0.000325 0.0800 0.0440 0.000325)
vel(0.0 0.0 0.0) mat(3)
```

```
   dwall fp(0.0500 0.0440 0.000325 0.0800 0.0440 0.000325)
vel(0.0 0.0 0.0) mat(3)
```

Specify the region in which generate the particles (inside the shoe):

```
   agglom cub 1 0.0500 0.0800 0.0160 0.0420 0.0 0.00065
   agglom cub 2 0.0500 0.0800 0.0160 0.0420 0.0 0.00065
```

Generate randomly the particles inside the shoe area (the number of particles is selected in order to obtain a specific mass concentration of caffeine and is resumed in Table 4.2):

```
   rgenerate n_CAF(%) 1 1 1
   rgenerate n_DCPA(%) 2 2 2
```

Generate particles in particular positions in the specified region (first particles position and tridimensional distance for the others):

```
   agenerate 1 1 1 0.050103505 0.016103505 0.000325 0.00041402 0.00041402 0
   agenerate 1 1 1 0.050310515 0.016310515 0.000325 0.00041402 0.00041402 0

   agenerate 2 2 2 0.050310505 0.016103515 0.000325 0.00041402 0.00041402 0
   agenerate 2 2 2 0.050103515 0.016310505 0.000325 0.00041402 0.00041402 0
```

Specify the time step fraction (0 1)

```
   frac 0.5
```

Show animations:

```
   anim on 1000
   layers 500
   plot wal axes cir vel
   pri zda
```

Run cycles until the the kinetic energy of the system is negligible:

```
   cyc 50000
   pri zda
   cyc 50000
   ...
```

Save file of particles settled in the shoe to use in the die filling step:

```
   save RELAX
```

A.2 Fluid field mesh - *flowdata* file

If the simulation is carried out in air environment, the properties adopted for the gas are the following.

```
Hydrodynamics model                              PGF
X fluid cells in bed                             138
Y fluid cells in bed                               1
Z fluid cells in bed                              75
Bed x-origin, xb0                             0.0010
Bed y-origin, yb0                           0.000075
Bed z-origin, zb0                             0.0010
Bed x-dimension, xbed (m)                     0.0790
Bed y-dimension, ybed (m)                     0.0005
Bed z-dimension, zbed (m)                     0.0430
Maximum Newton method iterates, itm_new         1000
Maximum ICG Method Iterates,itm_icg             1000
Relative error Newton iterates, eps_new        1.0e-6
Relative error ICG iterates, eps_icg          1.0e-12
Left boundary cell-flag, hxl                        3
Right boundary cell-flag, hxh                       3
Back boundary cell-flag, hyl                        3
Front boundary cell-flag, hyh                       3
Bottom boundary cell-flag, hzl                      3
Top boundary cell-flag, hzh                         6
Fluid temperature, TK (K)                       293.0
Fluid shear viscosity, Mhu_gas (kg/ms)         1.8e-5
Fluid bulk viscosity, Labda_gas (kg/ms)           0.0
Average gas molar mass, M_gas (kg/mol)         2.88e-2
Initial x-fluid velocity (m/s)                    0.0
Initial y-fluid velocity (m/s)                    0.0
Initial z-fluid velocity (m/s)                    0.0
Initial fluid pressure (Pa)                  101325.0
Left boundary fluid velocity (m/s)                0.0
Right boundary fluid velocity (m/s)               0.0
Back boundary fluid velocity (m/s)                0.0
Front boundary fluid velocity (m/s)               0.0
Bottom boundary fluid velocity (m/s)              0.0
Top boundary fluid velocity (m/s)                 0.0
Left boundary fluid pressure (Pa)            101325.0
Right boundary fluid pressure (m/s)          101325.0
Back boundary fluid pressure (m/s)           101325.0
Front boundary fluid pressure (m/s)          101325.0
Bottom boundary fluid pressure (m/s)         101325.0
Top boundary fluid pressure (m/s)            101325.0
Number of obstacles, nobs                           0
X fluid cells in die start from                    68
X fluid cells in die end to                        80
Y fluid cells in die start from                     1
```

```
  Y fluid cells in die end to                    1
  Z fluid cells in die start from                1
  Z fluid cells in die end to                   26
```

A.3 Die filling process - *RunAir*/*RunVac* algorithms

With this code the shoe with the settled particles is moved from right to left above the die, with the set velocity.

Restart the file saved in the previous step:

```
restart RELAX
```

Name the simulation:

```
Filling in Air / Vacuum test
```

Specify the time step fraction:

```
frac 0.5
```

Introduce air on run the simulation in vacuum conditions:

```
gas / *gas
```

Animation:

```
anim on 1000
plot wal axes cir fvel
```

Move the shoe with the specified shoe walls velocity:

```
   awall 6 fp(0.0010 0.0160 0.000325 0.0010 0.0460 0.000325)
vel(0.0 0.0 0.0) mat(3)

   awall 9 fp(0.049999 0.016100 0.000325 0.049999 0.0440 0.000325)
vel(-0.240 0.0 0.0) mat(3)
   awall 10 fp(0.080001 0.016100 0.000325 0.080001 0.0440 0.000325)
vel(-0.240 0.0 0.0) mat(3)
   awall 11 fp(0.049999 0.044000 0.000325 0.080001 0.0440 0.000325)
vel(-0.240 0.0 0.0) mat(3)
```

Run the cycles:

```
cyc 50000
pri mas zda cel bal
save fd_50k
...
```

Stop the simulation:

```
stop
```

A.4 Post-processing: Matlab code

The post-processing operation is performed with a Matlab algorithm. The selected file from the die filling simulation is imported in the code, writing its characteristic number instead of *file_number*. The code must be adjusted for the specific simulated CAF concentration, changing the *conc_min* and *conc_max* in the final graphs.

```
%% Concentration analysis of die filling DEM simulation

% Die divided in 10 drawers (5 layers divided in far-end/near-end)
% Concentration analysis based on MASS

clear; clc; clf;

% Data file
fnoair=file_number;     % number of the simulation file to import

% Die characteristics
x0=0.0400;      % [m], left side of the die
y0=0.0010;      % [m], bottom of the die
len_x=0.0060;     % [m], width of the die
len_y=0.0160;     % [m], height of the die
nx=2;     % horizontal division of the die (far-end / near-end)
ny=5;     % number of vertical layers within the die
dx=len_x/nx;  dy=len_y/ny;
d_caf=207.0e-6;      % [m], diameter of CAF particles
d_dcpa=196.0e-6;     % [m], diameter of DCPA particles
rho_caf=1460;     % [kg/m3], density of CAF particles
rho_dcpa=2860;    % [kg/m3], density of DCPA particles
xf=0.1;

%% File import

    fname1=sprintf('%dp',fnoair);
    fid1=fopen(fname1,'r');
    part1=fscanf(fid1, '%i %f %f %f %f %i %f',[7 inf]);
    part1=part1';
    fclose(fid1);
    part_n1=part1(:,1);
    xa=part1(:,2);ya=part1(:,3);za=part1(:,4);
    ra=part1(:,5);rhoa=part1(:,7);
    [nball_1, con_1]=size(part_n1);

%% Concentration analysis

    r=ra./2;
    partcount=[1,0;2,0;3,0;4,0;5,0];
    conc=zeros(5,2);
    partcaf=zeros(2,nball_1);
    partdcpa=zeros(2,nball_1);
    yp=zeros(1,5);
    s_1=[];

    for i=1:ny       % each layer
        yp(i)= y0+(i-1)*dy+dy/2;
```

```
      yl=y0+(i-1)*dy;
      yh=y0+i*dy;
      vol_caf=0;
      vol_dcpa=0;

   for j=1:nx      % far-end and near-end
         xp=[-len_x/4,len_x/4];

         xl=x0+(j-1)*dx;
         xh=x0+j*dx;

       for n=1:nball_1  % check the position of every particle

       if (ra(n)==d_caf/2.0)
          partcaf(1,n)=xa(n);
          partcaf(2,n)=ya(n);
          if (xa(n)>(xl-r(n)))&&(xa(n)<(xh+r(n)))&&(ya(n)>...
             (yl-r(n)))&&(ya(n)<(yh+r(n)))
              if (xa(n)>=(xl+r(n)))&&(xa(n)<=(xh-r(n)))&&...
                 (ya(n)>=(yl+r(n)))&&(ya(n)<=(yh-r(n)))
                           vol_caf=vol_caf+4*pi*ra(n)^3/3;
                           partcount(i,2)=partcount(i,2)+1;
              elseif (xa(n)>=(xl+r(n)))&&(xa(n)<=(xh-r(n)))||...
                     (ya(n)>=(yl+r(n)))&&(ya(n)<=(yh-r(n)))
                           vol_caf=vol_caf+(1/2)*4*pi*ra(n)^3/3;
                           partcount(i,2)=partcount(i,2)+1/2;
              else
                           vol_caf=vol_caf+(1/4)*4*pi*ra(n)^3/3;
                           partcount(i,2)=partcount(i,2)+1/4;
              end
          end
              if partcaf(2,n)>0.02
                  if partcaf(1,n)~=0
                     s_1=[s_1 ; partcaf(1,n)];
                  end
              end
              elseif (ra(n)==d_dcpa/2.0)
                   partdcpa(1,n)=xa(n);
                   partdcpa(2,n)=ya(n);
              if (xa(n)>(xl-r(n)))&&(xa(n)<(xh+r(n)))&&(ya(n)>...
                           (yl-r(n)))&&(ya(n)<(yh+r(n)))
              if (xa(n)>=(xl+r(n)))&&(xa(n)<=(xh-r(n)))&&...
                  (ya(n)>=(yl+r(n)))&&(ya(n)<=(yh-r(n)))
                  vol_dcpa=vol_dcpa+4*pi*ra(n)^3/3;
              elseif (xa(n)>=(xl+r(n)))&&(xa(n)<=(xh-r(n)))...
                     ||(ya(n)>=(yl+r(n)))&&(ya(n)<=(yh-r(n)))
                     vol_dcpa=vol_dcpa+(1/2)*4*pi*ra(n)^3/3;
              else
                  vol_dcpa=vol_dcpa+(1/4)*4*pi*ra(n)^3/3;
              end
            end
         end
   conc(i,j)=vol_caf*rho_caf/(vol_caf*rho_caf+vol_dcpa*rho_dcpa);
       end
    end
  end
```

```
layers=mean(conc,2);     % mean layers concentrations
fene=mean(conc);         % mean concentrations far-end / near-end

%% Segregation Index

mean_conc=mean(mean(conc));         % mean concentration in the die

SI=sum(sum(abs(conc-mean_conc)/mean_conc));      % S.I. calculation

%% Plots

figure(1) % far-end/near-end side concentration comparison

plot(xp,fene*100,'rs:',...
    'MarkerEdgeColor','r',...
    'MarkerFaceColor','r',...
    'MarkerSize',12);
hold on;
axis([-0.0028 0.0028 conc_min conc_max]);
 set(gca,'plotboxaspectratio',[1 1 1]);
xlabel('          far-end | near-end [m]','fontname','times',...
    'FontSize',12,'FontWeight', 'bold');
ylabel('CAF concentration [%]','fontname','times','FontSize',12,...
    'FontWeight', 'bold');
title('CAF concentration vs far-end/near-end','Fontsize',14);
hold off;


figure(2)    % different layers concentration comparison

plot(layers*100,yp,'rs:',...
    'MarkerEdgeColor','r',...
    'MarkerFaceColor','r',...
    'MarkerSize',12);
hold on;
axis([conc_min conc_max 0.0010 0.0170]);
 set(gca,'plotboxaspectratio',[1 1 1]);
xlabel('CAF concentration [%]','fontname','times','FontSize',12,...
    'FontWeight', 'bold');
ylabel('Die height [m]','fontname','times','FontSize',12,...
    'FontWeight', 'bold');
title('CAF concentration vs Die height','Fontsize',14);
hold off;

figure(3)    % total system 2D representation

x1=0;
x2=0.04;
x3=0.046;
x4=0.082;
y1=0.0009;
y2=0.0159;
y3=0.044;
x = [x1, x2, x2, x3, x3, x4];
y = [y2, y2, y1, y1, y2, y2];
```

```
plot(x, y, 'k-', 'LineWidth', 3);

hold on;

s1=min(s_1)-0.0002;
s2=max(s_1)+0.0002;
y1=0.016;
y2=0.035;
x = [s1, s1, s2, s2];
y = [y1, y2, y2, y1];
plot(x, y, 'k-','LineWidth',2);

xlim([0 0.082]);
ylim([0 0.04]);
 set(gca,'plotboxaspectratio',[1 0.6 1]);

plot(partdcpa(1,:),partdcpa(2,:),'.b','MarkerSize',8)
plot(partcaf(1,:),partcaf(2,:),'.r', 'MarkerSize',6)

xlabel('Simulated lenght [m]','fontname','times','FontSize',12,...
    'FontWeight', 'bold');
ylabel('Simulated height [m]','fontname','times','FontSize',12,...
    'FontWeight', 'bold');
title('Simulated die filling device','Fontsize',14);

hold off

 figure(4)    % any drawer concentration comparison

plot(conc(:,1)*100,yp,'rs:',...
    'MarkerEdgeColor','r',...
    'MarkerFaceColor','r',...
    'MarkerSize',12);
hold on;
plot(conc(:,2)*100,yp,'bs:',...
    'MarkerEdgeColor','b',...
    'MarkerFaceColor','b',...
    'MarkerSize',12);
axis([conc_min conc_max 0.0010 0.0170]);
 set(gca,'plotboxaspectratio',[1 1 1]);
xlabel('CAF concentration [%]','fontname','times','FontSize',12,...
    'FontWeight', 'bold');
ylabel('Die height [m]','fontname','times','FontSize',12,...
    'FontWeight', 'bold');
title('CAF concentration vs Die height','Fontsize',14);
hold off;
```

Acknowledgements

Prof. Chuan-Yu (Charley) Wu

For your help and trust in me, which allowed me to extricate myself from a complex subject such as Powder Technology. It was an honor and a pleasure to confront with such an expert.

Prof. Andrea Claudio Santomaso

Per la disponibilità e i confronti in fase di commento dei risultati e revisione del testo. La ringrazio per aver messo la sua competenza e solida conoscenza a mia disposizione e di avermi permesso in questo modo di trarre il massimo dal mio lavoro.

Office 17BC02

Thank you for your help and friendship during these months. You accepted me immediately as a member of your team and were available to give me advice at any time. I'm glad I have worked with you.

MSc Anastasia Zakhvatayeva

Grazie per avermi sempre dato con pazienza e chiarezza tutte le informazioni di cui avevo bisogno per completare il mio lavoro e per sopravvivere alle lunghe ore in laboratorio.

La mia famiglia

Grazie perché dimostrate sempre di tenere a me e mi siete vicine in ogni momento della mia vita. Spero di rendervi orgogliose e felici quanto lo sono io di appartenere alla nostra famiglia.

I miei amici

Infinite volte grazie ad una schiera di persone magnifiche che non si tirano mai indietro dal ricordarmi quanto io sia fortunato. Agli amici di una vita, perché gli anni non consumino il nostro rapporto e a tutti gli altri, perché lo diventino.

Marta

A te che mi hai fatto scoprire il mondo, ma ancor più mi hai fatto scoprire me stesso, non ci sono parole per ringraziarti. Mi hai spinto a dare sempre il massimo e mi sei sempre vicina, nonostante la distanza a cui siamo costretti. Ti amo.